ENGINEERING RESEARCH INSTITUTE
UNIVERSITY OF MICHIGAN
ANN ARBOR

THEORETICAL STUDY, DESIGN AND CONSTRUCTION OF C-W MAGNETRONS FOR FREQUENCY MODULATION

FINAL REPORT

Technical Report No. 17
Electron Tube Laboratory
Department of Electrical Engineering

by

J. R. BLACK G. E. DOMBROWSKI
J. A. BOYD W. W. PETERSON
P. E. DICKER J. W. VAN NATTER

Approved by: W. G. DOW

Project 2009

CONTRACT NO. DA-36-039 sc-15450
SIGNAL CORPS, DEPARTMENT OF THE ARMY
DEPARTMENT OF THE ARMY PROJECT NO. 3-99-13-02[illegible]
SIGNAL CORPS PROJECT 27-112B-0

December 1953

TABLE OF CONTENTS

	Page
LIST OF ILLUSTRATIONS	ii
PERSONNEL	vi
MAJOR REPORTS ISSUED TO DATE	vii
PAPERS PRESENTED DURING THE PERIOD	x
ABSTRACT	xi
1. Objectives for the Period	1
2. Technical Reports and Articles Published During the Period	2
3. Model 8 - Rectangular Cavity Interdigital Magnetron	8
4. Circuit Studies for the Model 9 Coaxial Voltage-Tunable Magnetron	15
5. High Power Coaxial Voltage-Tunable Magnetron (Model 10)	31
6. Model 11, 11A, and 11B Interdigital Anode Voltage-Tunable Magnetrons Operating in the S-Band Region	36
7. A Ten-Watt Interdigital Voltage-Tunable Magnetron (Model 12)	59
8. A Study of the Effect of the Cathode-Filament Circuit on the Operation of Magnetrons	64
9. An Experimental Investigation of the Effects of Interaction Space Geometry on the Operation of Voltage-Tunable Magnetrons	79
10. The Trajectron, An Experimental Tube for Determining the Space-Charge Distribution in a D-C Magnetic Diode	81
11. Conclusions	94
12. Appendix	97
A. Tubes Constructed During the Period Covered by This Report	99
B. Assembly and Detail Drawings for Model 11B Magnetron	108
C. Construction Techniques for 11 Series Magnetrons	121
Distribution List	131

LIST OF ILLUSTRATIONS

Figure		Page
3.1	Possible Types of Magnetrons Employing the Model 8 Resonant System	9
3.2	Tunable Magnetron Model 8C	11
3.3	Photograph of Model 8C	12
3.4	Tuning Curve for Model 8C - Cathode Modification No. 1	13
3.5	Tuning Curve for Model 8C - Cathode Modification No. 2	14
3.6	Tunable Magnetron Model 8D	16
3.7	Model 8D - A Mechanically Tunable Rectangular Cavity Interdigital Anode Magnetron	17
4.1	Low Power Magnetron Model 9B	20
4.2	Coaxial-T-Resonator	21
4.3	Tuning Curves for Coaxial-T-Resonator	22
4.4	Coaxial-T- Stub Tuner No. 2 for Model 9B Magnetron	24
4.5	Ground Plane Resonator	27
4.6	Model 9 Tube to Waveguide Adapter	28
4.7	Ground Plane Coaxial Output System	30
4.8	Modified Model 9B Bar-and-Vane Geometries	32
5.1	Photograph of Model 10 Magnetron	34
5.2	Assembly Drawing of Interdigital External Cavity Magnetron Model 10	35
6.1	Dual Output Cavity - Model 11 Magnetron	38
6.2	Interdigital External Cavity Magnetron - Model 11	41
6.3	Photograph of Model 11 Magnetron	42
6.4	Test Equipment for Pulsed Operation of Magnetron	44

LIST OF ILLUSTRATIONS
(Continued)

Figure		Page
6.5	Experimental Set-Up Using Model 11 Magnetron as Local Oscillator for Spectrum Analyzer	46
6.6	Circuit Arrangement Used to Observe Output Signal vs. Anode Voltage	48
6.7	Voltage-Tuning Characteristics, Model 11, No. 80	50
6.8	Voltage-Tuning Characteristics of Model 11B, No. 88	52
6.9	Frequency vs. Anode Potential, Model 11B, No. 112	54
6.10	Power and Current Characteristics of Model 11B, No. 112	55
7.1	High Power S-Band Interdigital Magnetron	61
8.1	Equivalent Circuit of Magnetron and Cavity	66
8.2	Expected Circuit Effect for Simple Cathode Lead Structure	67
8.3	Expected Cathode Unbalance Effect for Simple Cathode By-Pass Structure	68
8.4	Assembly of Magnetron Cavity and Experimental By-Pass Structure	69
8.5	Cathode Circuit Tuning Characteristics Model 9B Magnetron, No. 68	70
8.6	Cathode Circuit Tuning Characteristic Model 9B Magnetron, No. 68 in Model 3 Cavity	71
8.7	Coaxial Voltage-Tunable Magnetron, Model 11C	73
8.8	Equivalent Circuit of Magnetron and Cavity	75
8.9	Properties of Model 11 Filament as a Transmission Line	76
8.10	Comparison of Calculated Impedance and Experimental Characteristics	78
10.1	Assembly Drawing of Trajectron	84

LIST OF ILLUSTRATIONS
(Continued)

Figure		Page
10.2	The Trajectron Ready for Recording of Data	85
10.3	The Trajectron, Vacuum Station and Power Supplies	85
10.4	Trajectron Data for the Case of Non-Emitting Cathode with Magnetic Field ($\alpha = 2.48$)	87
10.5	Beam Displacement as a Function of Transit Time (With No Space Charge)	88
10.6	Trajectron Data for the Cylindrical Diode	89
10.7	Typical Data Photographs for Cutoff Magnetron Case	91
12B.1	Interdigital External Cavity Magnetron Model 11B	108
12B.2	Anode and Pole Piece Sub-Assembly	109
12B.3	Kovar Sleeve	110
12B.4	Pole Piece	111
12B.5	Kovar Flanged Flat-Bottom Cup	112
12B.6	Anode Fingers, Model 11B Magnetron	113
12B.7	Tungsten Cathode for Models 11B and 11E Magnetron	114
12B.8	Upper End Hat	115
12B.9	Lower End Hat	116
12B.10	Tungsten Filament	117
12B.11	Insulator	118
12B.12	Center Conductor	119
12B.13	Lower Stem	120
12C.1	Filament Firing Jig - Model 11 Magnetron	124
12C.2	Brazing Jig for Models 11B, 11G, 11GA, 13 and 14 Magnetrons - Part 1	125

LIST OF ILLUSTRATIONS
(Continued)

Figure		Page
12C.3	Anode Wire Brazing Jig - Part 2	126
12C.4	Glassing Jig - Part 1	127
12C.5	Glassing Jig - Part 2	128
12C.6	Glassing Jig - Part 3	129
12C.7	Glassing Jig - Part 4	130

PERSONNEL

Scientific and Engineering Personnel

		Time Worked in Man Months**
W. Dow	Professor of Electrical Engineering	Supervisor
H. Welch	Assoc. Prof. of Electrical Engineering	.87
J. Black	Research Engineer	13.26
J. Boyd	Project Engineer*	3.08
G. Hok	Professor of Electrical Engineering	2.69
J. Needle	Asst. Prof. of Electrical Engineering	2.41
P. Dicker	Research Associates	9.78
G. Dombrowski		16.98
W. Peterson		7.08
D. Hoover	Research Assistant	5.67

Service Personnel

V. Burris	Machine Shop Foreman	7.85
R. Steiner	Assembly Technicians	12.78
J. Van Natter		20.03
R. Denning	Instrument Makers	2.16
E. Kayser		1.55
T. Keith		12.78
T. Knopf		2.53
E. Murphy		1.84
R. Beavis	Laboratory Assistants	1.22
E. Burnais		1.83
R. Eschelbach	Technician	1.15
N. Navarre	Draftsmen	3.09
P. Woodhead		11.69
M. Gotanda	Secretaries	5.71
F. O'Harra		3.69
L. Reeder		4.12

* This title s to another project.

** Time worked is based on 172 hours per month.

MAJOR REPORTS ISSUED TO DATE

Contract No. W-36-039 sc-32245. Subject: Theoretical Study, Design and Construction of C-W Magnetrons for Frequency Modulation.

Technical Report No. 1

H. W. Welch, Jr., "Space-Charge Effects and Frequency Characteristics of C-W Magnetrons Relative to the Problem of Frequency Modulation," November 15, 1948.

Technical Report No. 2

H. W. Welch, Jr., G. R. Brewer, "Operation of Interdigital Magnetrons in the Zero-Order Mode," May 23, 1949.

Technical Report No. 3

H. W. Welch, Jr., J. R. Black, G. R. Brewer, G. Hok, "Final Report," May 27, 1949.

Contract No. W-36-039 sc-35561. Subject: Theoretical Study, Design and Construction of C-W Magnetrons for Frequency Modulation.

Technical Report No. 4

H. W. Welch, Jr., "Effects of Space Charge on Frequency Characteristics of Magnetrons," Proc. IRE, 38, 1434-1449, December 1950.

Technical Report No. 5

H. W. Welch, Jr., S. Ruthberg, H. W. Batten, W. Peterson, "Analysis of Dynamic Characteristics of the Magnetron Space Charge, Preliminary Results," January 1951.

Technical Report No. 6

J. S. Needle, G. Hok, "A New Single-Cavity Resonator for a Multianode Magnetron," January 8, 1951.

Technical Report No. 7

J. R. Black, H. W. Welch, Jr., G. R. Brewer, J. S. Needle, W. Peterson, "Theoretical Study, Design and Construction of C-W Magnetrons for Frequency Modulation," Final Report, February 1951.

Contract No. DA-36-039 sc-5423. Subject: Theoretical Study, Design and Construction of C-W Magnetrons for Frequency Modulation.

Technical Report No. 8

G. R. Brewer, "The Propagation of Electromagnetic Waves in a Magnetron-Type Space Charge," July 1951.

Technical Report No. 10

G. Hok, "Space-Charge Equilibrium in a Magnetron: A Statistical Approach," July 13, 1951.

Technical Report No. 11

J. S. Needle, "The Insertion Magnetron: A New External-Cavity Magnetron for Low-Power Electronically-Tunable Operation in the 10 to 20-cm Wavelength Range," August 1951.

Technical Report No. 12

H. W. Welch, Jr., "Dynamic Frequency Characteristics of the Magnetron Space Charge; Frequency Pushing and Voltage Tuning," November 1951.

Technical Report No. 13

J. R. Black, J. A. Boyd, G. R. Brewer, G. Hok, J. S. Needle, W. Peterson, S. Ruthberg, R. F. Steiner, H. W. Welch, "Theoretical Study, Design and Construction of C-W Magnetrons for Frequency Modulation," Final Report, January 1952.

Contract No. DA-36-039 sc-15450. Subject: Theoretical Study, Design and Construction of C-W Magnetrons for Frequency Modulation.

Technical Report No. 9

G. R. Brewer, translator. "On the Properties of Tubes in a Constant Magnetic Field," by O. Doehler, J. Brossart and G. Mourier. Annales de Radioelectricite, 1948-1950.

Technical Report No. 15

J. A. Boyd, "A Voltage-Tunable Magnetron for Operation in the Frequency Range 1500 to 3000 Megacycles," November 1953.

Technical Report No. 16

G. Hok, "Theoretical Study of the Initiation of Oscillations in Electron Streams through Crossed Fields," November 1953.

University of Michigan, Engineering Research Institute, Electron Tube Laboratory

Technical Report No. 14

G. Hok, "Calculations of a Wave-Guide-Loaded Resonator for Interdigital Magnetrons," September 1952.

PAPERS PRESENTED DURING THE PERIOD

H. W. Welch, Jr., "Method for Prediction of Magnetron Characteristics Relating Frequency and Anode Voltage to Power Output," presented at the Institute of Radio Engineers' National Convention, Waldorf-Astoria Hotel, New York City, March 1952.

G. Hok, "Initial Space Charge Waves in Magnetrons," presented at the Institute of Radio Engineers' Tenth Annual Conference on Electron Tubes held in Ottawa, Canada, June 17, 1952.

J. A. Boyd, "Recent Progress on Voltage-Tunable Magnetrons," presented at the Institute of Radio Engineers' Tenth Annual Conference on Electron Tubes held in Ottawa, Canada, June 17, 1952.

J. S. Needle and P. E. Dicker, "New Types of Magnetron Anodes," presented at the Institute of Radio Engineers' Tenth Annual Conference on Electron Tubes held in Ottawa, Canada, June 17, 1952.

G. Hok, "The Initiation of Oscillations in Electron Streams through Crossed Fields," presented at the Institute of Radio Engineers' Eleventh Annual Conference on Electron Tubes held at Stanford University, Stanford, California, June 19, 1953.

G. E. Dombrowski, "The Effects of the Cathode Line on the Operation of the Magnetron," presented at the Institute of Radio Engineers' Eleventh Annual Conference on Electron Tubes held at Stanford University, Stanford, California, June 20, 1953.

ABSTRACT

A program for developing an S-band voltage-tunable magnetron capable of producing one-half watt of power over a two-to-one frequency range is presented. Operating characteristics of preliminary models as well as the final model developed to date are given. The tube structure consists of an interdigital anode and its associated cathode enclosed in a vacuum envelope. The magnetron operates in a ridge-waveguide structure.

Results of preliminary tests of a new structure for a mechanically tunable magnetron are given. An interdigital magnetron anode and a mechanically variable capacitor are placed at the voltage maxima points in a rectangular cavity supporting one wavelength. This work was dropped at an early date in favor of the voltage-tunable magnetron program.

A study of a variety of circuits for operating a coaxial vane-bar anode magnetron is reported on. Mechanically tunable and voltage tunable operation was investigated. One mechanically tunable structure covers the frequency range 375-3750 mc.

A brief discussion of results obtained in an effort to obtain high power voltage tunable operation in a coaxial vane-bar anode structure is presented. This effort was terminated at an early date in favor of low-power voltage-tunable work.

Results obtained on a program to develop in the order of ten watts of voltage-tunable S-band power are presented.

Included is a study of the effects of the cathode-filament circuit on the operation of magnetrons.

Also included are the results obtained on an experiment for determining the space charge distribution in a d-c magnetic diode.

THEORETICAL STUDY, DESIGN AND CONSTRUCTION OF C-W MAGNETRONS FOR FREQUENCY MODULATION

FINAL REPORT

1. Objectives for the Period (J. R. Black)

This report summarizes the progress made at the University of Michigan's Electron Tube Laboratory during the period, December 1, 1951 through November 30, 1953 on Contract No. DA-36-039 sc-15450 for the Signal Corps.

The general objectives of this program are to increase the knowledge of space-charge effects and frequency characteristics in c-w magnetrons and to apply this knowledge to the development of magnetrons which can be frequency modulated. The main effort during this period was to develop practical, usable tubes with voltage-tunable magnetrons receiving the major interest. Some effort, however, was devoted to basic studies of the space charge distribution within a d-c magnetron and to the initiation of oscillations in electron beams through crossed electric and magnetic fields.

A portion of the earlier work done on this program was a continuation of work started on the previous contract (Contract No. DA-36-039 sc-5423) where effort had been devoted toward the development of mechanically tunable low power test oscillators and power tubes developing 500 watts which were capable of being frequency modulated over a narrow frequency range.

2. Technical Reports and Articles Published during the Period

Technical Report No. 9

During the past three to four years several articles presenting theoretical considerations on the subject of the magnetron and the proposed magnetron traveling-wave tube have appeared in the Annales de Radioelectricite. A series of four articles by O. Doehler et al. were of considerable interest to the personnel of the Electron Tube Laboratory and it is thought that they would be of greater interest to other workers in this field if available in an English translation. The following four articles have been translated and issued as Technical Report No. 9.

PART I "On the Properties of Tubes in a Constant Magnetic Field," by O. Doehler. Annales de Radioelectricite, Vol. 3, No. 11, January 1948, pp. 29-39.

Summary. This article treats the static and dynamic properties of the magnetron. Using the theories of L. Brillouin, the author gives the relations defining the space charge, the distribution of potential, and the characteristics for the magnetic field smaller than the critical magnetic field. The author then studies the oscillation frequencies of the multi-cavity magnetron and shows that the results of his calculations agree well with the measured values.

PART II "The Oscillations of Resonance," by O. Doehler. Annales de Radioelectricite, Vol. 3, No. 13, July 1948, pp. 169-183.

Summary. Starting with the results established in the first part of this article, the author considers the oscillations of resonance with high efficiency, that is to say, excited in the region above the critical point. He examines the differences existing between these oscillations and the electronic oscillations, then establishes a quantitative relation giving the conditions for optimum operation. The efficiency and the input impedances are calculated, and an empirical relation between the anode current and the current of rotation is given.

Finally, the dynamic electronic trajectories of a plane magnetron without space charge are calculated to serve as an introduction to the study of the traveling-wave tube in a magnetic field.

PART III "The Traveling-Wave Tube in a Magnetic Field," by J. Brossart and O. Doehler. Annales de Radioelectricite, Vol. 3, No. 14, October 1948, pp. 328-338.

Summary. In this article the authors study the behavior of the magnetron as a traveling-wave tube; they describe a new type of tube, the magnetron traveling-wave tube, and, neglecting the influence of space charge, they calculate the gain of this tube used as an amplifier. Finally, they point out the essential differences between the traveling-wave tube of the Kompfner-Pierce type and the magnetron traveling-wave tube.

PART IV "The Traveling-Wave Tube with a Magnetic Field," by O. Doehler, J. Brossart, and G. Mourier. Annales de Radioelectricite, Vol. 5, No. 22, October 1950, pp. 293-307.

Summary. The authors study again the linear theory of traveling-wave tubes with constant magnetic field without taking into consideration one of the assumptions made in the preceding issue.

Two additional waves are found in that case, which are neither amplified nor attenuated. By computing nonlinear effects, they point out that the essential fact is the absorption by the anode. The efficiency is then evaluated. When the electron beam is sent with a velocity small with respect to the anode voltage, its value is larger, and a simple expression can be found for it.

G. Hok, "A Statistical Approach to the Space Charge Distribution in a Cut-Off Magnetron," Jour. Applied Physics, 23, pp. 983-989, September 1952.

This report discusses the steady-state space-charge distribution in a d-c magnetron when its anode voltage is lower than its cut-off voltage. It is shown that the discrete electron-to-electron interaction has a cumulative effect on the space-charge distribution that is not negligible. The distributions derived by Brillouin, Slater, and others are not steady-state distributions, since they are obtained without regard to the discrete interaction. The actual distribution and its dependance on the ratio of anode voltage to cut-off voltage are discussed qualitatively, but no attempt is made to calculate the space-charge distribution explicitly.

Technical Report No. 14

G. Hok, "Calculation of a Waveguide Loaded Resonator for Interdigital Magnetrons," September 1952.

Abstract

PART I General Analysis of Discontinuities in Wave Guides and Cavities.

The transmission and reflection of electro-magnetic waves at the boundary surface between two systems of different geometry is studied by means of harmonic analysis. Attention is at first focused on such configurations that two-dimensional rather than three-dimensional analysis is possible. An equivalent network is given and a comprehensive expression derived for the wave admittance of the discontinuity in terms of the wave admittances of the normal anodes in the two systems and the coefficients of coupling between them. A coefficient of coupling is defined as a normalized non-orthogonality integral of the wave functions over the boundary surface between the two systems. The result is directly applicable to waveguide junctions and is extended to symmetrical obstacles in wave guides by combination of symmetrical and antisymmetrical illumination of the two discontinuities. Equivalent open-circuit and short-circuit impedances, T and π networks are given. The more general problem of three-dimensional harmonic analysis is considered in connection with a specific example: the junction between a rectangular wave guide and a cylindrical resonator. The general solution as well as an explicit approximate formula for the admittance of the junction.

PART II Solution of the Specific Problem.

This part of the paper considers the problem of designing a waveguide-ouput system for an interdigital magnetron so as to realize a specified slot conductance for the electronic operation of the magnetron. First the electromagnetic field at resonance is calculated in all parts of the system. Then the impedance transformation between the anode and the output wave guide is designed to meet the specifications. To facilitate experimental verification of the results, expressions are derived for the external and the internal Q of the resonator. Test results on a scale model are given and compared with computed values.

H. W. Welch, Jr., "Prediction of Traveling-Wave Magnetron Frequency Characteristics: Frequency Pushing and Voltage Tuning," Proceedings of the I.R.E., November 1953, pp. 1631-1653.

Summary. An approximate method has been developed for determining the shape and density of the spokes of electronic space charge when large r-f potentials exist in the magnetron. With the estimation of space-charge configuration which this method makes possible, induced current theory and knowledge of the magnetron electrode greometry and external cirucuit can be applied to the calculation of frequency characteristics. These characteristics relate frequency to operating anode potential and anode current and are defined as frequency pushing or voltage tuning characteristics. Relatively simple equations for these characteristics are presented. Calculated characteristics for typical values of the variables of magnetron design are presented. The correspondence of the results of the theory with experimental data is discussed very briefly.

Technical Report No. 15

J. A. Boyd, "A Voltage-Tunable Magnetron for Operation in the Frequency Range 1500-3000 Megacycles," November 1953.

Abstract. This report describes the design and construction of a microwave generator which can be used in many of the applications where electronically-tunable power is needed. This generator consists of an external-cavity interdigital magnetron and its associated cavity structure. This magnetron operates in the frequency range of 1500 to 3000 mc with a power output of the order of 250 milliwatts.

In the design of this magnetron, emphasis was placed on maintaining the anode-to-anode capacitance at a minimum, and on shaping the anode bars in such a manner that higher-order space harmonics would be reduced. Several types of cathodes were tested, including oxide-coated, thoriated tungsten, and pure tungsten. Results indicate that a pure tungsten cathode is most satisfactory for use in this tube. The cavity structure consists of a ridge waveguide, tapered at each end to a 50-ohm coaxial output.

A number of tubes have been built and tested. Results of these experimental investigations indicate that this magnetron is useful as a local oscillator for use in spectrum analyzers, microwave receivers, and as a source of electronically-tunable microwave power for general microwave measurement and development work.

A universal voltage-tuning equation for a magnetron has been derived. The experimental data are interpreted in terms of this theoretical tuning curve and the properties of the r-f circuit arrangment. The importance of the circuit impedance in determining the power output of a voltage-tunable magnetron is discussed. The sensitivity of the Model 11 voltage-tunable magnetron operation to the temperature of the cathode is related to the low impedance of the r-f circuit.

Technical Report No. 16

G. Hok, "Theoretical Study of the Initiation of Oscillations in Electron Streams through Crossed Fields," November 1953.

Discussion of Results. The theoretical investigation presented studies the modes of oscillation in a reentrant system formed by an ideal laminar stream of electrons partly filling the space between two plane boundaries of specified wave admittances. Comparisons are made between propagation parallel and perpendicular to the constant magnetic field. The particular purpose of the study is to survey the conditions under which modes exist that in the small-signal range show exponential growth of amplitude with time, in the hope that the result provide some better understanding of the limits for spontaneous initiation of oscillations in traveling-wave oscillators and magnetrons.

When at least one of the boundary admittances contains inductance components, the wave guide formed by the admittance walls and the space between them is a propagating structure, and the classical small-signal traveling-wave-amplifier theory applies. More interesting are the cases where this structure is operated under cut-off conditions and attenuates only, in the absence of the beam. The wall admittances are then resistive and capacitive, and the analysis indicates that within certain ranges of the parameters spontaneous oscillations can still occur.

Each root to the characteristic equation obtained for a specific case of boundary admittances leads to a relation between the radian wave numbers α and γ , on the one hand, and the complex frequency on the other hand, with beam velocity and dimensions as parameters. A study of this relation reveals the range of the parameters for which self-excited oscillations can be obtained, the electronic tuning obtainable by varying the parameters, primarily the beam voltage, and the mode selection rules when a set of different wave numbers are permitted.

In this report only those natural modes have been considered for which either α or γ is zero, because a comparison of these modes appears particularly instructive. Actually any cavity, limited in all three dimensions, with or without a stream of electrons, has an infinite number of natural modes with non-vanishing values of both α and γ. In the presence of an electron stream and under appropriate conditions of approximate synchronism between electron and phase velocity in one dimension natural modes may exist that are growing waves. A closer study may reveal that the complex frequencies of these modes differ very little from each other, so that an oscillator may switch from one mode to another for very small variations of the operating conditions. In many space-harmonic slow-wave structures, however, modes of this kind are more or less effectively suppressed. This is in general true about traveling-wave tubes but not about magnetrons.

The significance of the lower boundary ($y = 0$) and of its admittance is apparent in a magnetron, where the cathode surface forms a boundary which may have considerable wave resistance and, in case of a helical shape, also appreciable wave reactance. When a potential minimum exists, it is a rather complicated problem to state the boundary conditions realistically. The analysis shows definitely, however, that even for very small perturbations the space charge is by no means a perfect shield around the cathode, and that the finite cathode admittance has an appreciable effect on the natural modes of oscillation of the system.

The wide-range operation of voltage-tunable magnetrons may possibly be explained on the basis of this analysis. It is too early to present such a detailed interpretation here; only a general outline may be in order. When the anode admittance is large, the resistivity of the cathode may provide the necessary condition for the existence of growing waves even at frequencies where the anode is primarily capacitive, thus making the oscillation only to a minor extent dependent on the anode circuit. The mode selection and the variation of output power with frequency is still likely to be determined by the anode circuit and its matching network, even if the frequency range over which oscillations occur is not to any appreciable degree.

Some attempts have been made to show that viscous losses in the space charge, produced, for instance, by the presence of a small amount of gas, may also create conditions favorable to the existence of growing waves.

More important than the viscous losses in the space charge itself are the r-f losses due to "backheating," and it is reasonable to assume that the latter can be taken into account as increased resistance losses in the cathode surface.

3. Model 8 Rectangular Cavity Interdigital Magnetron (J. R. Black)

In the period preceding that covered by this report a new resonant structure for an interdigital magnetron anode was proposed. This essentially is a rectangular waveguide shorted at either end so that it operates in the full wavelength mode when capacitances are placed at the voltage maxima. Figure 3.1 shows possible variations of the structure which would produce four different types of magnetrons. Figure 3.1A shows two interdigital anodes placed at the voltage maxima points in the waveguide forming a high power fixed frequency magnetron with the anode sets operating in parallel.

A f-m magnetron could be produced when an interdigital oscillator anode and an anode employing a space charge variable reactance element are placed at the voltage maxima as depicted in Fig. 3.1B.

A mechanically tunable magnetron would be formed if the rectangular waveguide structure contained at the two voltage maxima points an interdigital oscillator anode and a mechanically variable capacitor. This structure is depicted in Fig. 3.1C.

A further proposed variation of this structure is shown in Fig. 3.1D where the interdigital anode structure operating in the rectangular waveguide couples directly through a window into a load. This heavy coupling can produce a voltage-tunable magnetron.

Initially the effort, previous to the period being reported on, was directed toward the development of a high power magnetron as depicted in Fig. 3.1A. Two such tubes designated as Model 8 and 8B were constructed, however, they operated in parasitic modes associated with the cathode lines. (See Technical Reports No. 7 and No. 13.)

FIG. 3.1

POSSIBLE TYPES OF MAGNETRONS EMPLOYING THE MODEL 8 RESONANT SYSTEM

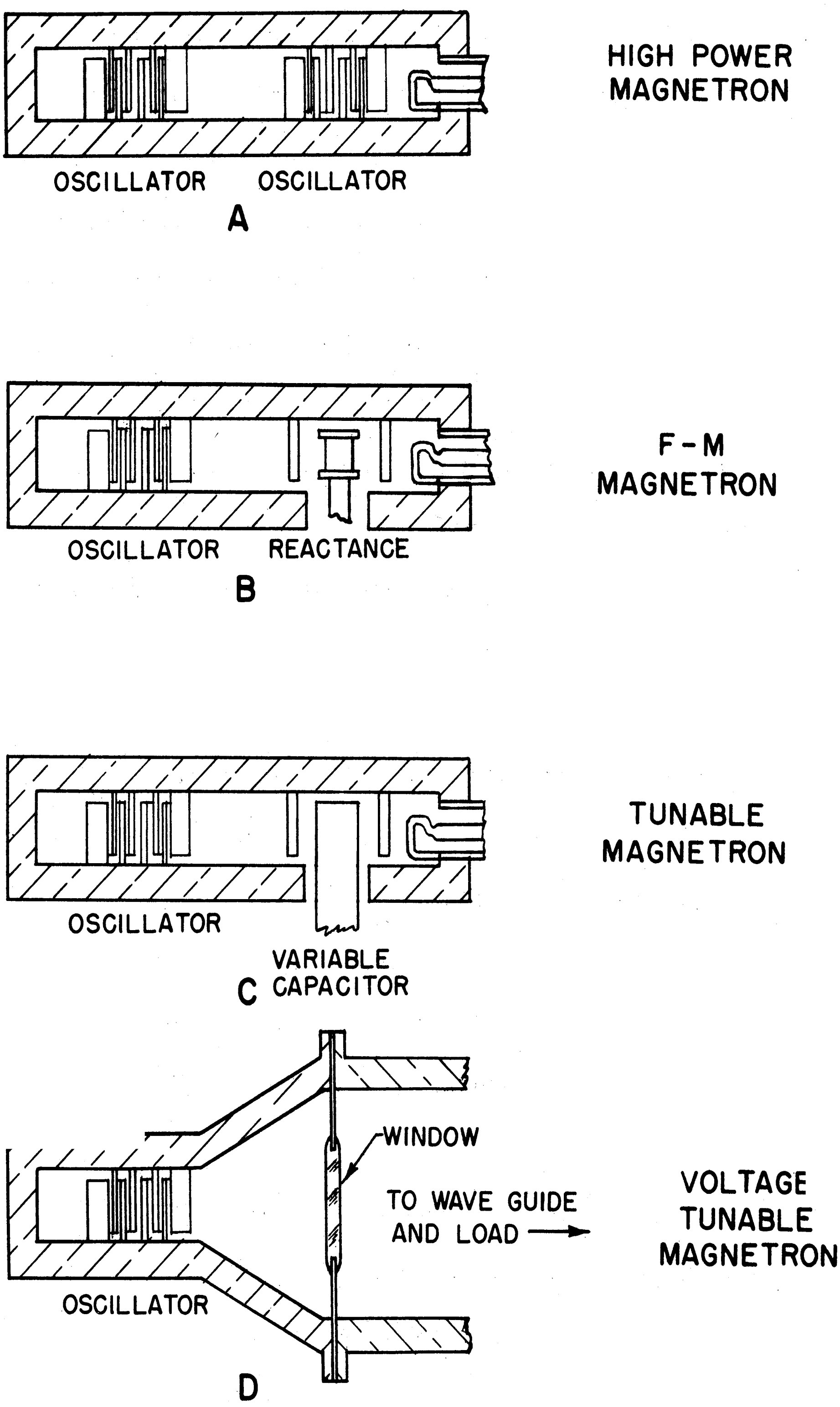

In order to investigate the role played by the cathode lines in this structure a mechanically tunable tube was constructed along the lines depicted in Fig. 3.1C and called Model 8C. This tube was reported on in our Technical Report No. 13. It tuned from 1500 to 2500 mc but exhibited non-tunable modes at 2060 and 1690 mc. The maximum mode-jump current boundary was extremely low (30-40 ma) limiting the power output to between 20 and 35 watts at efficiencies between 33 to 45 percent. The low mode boundary current was attributed to the high capacitance of the anodes and to the low unloaded Q caused by current circulating in the cathode stem circuit. A drawing of the Model 8C is presented in Fig. 3.2 and a photograph appears in Fig. 3.3.

During the period being reported on three modifications of the cathode line were made in an attempt to identify the two fixed frequency modes.

In the first case the cathode choke of Model 8C was modified as shown in the insert of Fig. 3.4. As the tuning curve of Fig. 3.4 indicates the higher frequency parasitic mode was entirely eliminated and the lower frequency parasitic mode shifted to 1875 mc.

Next the entire cathode choke skirt was eliminated leaving only a capacitive slug as shown in the insert of Fig. 3.5. The tuning curve of Fig. 3.5 shows only a slight change from the previous curve.

The third change made in the cathode line was the removal of 1.61 cm of the cathode upper end hat with results identical to the previous experiment.

It was determined that the parasitic mode appearing at 1875 mc was associated with the cavity. It is the expected frequency of operation of the anode placed in a square cavity equivalent to one-half the

DWG. NO. B

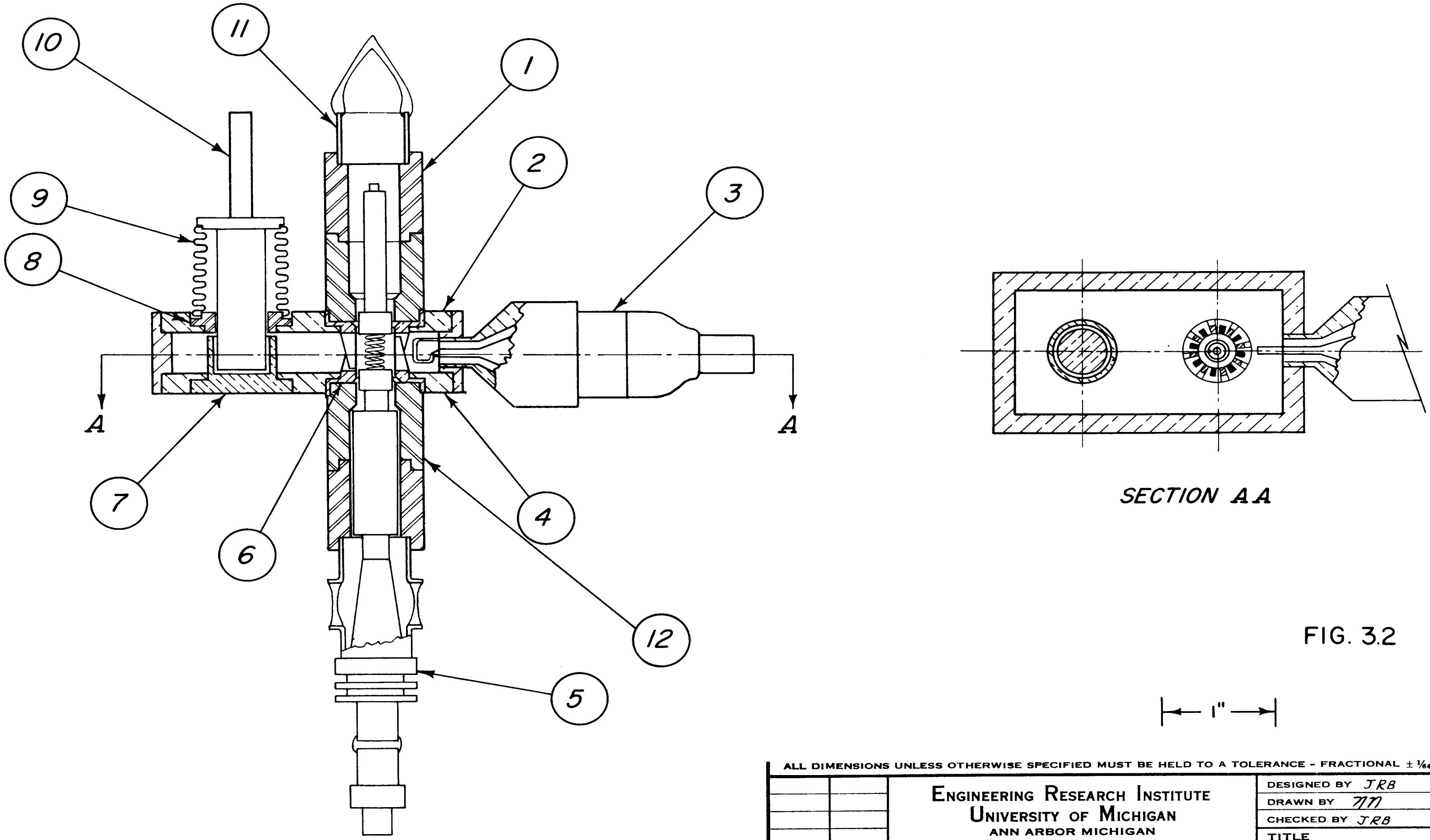

FIG. 3.2

ALL DIMENSIONS UNLESS OTHERWISE SPECIFIED MUST BE HELD TO A TOLERANCE - FRACTIONAL ± 1/64," DECIMAL ± .005," ANGULAR ± 1/2°

ISSUE	DATE	ENGINEERING RESEARCH INSTITUTE UNIVERSITY OF MICHIGAN ANN ARBOR MICHIGAN	DESIGNED BY JRB DRAWN BY 7117 CHECKED BY JRB	APPROVED BY SCALE FULL DATE 10-5-51
		PROJECT M- 921	TITLE TUNABLE MAGNETRON MODEL 8C	
		CLASSIFICATION	DWG. NO. B- 10,008C	

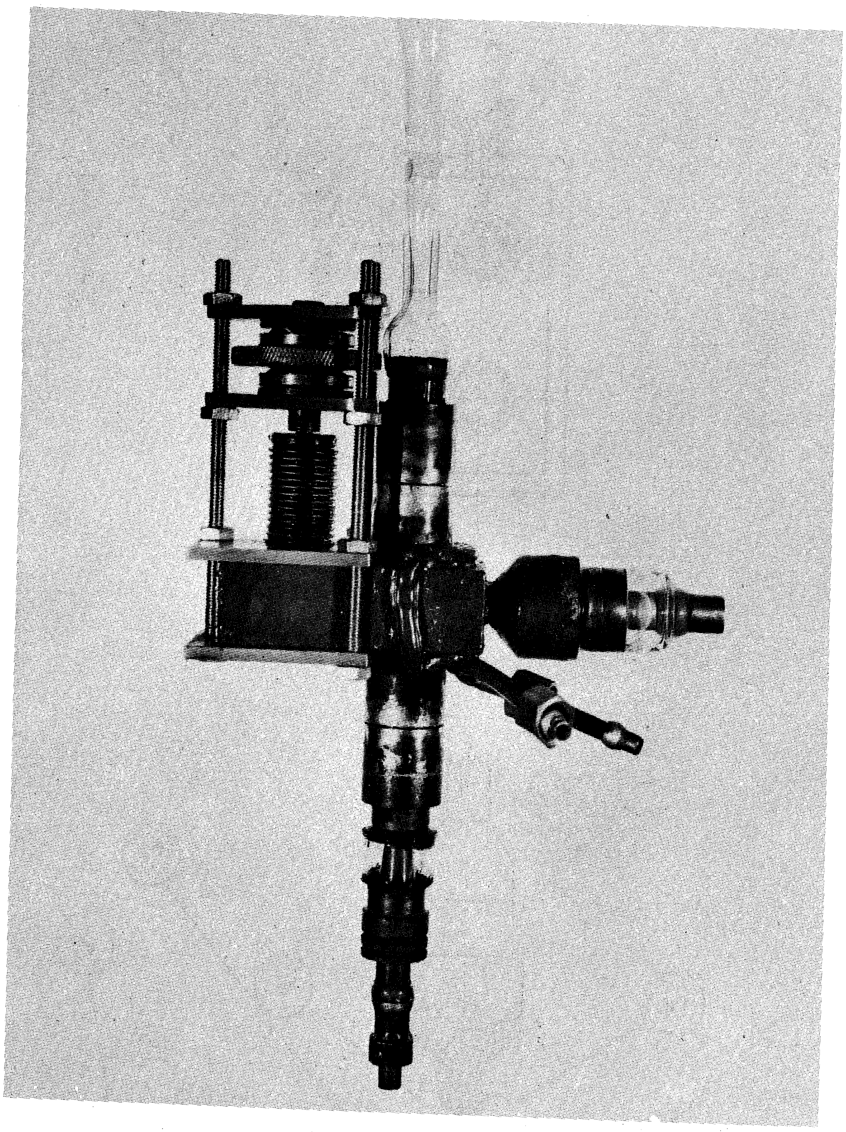

FIG. 3.3
PHOTOGRAPH OF MODEL 8C

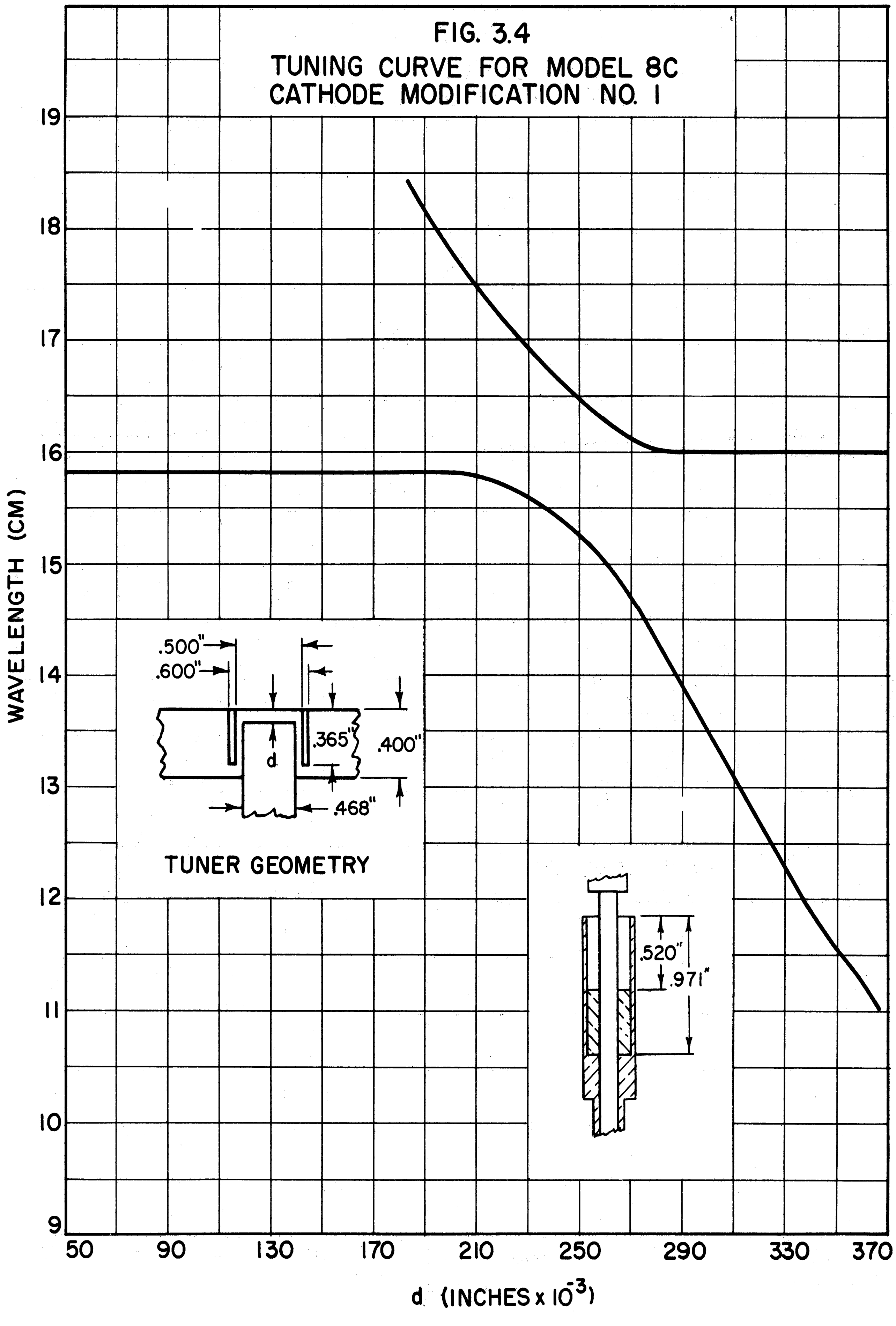
FIG. 3.4
TUNING CURVE FOR MODEL 8C
CATHODE MODIFICATION NO. 1
WAVELENGTH (CM)
19
18
17
16
15
14
13
12
11
10
9
50
90
130
170
210
250
290
330
370
d (INCHES x 10^{-3})
.500"
.600"
.365"
.400"
d
.468"
TUNER GEOMETRY
.520"
.971"

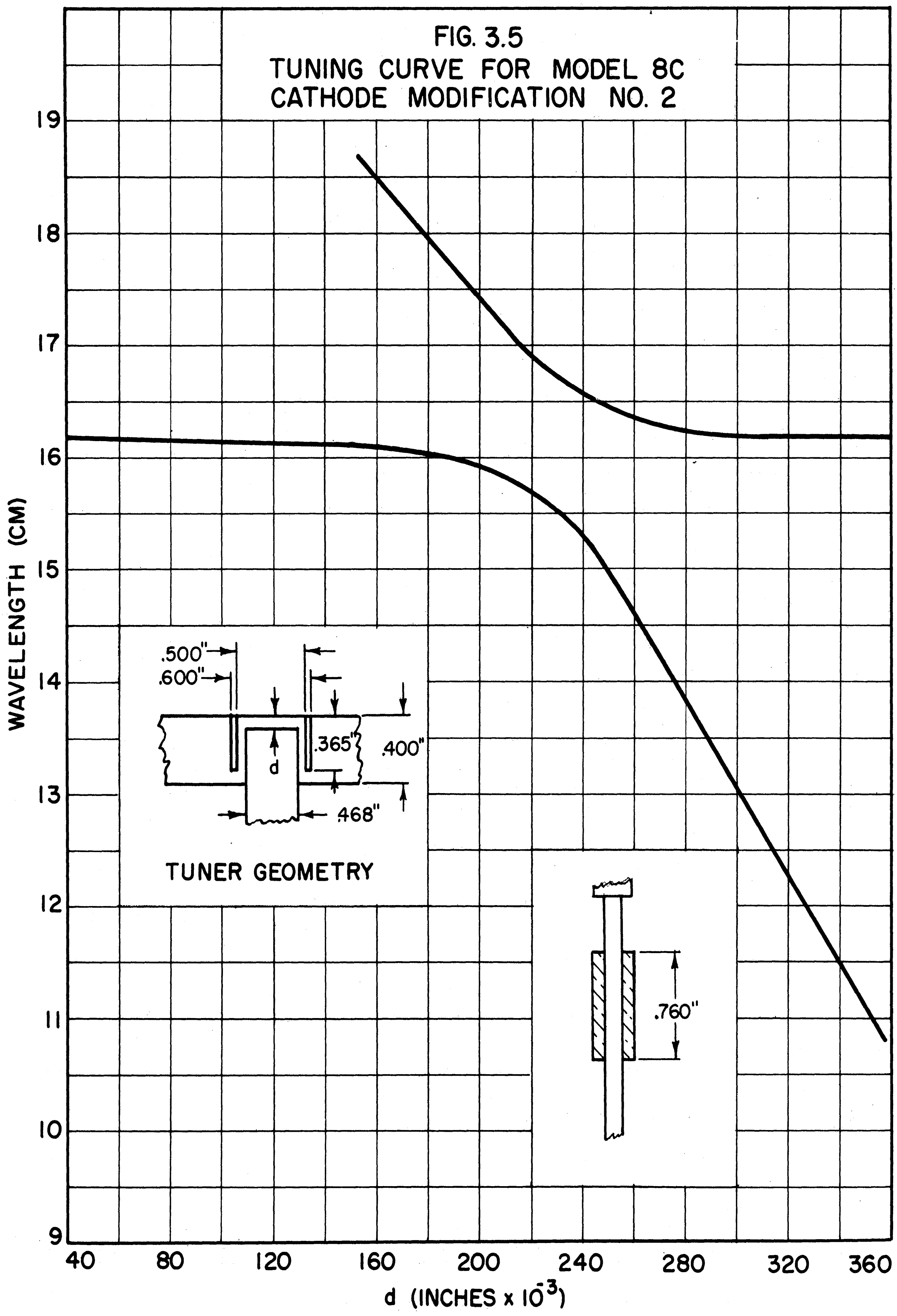
FIG. 3.5
TUNING CURVE FOR MODEL 8C
CATHODE MODIFICATION NO. 2
WAVELENGTH (CM)
19
18
17
16
15
14
13
12
11
10
9
40
80
120
160
200
240
280
320
360
d (INCHES x 10^{-3})
.500"
.600"
.365"
.400"
d
.468"
TUNER GEOMETRY
.760"

rectangular cavity employed with this tube.

A new tube Model 8D was then designed in an attempt to remove the parasitic resonances from the desired tuning range. A drawing and photograph of this tube appears in Figs. 3.6 and 3.7. Molybdenum wire anodes were employed to reduce the anode capacitance and to also reduce the coupling to the cathode line.

With the cathode removed the Model 8D cold tested to tune from 1550 to 2600 mc with no parasitic modes present in that range. However, with the tube operating hot two modes were present, neither of them being the desired tunable cavity mode. These modes appeared at 2900 mc and at 1660 mc. The high frequency mode is associated with the two full wavelength modes of the cavity while the low frequency mode is associated with the resonant circuit formed by the cathode line, the cathode chokes and the pole pieces.

The Model 8 program was discontinued in order to allow more time to be devoted to the development of voltage-tunable tubes.

It is felt that the method of mechanical tuning employed by the Model 8 structure is a promising technique for accomplishing wide tuning range magnetrons in the frequency range above 5000 mc and warrants further development at a later date.

4. Circuit Studies for the Model 9 Coaxial Voltage-Tunable Magnetron

(P. E. Dicker)

The lack of adequate sources of continuously tunable microwave frequency power has been one of the most serious obstacles encountered in microwave measurement techniques. The objective of the investigation de-

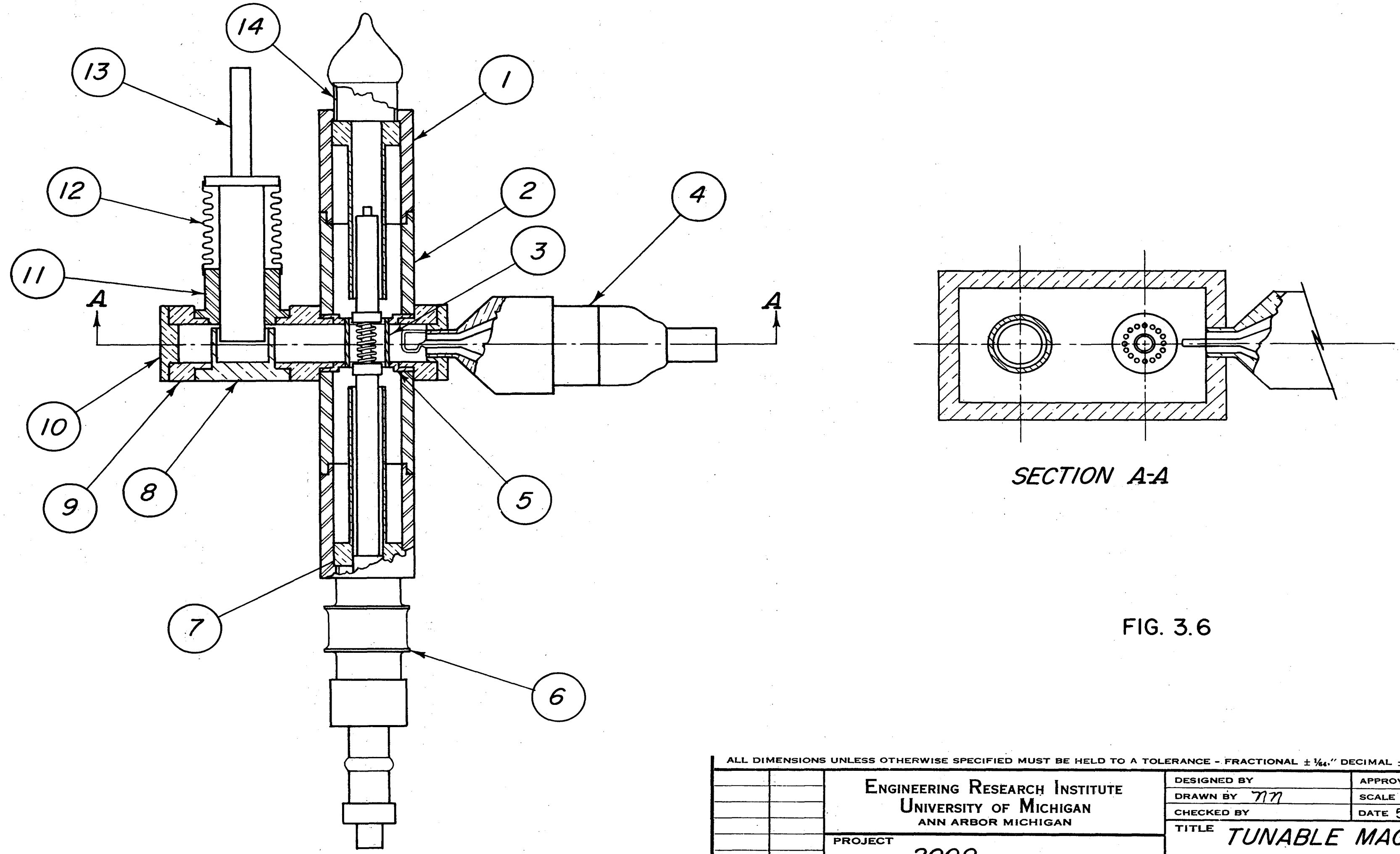

FIG. 3.6

ALL DIMENSIONS UNLESS OTHERWISE SPECIFIED MUST BE HELD TO A TOLERANCE - FRACTIONAL ± 1/64," DECIMAL ± .005," ANGULAR ± 1/2°

ENGINEERING RESEARCH INSTITUTE
UNIVERSITY OF MICHIGAN
ANN ARBOR MICHIGAN

PROJECT 2009

CLASSIFICATION

ISSUE | DATE

DESIGNED BY
DRAWN BY ՊՊ
CHECKED BY
APPROVED BY
SCALE FULL
DATE 5-16-52

TITLE TUNABLE MAGNETRON MODEL 8D

DWG. NO. B- 10,008D

DWG. NO. B

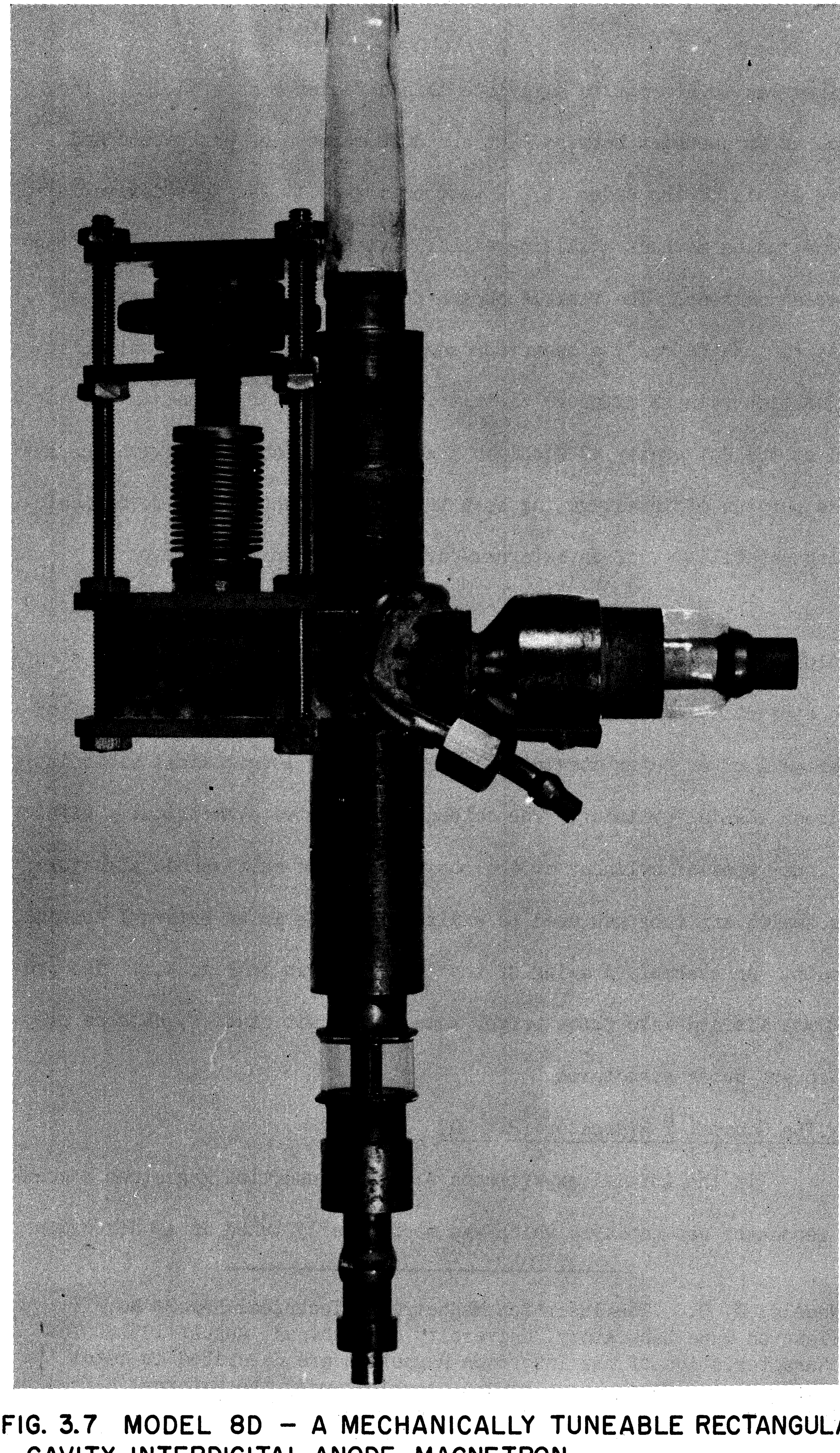

FIG. 3.7 MODEL 8D – A MECHANICALLY TUNEABLE RECTANGULAR CAVITY INTERDIGITAL ANODE MAGNETRON.

scribed was to attempt to alleviate this deficiency especially in the range of frequencies between 1500 and 3000 megacycles per second and power levels of the order of 1/2 watt or more. It was felt desirable to pursue tuning methods utilizing either mechanical or electrical (voltage-tunable) methods. The vehicle chosen for this investigation was the "Insertion Magnetron"; a magnetron designed for low power operation in conjunction with an external circuit[1]. The Insertion Magnetron was developed at the University of Michigan Electron Tube Laboratory with the express purpose of investigating both the voltage-tunable and mechanical tuning capabilities of an external-cavity magnetron oscillator.

The Model 9 magnetron consisted of a short hermetically-sealed section of coaxial transmission line which contained a multi-anode structure consisting of six equally-spaced vanes extending radially from the inner wall of an outer coaxial cylinder into six longitudinal slots in an inner coaxial cylinder. The cathode was located symmetrically within the inner coaxial cylinder at the position of the multi-anode structure. This sealed off tube was used to excit a TEM mode in an external coaxial circuit. An assembly drawing of the tube is shown in Fig. 4.1. The program was divided into three parts, namely: circuit studies, cathode properties and anode structures.

4.1 The Coaxial-T Resonator (High Q)

In the initial experiments with the Insertion Magnetron a coaxial resonator was employed which was mechanically tuned in a direction

1 Needle, J. S., "The Insertion Magnetron", Technical Report No. 11, Electron Tube Laboratory, University of Michigan, August 1951. The characteristics of the Insertion Magnetron are described in detail in this report. The present report describes only the external circuitry investigated and the results of this investigation.

coincident with the axis of the magnetron cathode. The coaxial configuration was severely limited in frequency range in view of the mechanical limitations imposed by the magnetic circuit requirements. To overcome these mechanical and magnetic circuit deficiencies, a circuit configuration which showed promise as a mechanically-tunable high Q structure for signal generator applications was designed. This coaxial-T resonator is shown in Fig. 4.2. The magnetron operating in conjunction with this high Q coaxial-T resonator was capable of being tuned from 375 to 2140 mc/sec.

Tuning curves for this magnetron and circuit arrangement are shown in Fig. 4.3. The upper wavelength limits indicated on the curves in this figure are not considered as boundaries of the operating range of this magnetron system. The upper wavelength of the high voltage mode may be increased beyond those shown in Fig. 4.3 by increasing the maximum length of the tuner stub. The upper wavelength shown for the low voltage mode in Fig. 4.3 was the longest wavelength which could be measured with the available measuring equipment. The power output over the tuning range varied within wide limits since the position of the coupling loop was fixed. The maximum c-w output was estimated to be of the order of one to three watts. Magnetic fields of the order of 1200 gausses were supplied by an electromagnet.

A packaged version of this oscillator built with two type QK 59-62 magnetron permanent magnets in parallel gave satisfactory mechanically tunable operation. The problems which arose in connection with the coaxial-T oscillator were (a) cathode back heating, which eventually caused instability of operation, and (b) the restriction of tuning speed by the mechanical structure of the tuning stub. Neither of these points

DWG. NO. B - 10,009 B

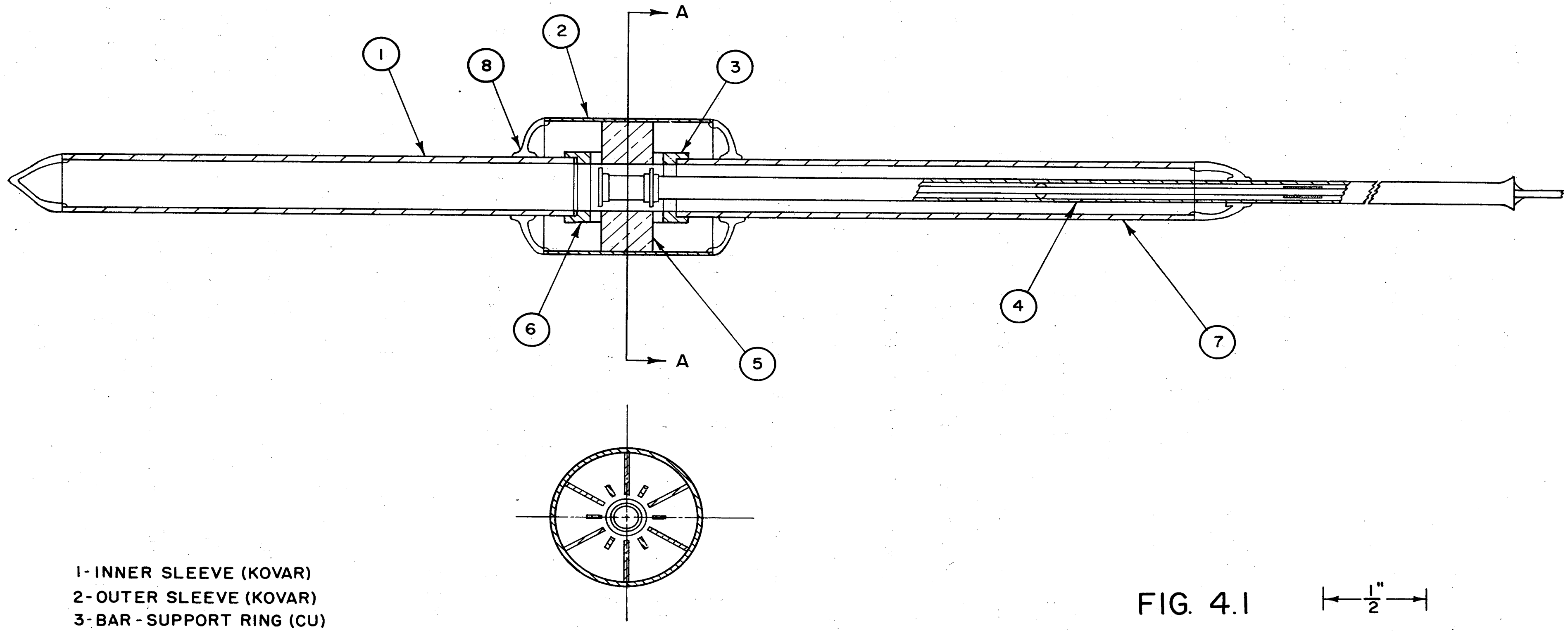

SECTION AA

FIG. 4.1

1"/2

1-INNER SLEEVE (KOVAR)
2-OUTER SLEEVE (KOVAR)
3-BAR-SUPPORT RING (CU)
4-CATHODE STEM (KOVAR)
5-VANE (CU)
6-BAR-SUPPORT RING (CU)
7-INNER SLEEVE (KOVAR)
8-GLASS SEAL

ALL DIMENSIONS UNLESS OTHERWISE SPECIFIED MUST BE HELD TO A TOLERANCE - FRACTIONAL ± 1/64," DECIMAL ± .005," ANGULAR ± 1/2°

ENGINEERING RESEARCH INSTITUTE
UNIVERSITY OF MICHIGAN
ANN ARBOR MICHIGAN

DESIGNED BY [illegible]	APPROVED BY
DRAWN BY [illegible]	SCALE 2X
CHECKED BY	DATE 1-22-51

PROJECT M-921

TITLE LOW-POWER MAGNETRON MODEL 9B

CLASSIFICATION

DWG. NO. B-10,009 B

ISSUE | DATE

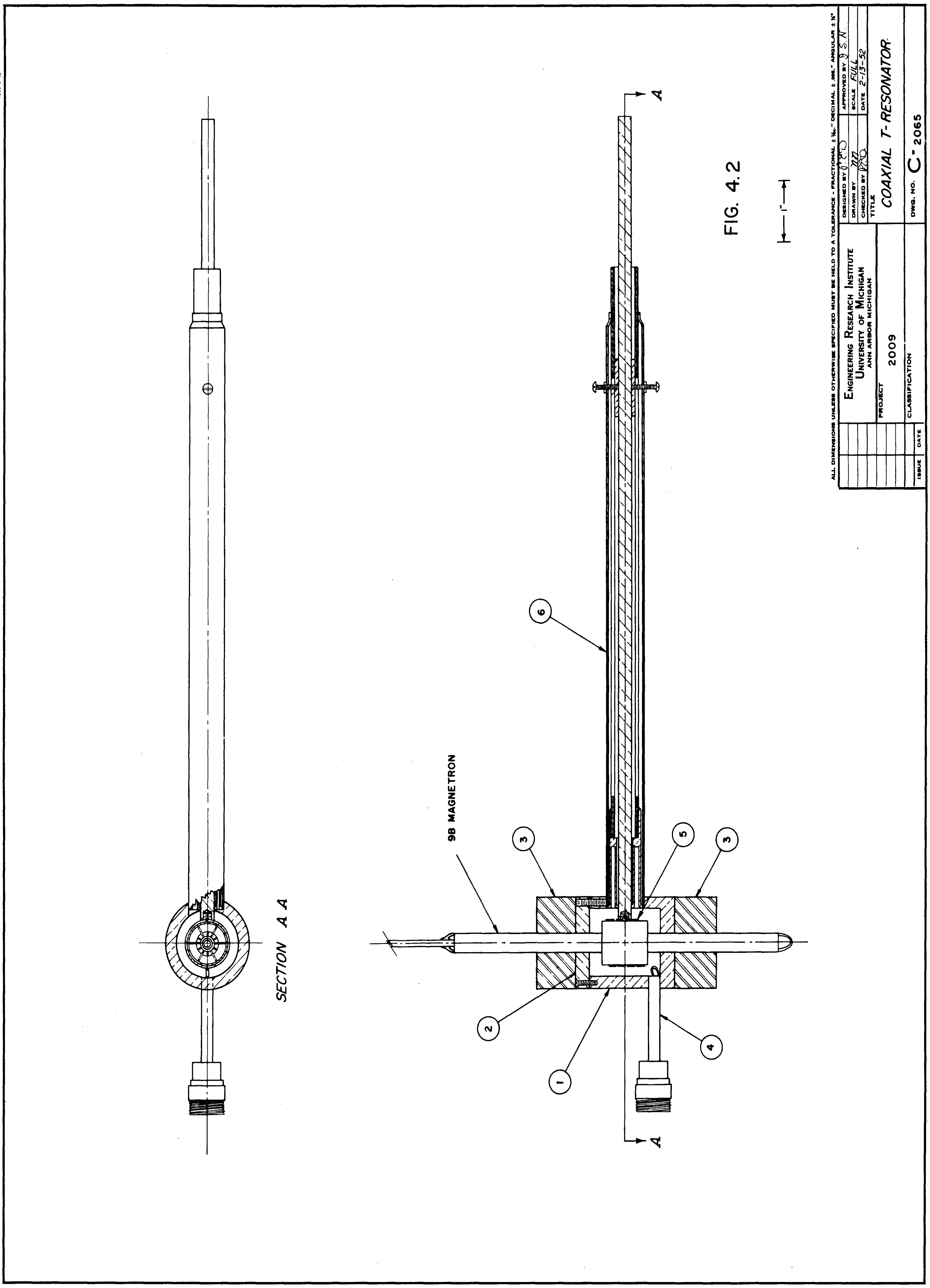

FIG. 4.2
9B MAGNETRON
SECTION A A
ENGINEERING RESEARCH INSTITUTE
UNIVERSITY OF MICHIGAN
ANN ARBOR MICHIGAN
PROJECT 2009
CLASSIFICATION
SCALE FULL
DATE 2-13-52
COAXIAL T-RESONATOR
DWG. NO. C-2065

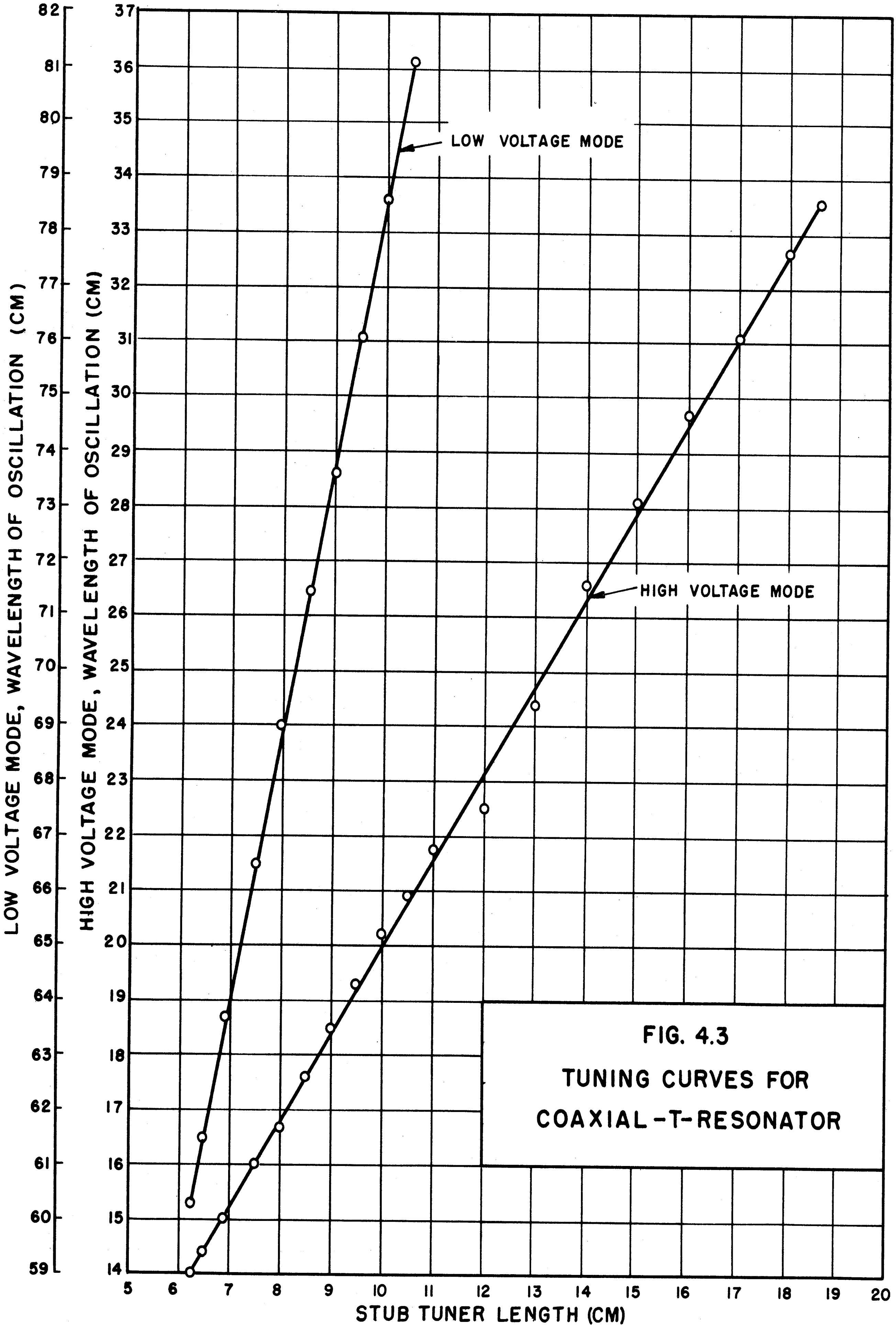

FIG. 4.3
TUNING CURVES FOR
COAXIAL-T-RESONATOR

was investigated fully enough to provide final solutions; however, attempts were made to attain faster tuning by employing a butterfly tuner in the tube cavity portion of this resonator. The results of the butterfly tuning method proved that the frequency shift was too small to be of interest and confirmed earlier indication that the tuning range covered by the "T" resonator is virtually independent of the coaxial cavity length and is primarily a function of the tuner stub length.

4.2. Coaxial-T Circuit (Low Q)

A second type of coaxial-T circuit shown in Fig. 4.4 was built primarily to determine the character of low Q voltage-tunable operation attainable with this design. The structure differs from the coaxial-T high Q oscillator only to the extent that it is more heavily loaded. One side of this low Q circuit feeds directly into a 50 ohm coaxial output terminal through a tapered coaxial line. This oscillator arrangement was found to be mechancially tunable from 375 to 3750 mc/sec with a maximum output of approximately one watt c-w over the tuning range. This direct dependence of frequency on tuner length indicates that the Q of the structure cannot be reduced to a low enough level for satisfactory voltage-tunable operation. In addition the magnetic circuit requirements are more difficult to satisfy than in the case of the high Q oscillator described above. The conclusions reached with regard to this structure are that (a) it does not satisfy the low Q conditions for voltage-tunable operation, and (b) it is not as good as the high Q structure when mechanical tuning is desired.

4.3. Ground Plane Resonator

The initial Electron Tube Laboratory investigation of the Insertion Magnetron resulted in the conclusion that, for voltage-tunable opera-

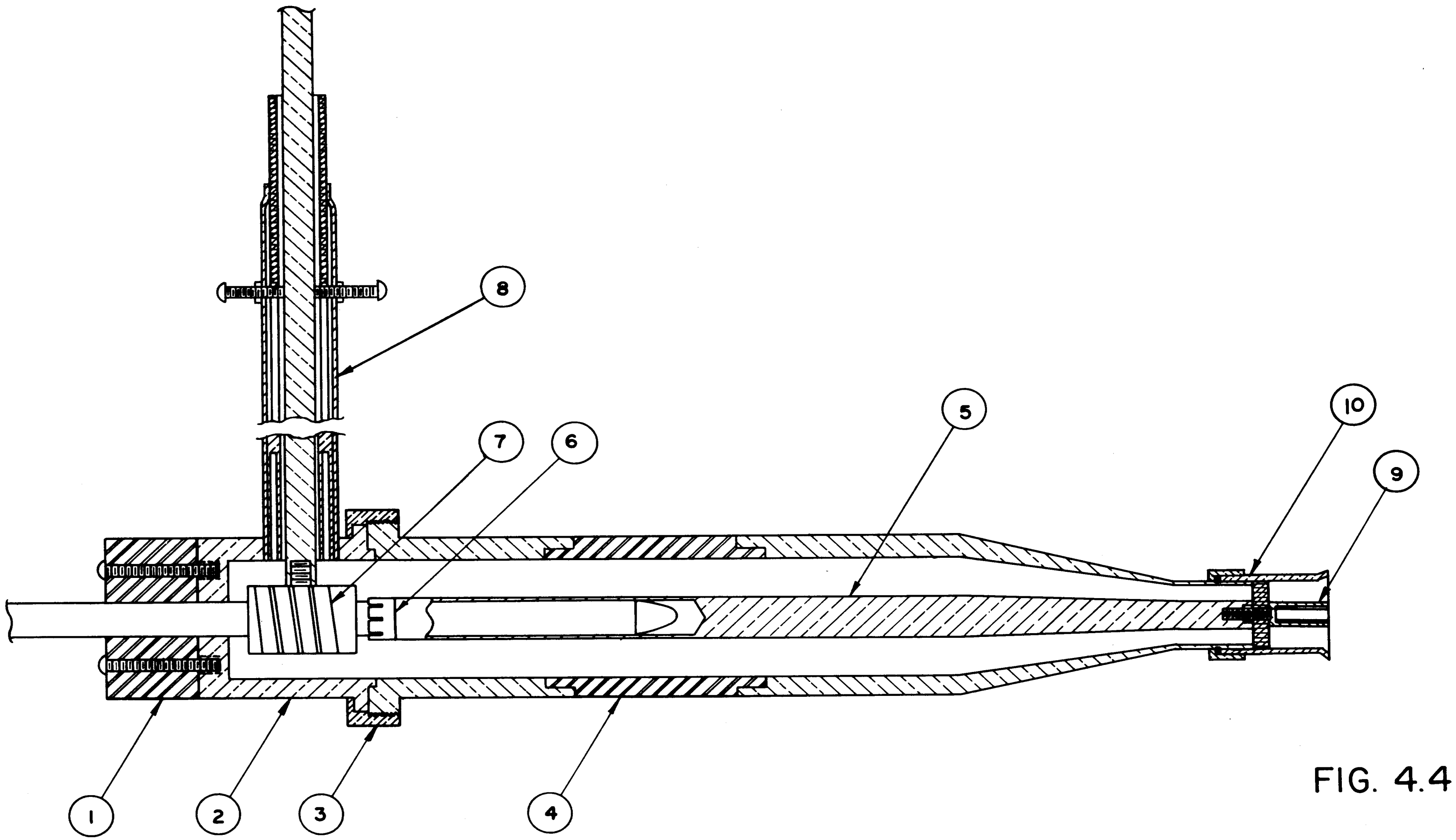

FIG. 4.4

ALL DIMENSIONS UNLESS OTHERWISE SPECIFIED MUST BE HELD TO A TOLERANCE - FRACTIONAL ± 1/64." DECIMAL ± .005," ANGULAR ± 1/2°

ENGINEERING RESEARCH INSTITUTE UNIVERSITY OF MICHIGAN ANN ARBOR MICHIGAN	DESIGNED BY PRD DRAWN BY PLW CHECKED BY	APPROVED BY SCALE FULL DATE 7-15-52	
PROJECT 2009	COAXIAL T-STUB TUNER #2 FOR MODEL 9B MAGNETRON		
ISSUE 1 / DATE 7-15-52 / CLASSIFICATION	DWG. NO. B- 2063		

DWG. NO. B

tion, it would be desirable to operate the tube into as high an impedance as possible and still maintain the low Q properties of the external circuit. This conclusion was based on the concept that the electrons in the low Q magnetron oscillator are bunched, mainly because of the electric field between adjacent anodes and that the r-f amplitude is, to a great extent, a function of the impedance between the magnetron anodes[1]. The circuits described below were designed with this concept in mind and represent a departure from the "usual" coaxial transmission line, whose practical upper limit of characteristic impedance is of the order of 75 ohms.

One of the structures investigated as an external cavity for the Insertion Magnetron was a "slab line" or "ground plane resonator". The development of this resonator was based on an article appearing in the March 1950, Proceedings of the I.R.E. entitled "A New Type of Slotted Line Section," by W. Bruce Wholey and W. Noel Eldred, p. 244. See also "Etched Sheets Serve as Microwave Components," by R. M. Barrett, June 1952, Electronics, pp. 114-118. The problem was one of obtaining a resonator system with a given characteristic impedance whose physical configuration would be compatible with the tube and would also be capable of being easily swept in frequency. A transmission line consisting of parallel planes seemed to have advantages and a conformal transformation was available for this development. The transformation used for mapping the coaxial line into the parallel plane line was $W = \tan Z$.

Using this transformation, and applying the resulting equations,

---

1 Welch, H. W., Jr., "Dynamic Frequency Characteristics of the Magnetron Space Charge; Frequency Pushing and Voltage Tuning", Technical Report No. 12, Electron Tube Laboratory, University of Michigan, November 1951.

one structure was made and tested. This structure is shown in Fig. 4.5. In this figure it is apparent that the Model 9B tube is centered in the parallel plane structure by means of parts (20) and (21). The kovar anode support ring is located in the cylindrical hole of the brass spacer (9). The two shorting slugs (7) and (8) are free to move and are used to tune the cavity. Power is coupled out through the loop (26).

Tests on the "Ground Plane Resonator" indicated that both mechanical and voltage tuning were feasible. The tube-and-cavity was operated both c-w and pulsed. The pulse was one of 15 microseconds duration and repetition rate of 60 pulses per second. The observed wavelengths of oscillation were at low voltages (order of 190-300 volts), and the wavelengths themselves were in the 60-80 cm range. This cavity may be swept over a narrow range by the insertion of a rotating member between the parallel plane side-walls in close proximity to the center conductor. The length of the transmission line between the insertion tube and the rotating disk "short" would then be a function of time.

This structure is bulky and heavy in its present form. It can be reduced in weight and somewhat in size. The magnetic field path can be shortened, thereby affording a reduction in the size and weight of the magnet used. However, the limitations are believed to outweigh the advantages for any application other than laboratory use.

4.4. Waveguide Circuits

It was felt desirable to attempt to operate the Insertion Magnetron into a waveguide transmission system. One of the waveguide circuits employed in this connection is shown in Fig. 4.6. The magnetron is used to excite the TE_{01} mode in a section of S-band waveguide. Here the axis

DWG. NO. C

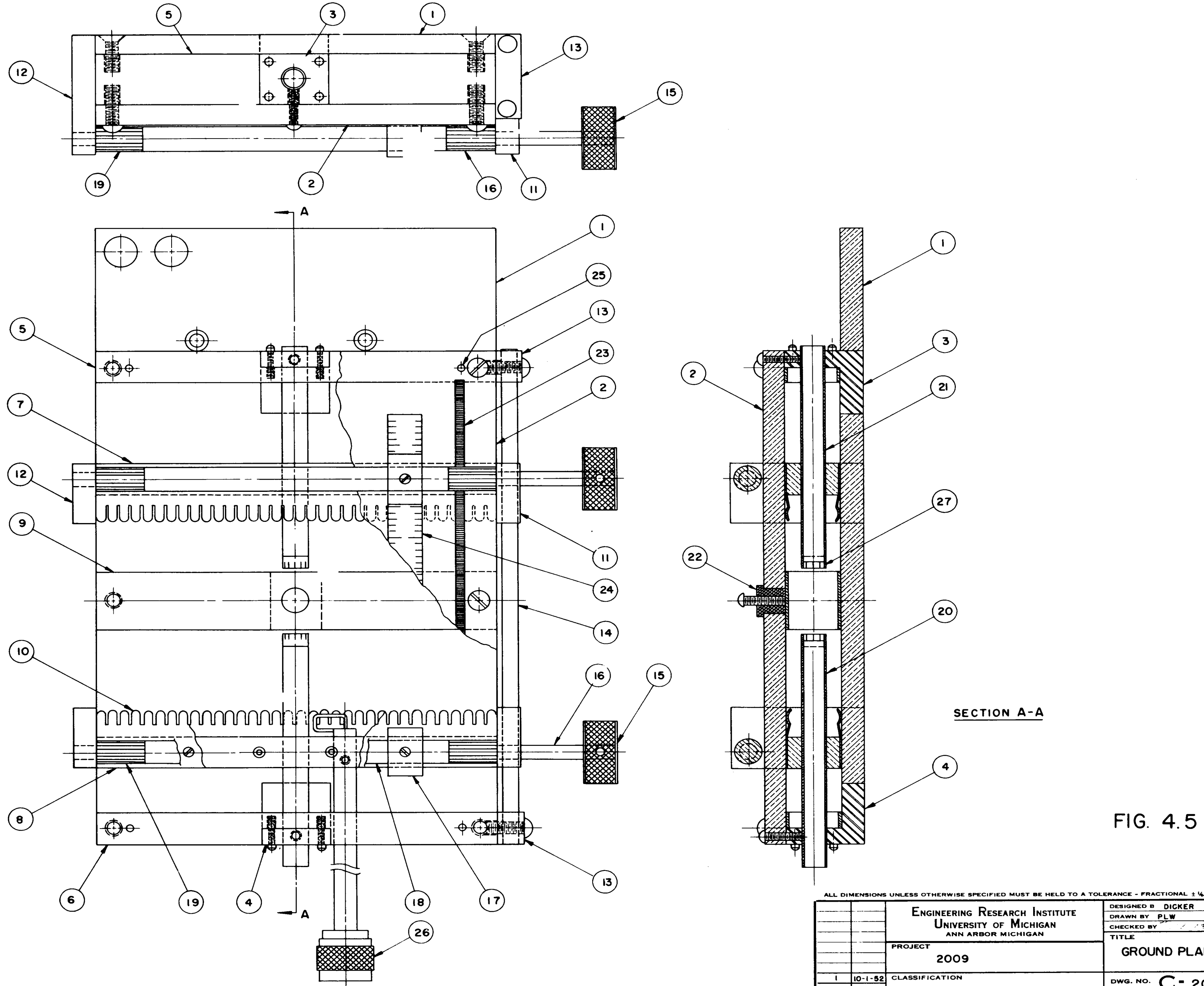

FIG. 4.5

ALL DIMENSIONS UNLESS OTHERWISE SPECIFIED MUST BE HELD TO A TOLERANCE - FRACTIONAL ± 1/64" DECIMAL ± .005" ANGULAR ± 1/2°

ENGINEERING RESEARCH INSTITUTE UNIVERSITY OF MICHIGAN ANN ARBOR MICHIGAN		DESIGNED B DICKER	APPROVED BY	
		DRAWN BY PLW	SCALE FULL	
		CHECKED BY	DATE OCTOBER 1, 1952	
PROJECT 2009		TITLE GROUND PLANE RESONATOR		
ISSUE 1	DATE 10-1-52	CLASSIFICATION	DWG. NO. C- 2072	

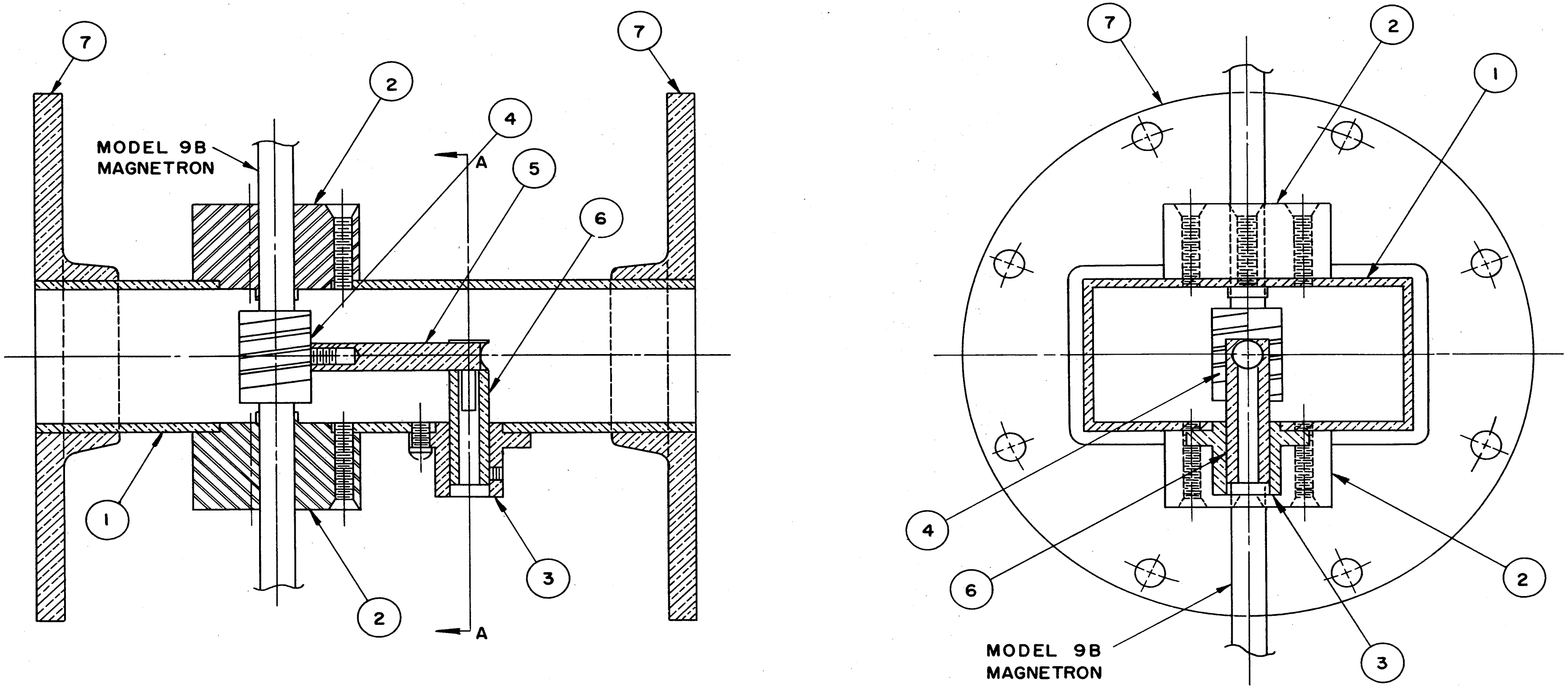

FIG. 4.6

ALL DIMENSIONS UNLESS OTHERWISE SPECIFIED MUST BE HELD TO A TOLERANCE - FRACTIONAL ± 1/64," DECIMAL ± .005," ANGULAR ± 1/2°

ENGINEERING RESEARCH INSTITUTE UNIVERSITY OF MICHIGAN ANN ARBOR MICHIGAN	DESIGNED BY P.E.D DRAWN BY PLW CHECKED BY VRB	APPROVED BY SCALE FULL DATE 7-10-52	
PROJECT 2009	TITLE TUBE TO WAVE-GUIDE ADAPTOR – FOR MODEL 9B MAGNETRON		
ISSUE 1 DATE 7-10-52	CLASSIFICATION	DWG. NO. B-2062	

of the tube is in the same direction as the TE_{01} electric field in the guide. An L-shaped loop which is joined to the vane anode ring of the magnetron at one end and to the larger guide wall at the other end is so oriented so as to excite the TE_{01} mode in the waveguide. Operation as a mechanically tunable oscillator was obtained by terminating one end of the waveguide in a matched load and tuning the opposite end with a non-contacting shorting plunger. It was possible in this way to tune the structure mechanically over a frequency range from 3000 to 4800 mc/sec. The size of the L-shaped loop to a great extent determines both the coupling into the waveguide and the upper frequency limit of operation. This type of transmission system is definitely better than any mechanically tuned coaxial system, especially at high frequencies. It can be packaged easily and has possibilities insofar as both low Q and rapid mechanical scanning are concerned.

Another waveguide circuit structure for operation with the Model 9 Insertion Magnetron is shown in Fig. 4.7. This circuit consists of a section of S-band waveguide and a cylindrical rod which is located on the longitudinal axis of the waveguide. It should be apparent from this figure that the magnetron will be coupled to a load through this modified ground-plane coaxial transmission line. The center conductor of the transmission line is attached to the vane anodes of magnetron and the bar anodes are connected to the waveguide.

The characteristic impedance of this ground-plane type of coaxial transmission line can conveniently be made as high as 150 ohms. In addition to providing a higher characteristic impedance than is practical with a concentric cylinder line, higher magnetic fields are more easily

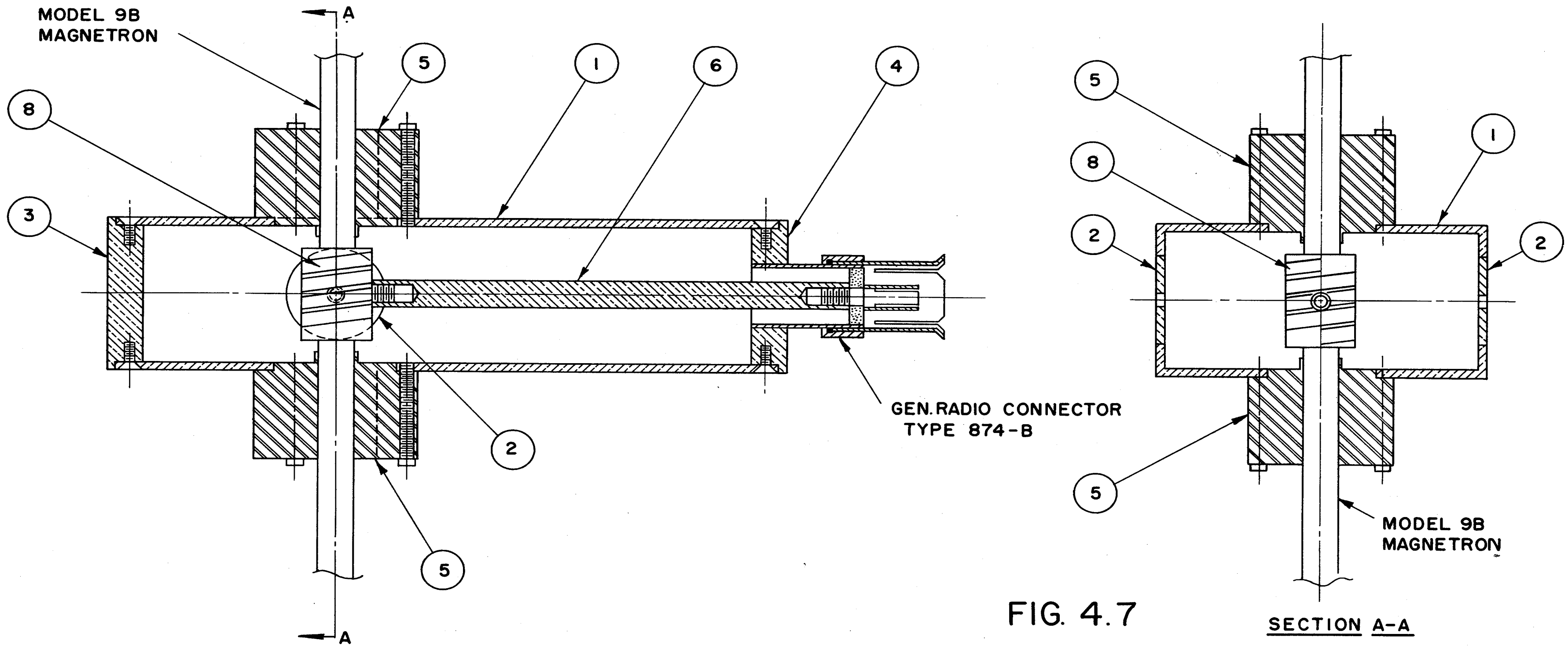

FIG. 4.7

NOTE –
PARTS -6 AND -7 ARE USED ALTERNATELY
-3 AND -4 ARE THEN REVERSED

ALL DIMENSIONS UNLESS OTHERWISE SPECIFIED MUST BE HELD TO A TOLERANCE - FRACTIONAL ± 1/64." DECIMAL ± .005." ANGULAR ± 1/2°

ENGINEERING RESEARCH INSTITUTE
UNIVERSITY OF MICHIGAN
ANN ARBOR MICHIGAN

DESIGNED BY JW	APPROVED BY
DRAWN BY PLW	SCALE FULL
CHECKED BY VRB	DATE 7-31-52

PROJECT 2009

TITLE GROUND-PLANE CO-AXIAL OUTPUT SYSTEM

ISSUE	DATE
1	7-31-52

CLASSIFICATION

DWG. NO. B-2069

obtainable with this circuit arrangement.

A limited amount of testing was carried out with this circuit and tube arrangement. The results of these limited tests indicate that higher power output can be obtained with this structure than with a coaxial system of practical dimensions; however, the bandwidth of this structure is smaller than the low Q coaxial circuits used to date.

4.5. Anode Structures

Some new anode structures were developed for the Model 9 series of tubes. These are shown in Fig. 4.8. Their advantage over the original 9B anode structure lay in the fact that they are easier to construct and they permitted the application of separate voltages to the bars. The effect of a differential potential applied between the two halves of the bar anodes could then be made. Two tubes were constructed with this anode geometry and operated in the "T" resonator described in Section 4.1. The tubes operated in the low voltage mode continuously from 375 to 790 mc with the lower limit set only by measuring equipment. Variation of the second anode voltage over a range 0-400 volts caused some frequency pushing. The signal was strong and appeared to be more stable than previously observed with other Model 9B tubes.

5. High Power Coaxial Voltage-Tunable Magnetron (Model 10) (G. E. Dombrowski)

An effort was made to obtain the voltage-tuned operation of the Model 9 design on a higher-power basis. The design of this version, Model 10, was therefore similar to that of Model 9, with modification to permit greater anode heat dissipation.

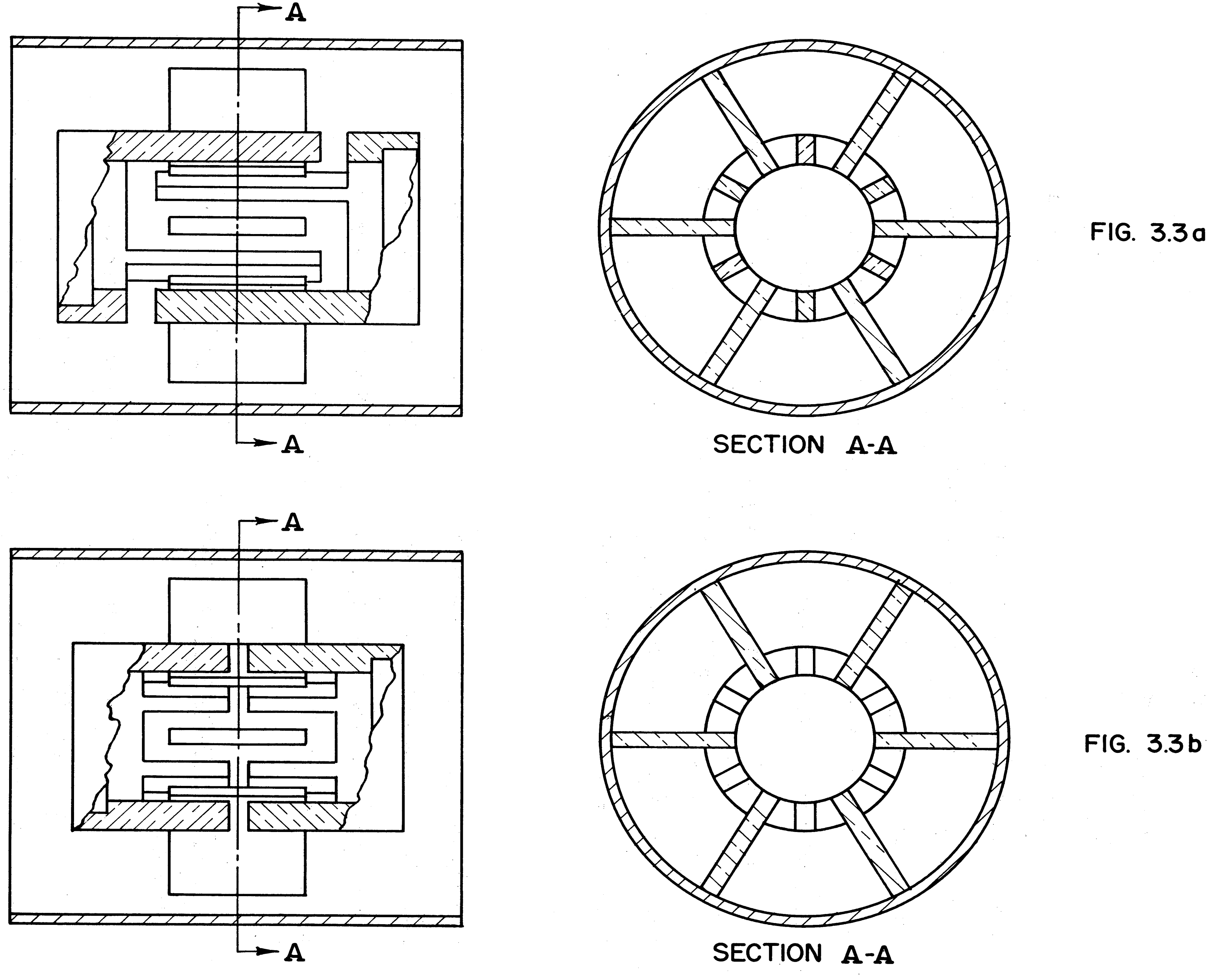

FIG. 4.8 MODIFIED MODEL 9B BAR-AND-VANE GEOMETRIES

Interaction-space design parameters are:

$$r_a = .45 \text{ cm}$$

$$r_c = .27 \text{ cm}$$

$$r_c/r_a = .60$$

$$N = 12 \text{ (6 bars and 6 vanes)}$$

π mode number, $n = 6$

frequency = 3000 mc

$$E_o = 540 \text{ volts}$$

$$B_o = 554 \text{ gausses}$$

The Model 10 magnetron is shown in the photograph, Fig. 5.1 and in the drawing, Fig. 5.2. The bars and vanes form part of a 52.3 ohm coaxial line. This line is short-circuited near one end of the interaction space; it is continued external to the glass seal on the other end.

This tube was first operated on a pulsed basis with the coaxial line terminated with a short circuit (high Q). A frequency range of 2000-2300 mc was covered in the resonance modes of the coaxial line. Mechanically tuned high power could be thus obtained. The magnetron also oscillated in the conventional 6-vane magnetron mode at fixed frequency.

The Model 10 magnetron was connected to a matched waterload for voltage-tuned operation, again on a pulsed basis. The frequency range 1900-2800 mc was tuned by voltage variation from 1500 to 3000 volts. Both anode current and r-f power were quite small; operation was critically dependent upon filament temperature. In an attempt to obtain measurable results on a c-w basis, the tube failed. Although this magnetron was repaired, no further data were taken. Effort was directed toward the more promising Model 11, described below.

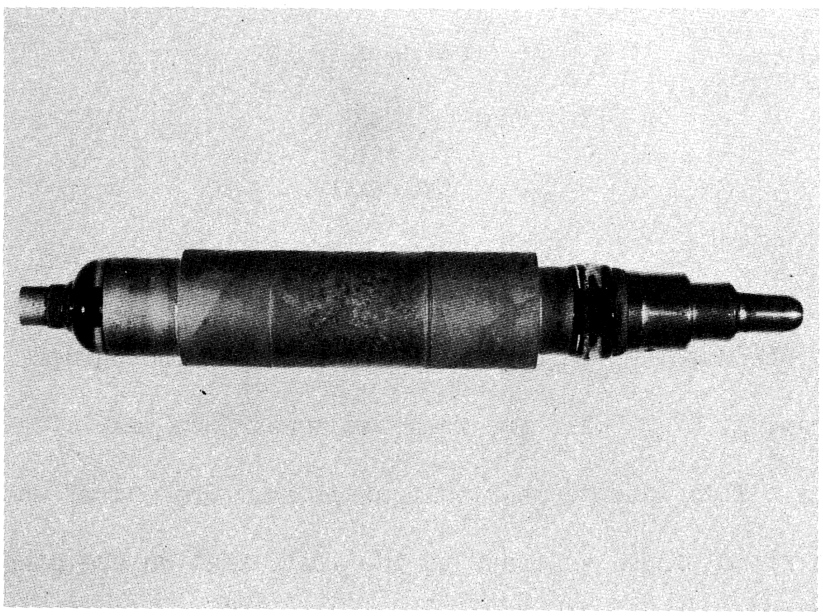

FIG. 5.1

PHOTOGRAPH OF MODEL 10 MAGNETRON

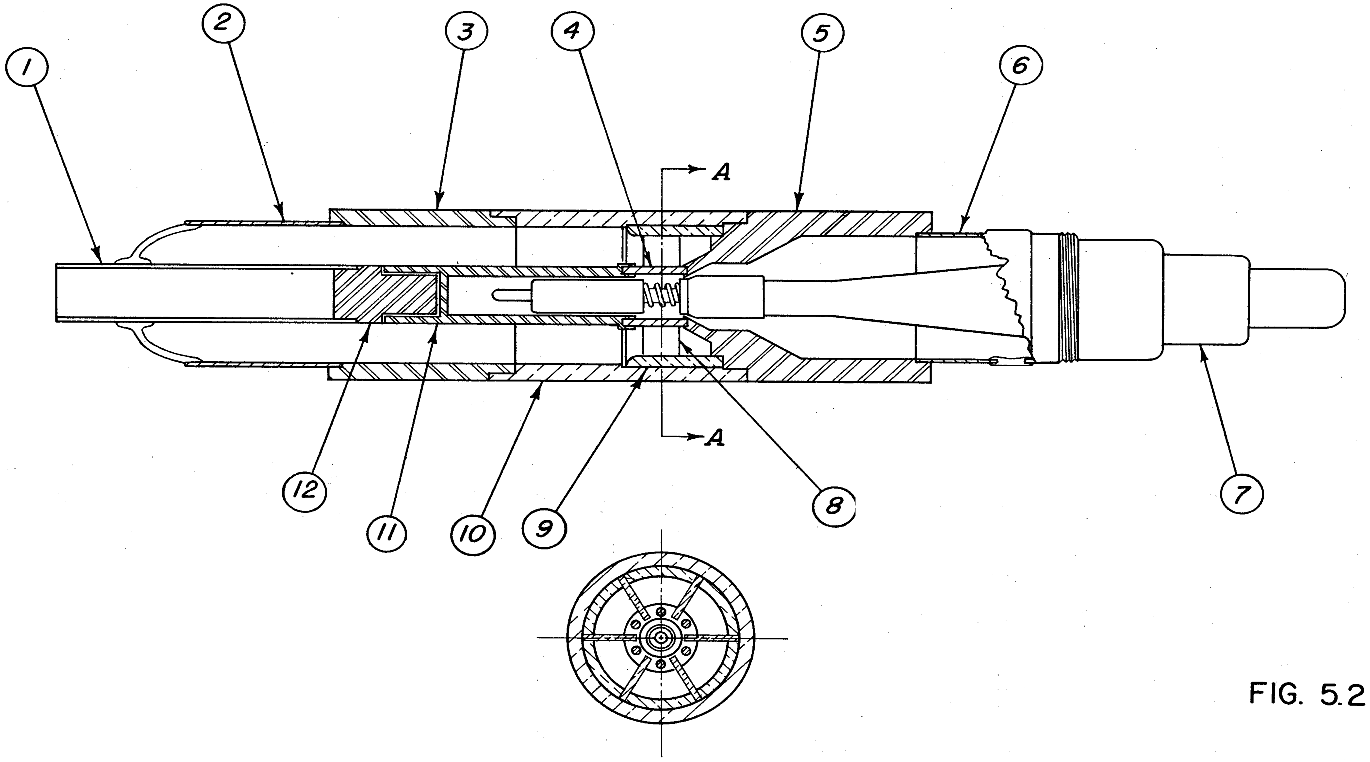

SECTION A-A

FIG. 5.2

1"

ALL DIMENSIONS UNLESS OTHERWISE SPECIFIED MUST BE HELD TO A TOLERANCE - FRACTIONAL ± 1/64," DECIMAL ± .005," ANGULAR ± 1/2°

ENGINEERING RESEARCH INSTITUTE
UNIVERSITY OF MICHIGAN
ANN ARBOR MICHIGAN

DESIGNED BY J.S.N — APPROVED BY J.S.N.
DRAWN BY nn — SCALE FULL
CHECKED BY J.S.N. — DATE 2-22-52

PROJECT 2009

TITLE COAXIAL VOLTAGE TUNABLE MAGNETRON MODEL 10

CLASSIFICATION

DWG. NO. B-10,010

ISSUE | DATE

6. Model 11, 11A, and 11B Interdigital Anode Voltage-Tunable Magnetrons Operating in the S-Band Region (J. A. Boyd)

This section summarizes the results of an effort to design and develop a voltage-tunable magnetron. The emphasis in this program was to obtain a tube which would be useful as a local oscillator and as a signal generator in many of the applications where electronically tunable r-f power is needed. A report presenting the results in detail has been issued[1]. What follows is essentially a summary of this report.

6.1. Design of the Model 11 Magnetron and Associated Cavity Structure.

In the design of this magnetron (designated the Model 11) and its associated cavity, two factors were considered essential if a satisfactory voltage-tunable magnetron was to be developed. These factors were:

a) Low anode-to-anode capacitance;

b) A high-impedance external cavity, the impedance being a slowly varying function of frequency. By high impedance, we mean in the order of 150 ohms.

The low anode-to-anode capacitance is necessary because this capacitance is in parallel with the external circuit and must be driven by the magnetron. The high over-all impedance is necessary if significant power output is to be obtained, since the induced current in the external circuit is proportional to the total d-c anode current, and the d-c anode current is limited (for voltage-tunable operation) by the temperature conditions under which the cathode must be operated. Since significant r-f fields

---

1 Boyd, J. A., "A voltage-Tunable Magnetron for operation in the Frequency Range 1500 to 3000 Megacycles", Technical Report No. 15, University of Michigan Electron Tube Laboratory.

are required to produce effective bunching, the small induced current obtainable in the external circuit requires that a high impedance be an essential design objective of the circuit.

For a low anode-to-anode capacitance it is desirable to have the anode bars as short as possible and still maintain the necessary length of interaction space. However, if the interdigital tube is to be mounted in a manner similar to that shown in Fig. 6.1, the circuit impedance will be reduced as the space between anode supports is reduced, since the characteristic impedance of a waveguide is directly proportional to its height.

The ridge waveguide offers a possibility for increasing the circuit impedance over that of a rectangular waveguide for a given spacing between anode supports. The ridge waveguide is characterized by its lowered cutoff frequency and lowered impedance (compared with a rectangular guide of equal dimensions), and by a wide bandwidth free from higher-mode interference.

A section of standard S-band waveguide, which has inside dimensions of 1.34 x 2.84 inches, was used. A single-ridge waveguide was used because of its mechanical simplicity.

Since it is desirable to have a coaxial output from the magnetron a tapered-ridge waveguide-to-coaxial-line junction was used to terminate each end of the ridge waveguide. This arrangement is shown in Fig. 6.1. These junctions have an upper cutoff frequency of approximately 4800 mc, therefore when used in conjunction with a ridge wavguide with a lower cutoff frequency of 1250 mc, give a very wide-band structure. The impedance which this circuit presents to the magnetron is, to a very

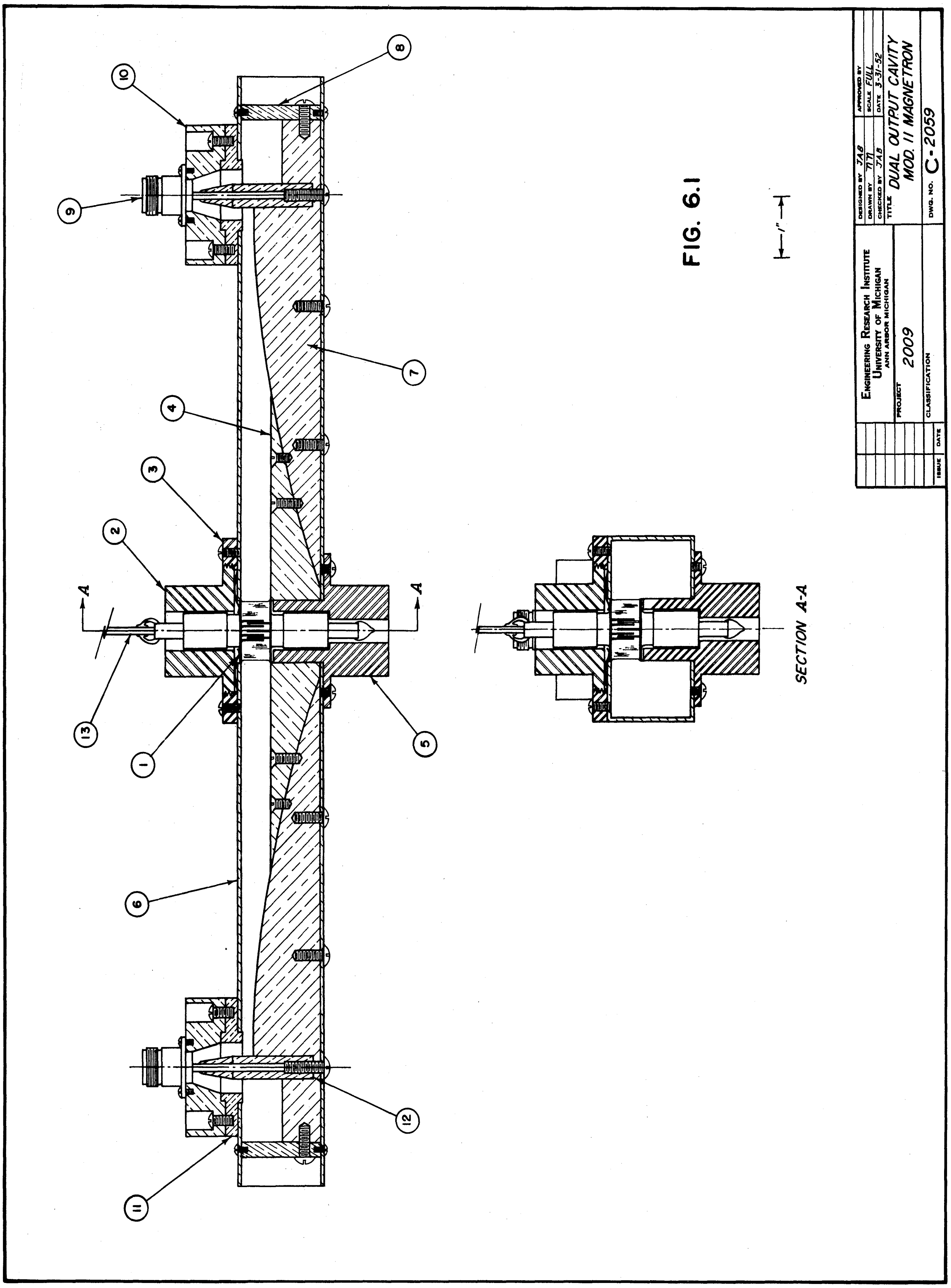
A
A
SECTION A-A
ENGINEERING RESEARCH INSTITUTE
UNIVERSITY OF MICHIGAN
ANN ARBOR MICHIGAN
PROJECT 2009
CLASSIFICATION
DESIGNED BY JAB
CHECKED BY JAB
SCALE FULL
DATE 3-31-52
TITLE DUAL OUTPUT CAVITY MOD. II MAGNETRON
DWG. NO. C-2059
ISSUE
DATE

FIG. 6.1

large extent, determined by the termination used on the coaxial output terminals. Theoretically, this impedance would be a pure resistance whose magnitude is given by

$$Z_o = \frac{Z_\infty}{\sqrt{1 - \left(\frac{f_c^{1}}{f}\right)^2}} \tag{6.1}$$

where in this case Z_∞ = 160

f_c^{1} = cutoff frequency of ridge waveguide

f = operating frequency

when the coaxial output terminals are terminated in their characteristic impedances. This type of cavity has two outputs, which makes it necessary to dissipate 50 percent of the power in a line termination.

The values of the parameters which resulted from the design of the interaction space are given below.

f = 3000 mc (chosen to suit available test equipment)

P_i = 50 watts

I_b = .050 amperes (required to satisfy the maximum power demand at an anode voltage of 1000 volts)

N = 12 (number of anode bars, based on existing magnetrons)

r_c/r_a = 0.6 (ratio of cathode to anode radii, based on existing magnetrons)

r_a = .233 inch (determined by size of molybdenum rod available, and anode radius of existing magnetrons)

L_c = .150 inch (length of emitting surface on cathode required to satisfy maximum power requirements with a safety factor of two)

ℓ_s = .290 inch (overlap length of anode bars; chosen to allow for length of emitting portion of cathode and end hats)

E_o = 250 volts

B_o = 550 gauss

C_p = $.9 \mu\mu$ f (anode-to-anode capacitance, no cathode present)

Figure 6.2 is a drawing of a Model 11 magnetron with an oxide cathode in place.

6.2 Experimental Results. Considerable data on the operation of the various forms of the Model 11 tube, (Model 11, 11A, and 11B) were obtained and in this section typical results are presented. A total of thirty-one tubes were studied in this investigation, in this section data is presented from four of these tubes. The data have been selected so that each tube reported on represents a significant step in the research program.

The results of experimental tests on the Model 11 tubes are presented first. This was the first model to be constructed and the results of the tests were in general quite satisfactory. Measurement techniques were designed and perfected during the testing of these Model 11 tubes. The Model 11B magnetron was designed in an attempt to improve the efficiency of the Model 11 tubes. Data are presented which indicate the improvement in operating characteristics of the Model 11B over the Model 11. Tungsten cathodes were used in all Model 11B tubes. The Model 11A tube was designed to allow comparison of the operating characteristics of two similar magnetrons, one having round anode bars and the other square anode bars.

Figure 6.3 shows a photograph of a tube and its various parts. In this investigation, the local oscillator application of the tube has been emphasized; therefore, most of the data presented below have resulted

DWG. NO. B

DWG. NO. B

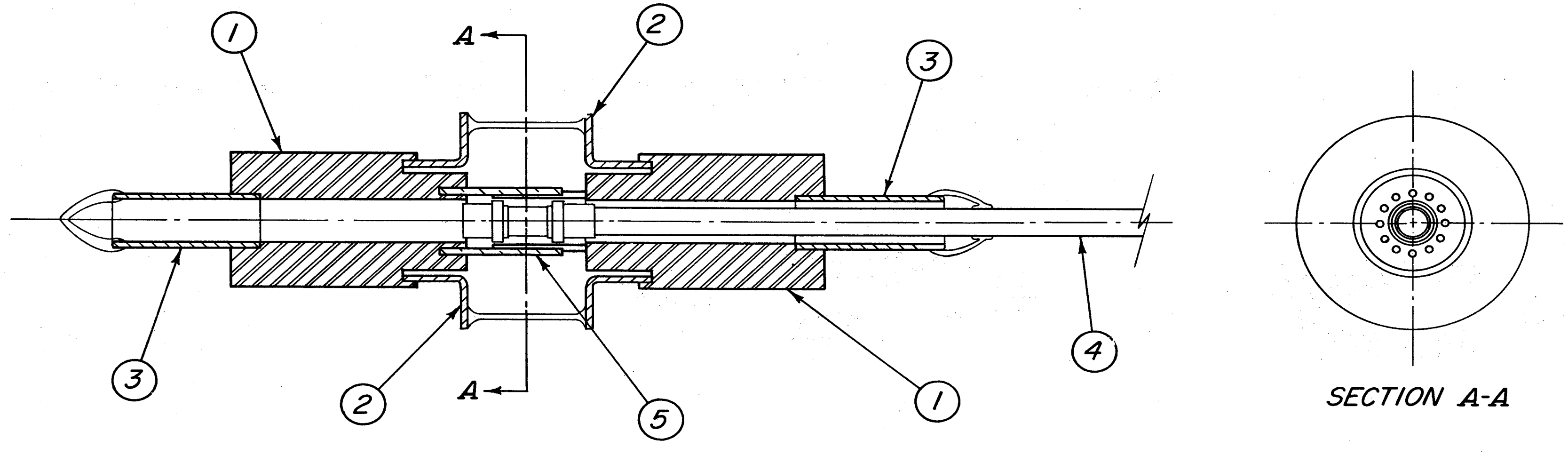

FIG. 6.2

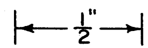

ALL DIMENSIONS UNLESS OTHERWISE SPECIFIED MUST BE HELD TO A TOLERANCE - FRACTIONAL ± 1/64" DECIMAL ± .005" ANGULAR ± 1/2°

ENGINEERING RESEARCH INSTITUTE
UNIVERSITY OF MICHIGAN
ANN ARBOR MICHIGAN

DESIGNED BY JAB | APPROVED BY
DRAWN BY MM | SCALE X2
CHECKED BY JAB | DATE 3-27-52

PROJECT 2009

TITLE INTERDIGITAL EXTERNAL CAVITY MAGNETRON MOD. II

CLASSIFICATION

ISSUE | DATE

DWG. NO. B- 10,011

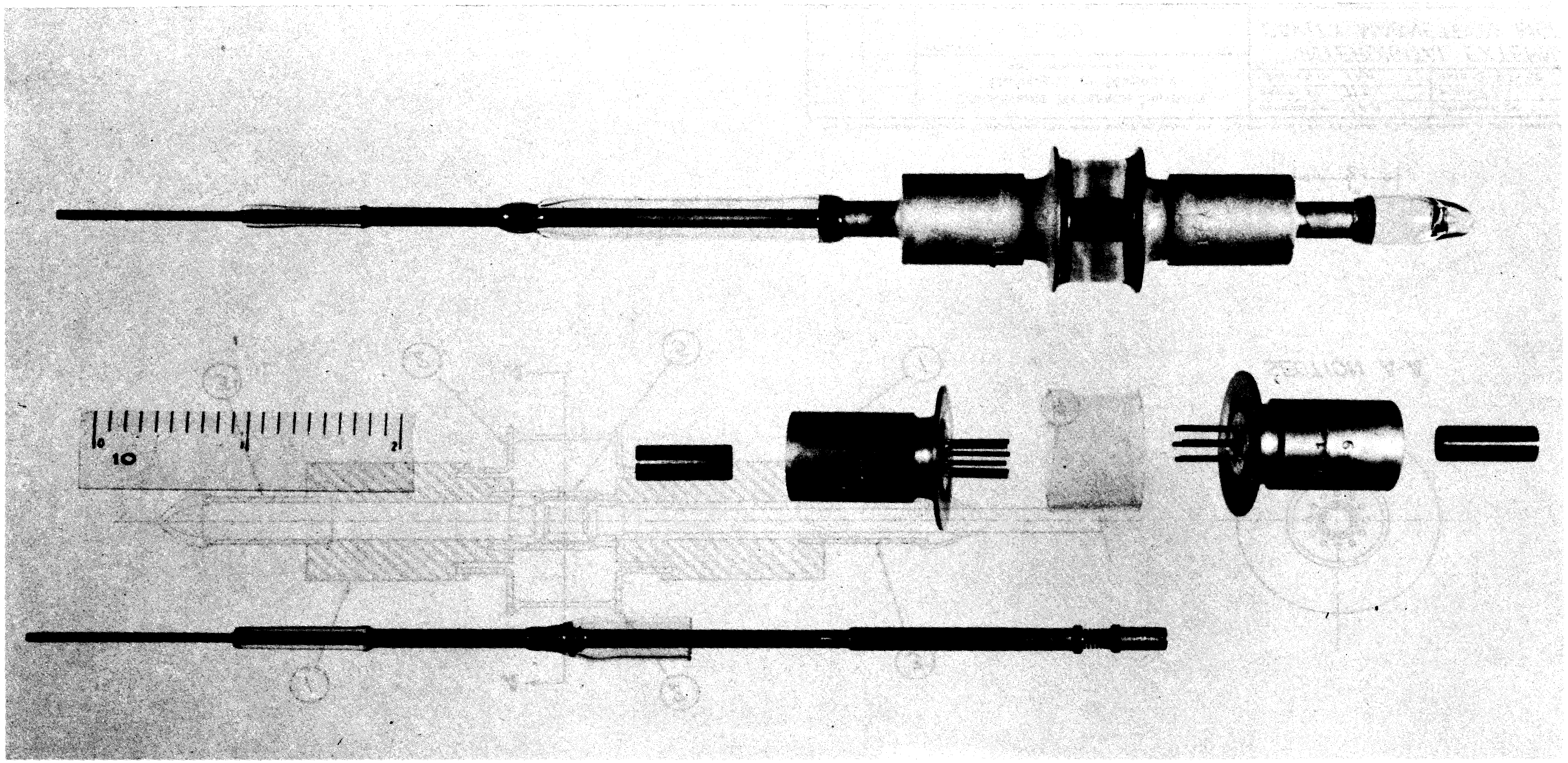

SCALE: INCHES

FIG. 6.3

PHOTOGRAPH OF MODEL II MAGNETRON

from measurements made under c-w conditions.

6.2.1 Model 11, No. 74. The first tube completed was the Model 11, No. 74. This tube used an oxide-coated cathode. Under pulsed operation, the tube was voltage-tunable from 2060 to 2750 mc. A schematic diagram of the test equipment used in these tests is shown in Fig. 6.4. As indicated there it is possible to observe either the volt-ampere characteristic of the tube, or to observe the output of the wavemeter as a function of the anode voltage. Thus by tuning the wavemeter and observing a continuous output over a wide voltage range, it was determined that the tube was operating over the frequency range of 2060 to 2750 mc. The cathode temperature was critical but could be adjusted for stable operation. The cathode temperature affects not only the stability of operation but also the frequency of oscillation. An increase in cathode temperature causes a decrease in the frequency of oscillation. An external choke was used on the cathode support while making these tests. It was impossible to test this tube under c-w conditions due to the back-heating of the cathode. Once the tube started to oscillate, the back-heating was sufficient to prevent the adjustment of the cathode temperature for voltage-tunable operation. There was a very narrow cathode temperature range in which the tube produced a coherent signal. The tube was operated with a magnetic field of 2625 gauss and a filament current of 1.25 amperes.

6.2.2 Model 11, No. 80. Results of the tests on the Model 11, No. 74, indicated a need for a change in the design of the cathode if c-w operation was to be obtained. In an attempt to satisfy this need, the No. 80 tube was built, using a thoriated tungsten cathode which was not carburized. In order to determine the feasibility of using this tube as a

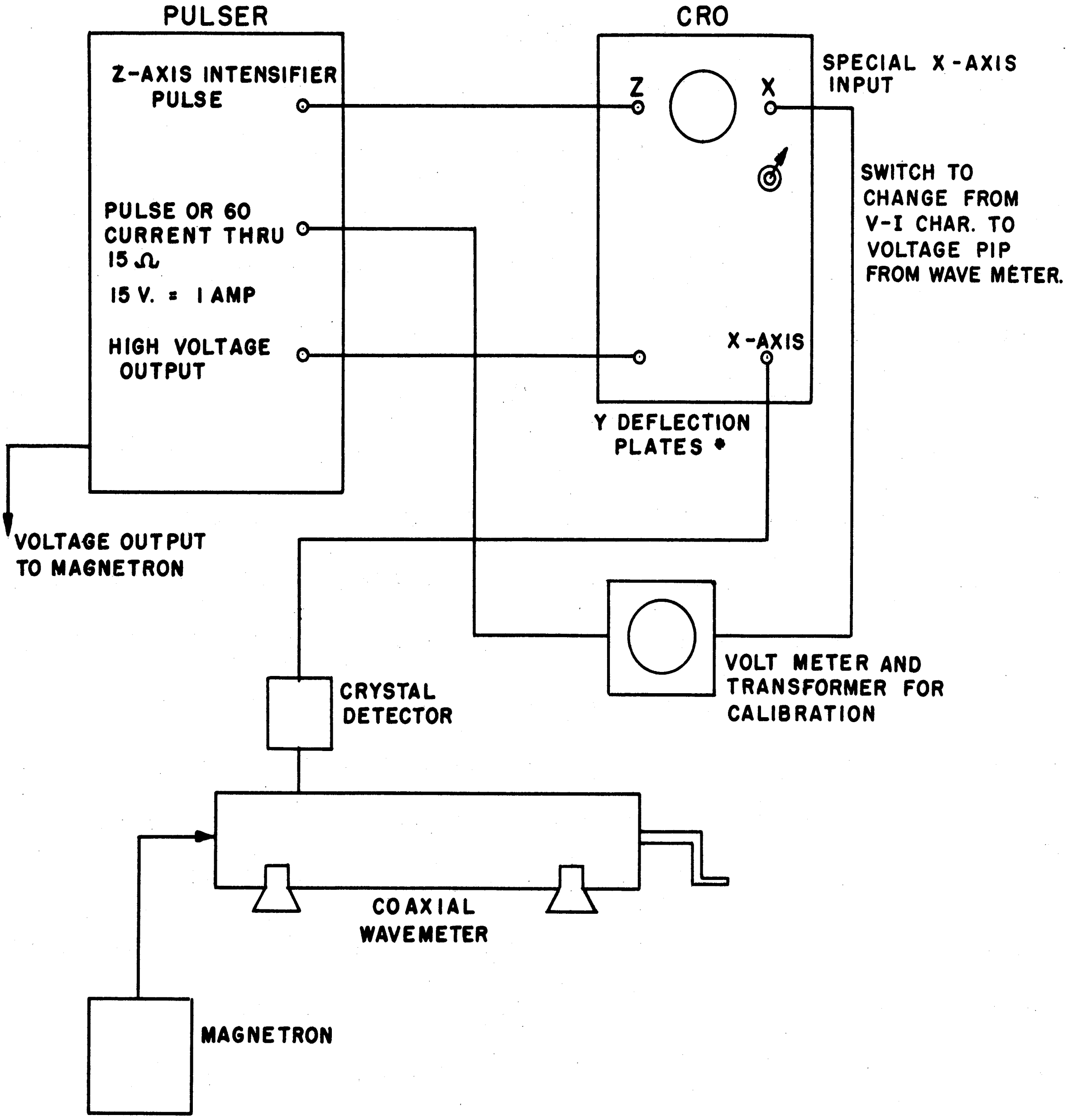

*VOLTAGE FROM PULSER IS APPLIED DIRECTLY TO THE VERTICAL DEFLECTOR PLATES OF THE SCOPE, THRU A VOLTAGE DIVIDER NETWORK WHICH IS USED FOR CALIBRATION.

FIG. 6.4

TEST EQUIPMENT FOR PULSED OPERATION OF MAGNETRON local oscillator, it was employed as such in an S-band spectrum analyser (as indicated in Fig. 6.5). The frequency was swept by superimposing an a-c voltage on the magnetron d-c anode supply.

The total range of the frequency sweep was determined by using the output of a klystron as the input to the spectrum analyzer and mechanically tuning this klystron over the range of frequencies covered by the magnetron local oscillator. The frequency of the klystron at the extreme points was determined by using a coaxial wavemeter. In this manner, it was determined that the magnetron frequency could be swept from 1760 to 2475 mc with continuous, and very nearly constant, power output. Initially, it was necessary to adjust the cathode temperature to a critical value, which once obtained, required no further adjustment over the frequency range. The voltage change corresponding to the frequency change of 715 mc was approximately 1000 volts. These tests indicated that the magnetron was quite satisfactory as a local oscillator in a spectrum analyser.

Qualitative measurements on the noise content of the magnetron output were made by comparing its output signal with the output of a reflex klystron. This comparison was made by alternately feeding the two signal into an S-band spectrum analyzer. When the magnetron was operated c-w, the signal as observed on the spectrum analyser appeared to be unstable in that there were random shifts in the frequency, and also, the signal was alternately noisy and clean. The cathode input power was a critical factor in this operation. When the anode voltage was modulated a very small amount at a 60 cycle rate the signal became steady and all visible noise disappeared. The magnetron output signal under these condi-

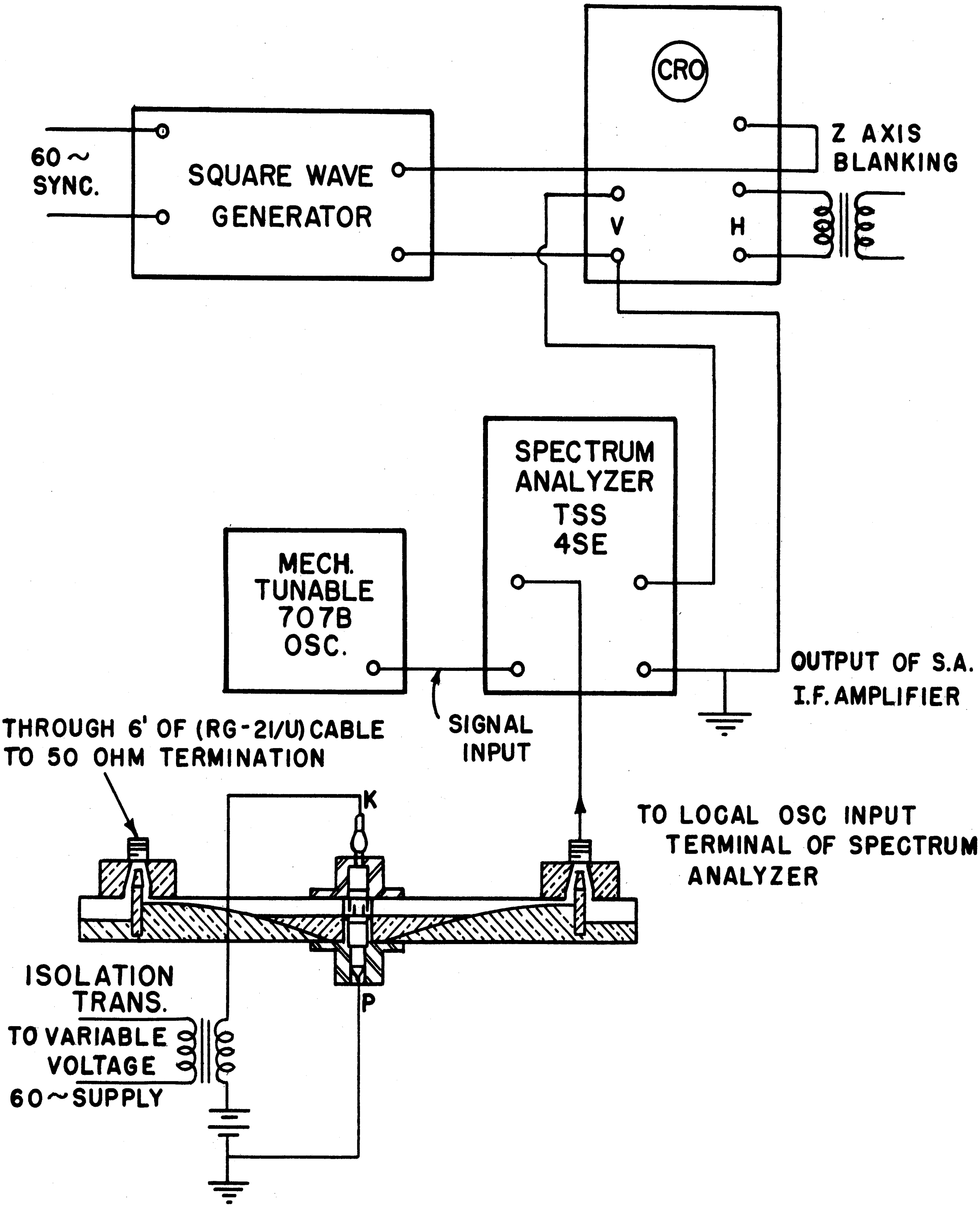

FIG. 6.5

EXPERIMENTAL SETUP USING MODEL II MAGNETRON AS LOCAL OSCILLATOR FOR SPECTRUM ANALYZER tions compared favorably, in both magnitude and noise content, with a 707-B reflex klystron oscillator. Qualitative tests indicated a detectable magnetron signal on the spectrum analyser screen at least 60 db above noise present. For the particular arrangement used, results were similar when the output from a reflex klystron was substituted for the magnetron.

An attempt was made to determine the effect of the cathode temperature on the operating characteristics of the tube. Since the cathode was visible through a small hole in the cavity, it was possible to measure cathode temperature optically. A Leeds and Northrup optical pyrometer was used; this allowed determination of the temperature to within 50 degrees out of approximately 1800 degrees centigrade. The cathode power input was changed very slightly but sufficiently to cause the output to change from a coherent signal to noise, and an attempt was made to measure the resulting cathode temperature change. It was found that this temperature change could not be optically detected with the instrument used.

The arrangement shown in Fig. 6.6 was used to monitor the output signal of the tube. This arrangement made it possible to observe the output as a function of voltage, and to determine the effects of changing various parameters. As indicated in Fig. 6.6, the x-axis sweeping voltage was obtained from the same source as the anode modulating voltage. Thus, with the proper phase shift adjustment, the horizontal sweep on the oscilloscope could be synchronized with anode sweep voltage. The z-axis input was used to blank the return trace from the screen. Since the frequency was linear with voltage it was possible to calibrate the oscilloscope to give power output as a function of frequency.

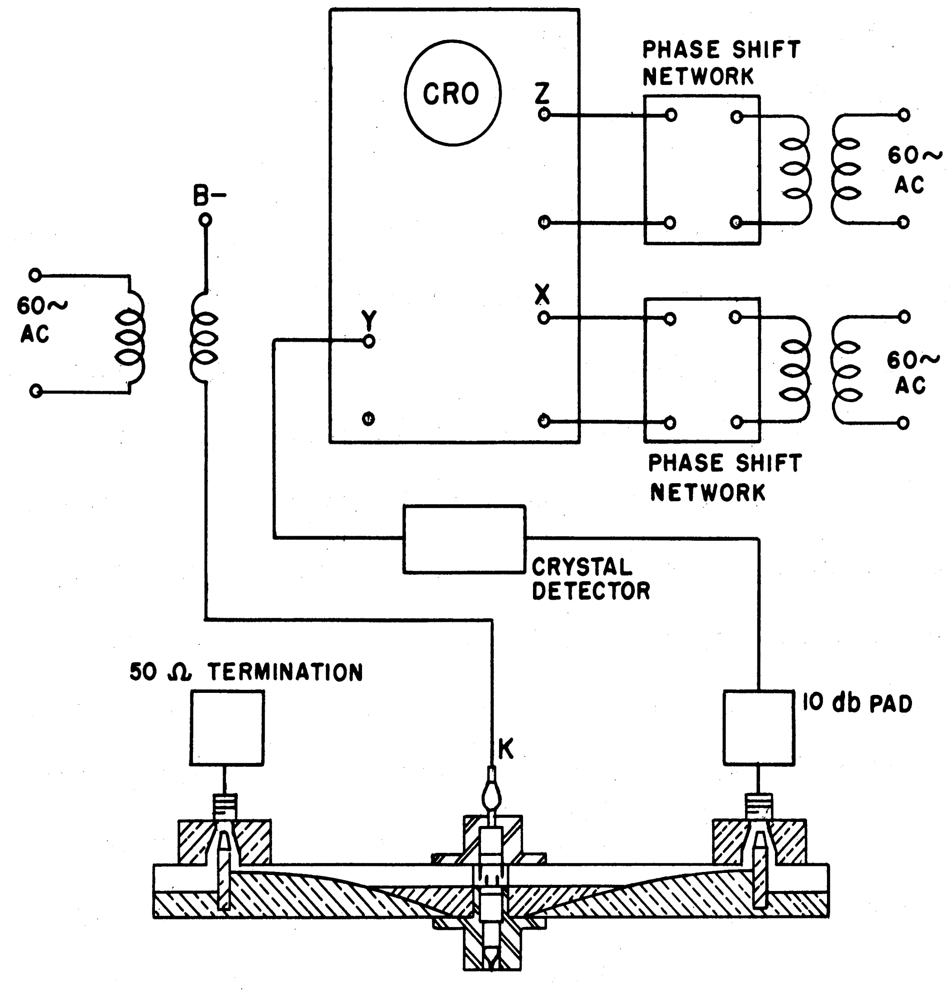

FIG. 6.6

CIRCUIT ARRANGEMENT USED TO OBSERVE OUTPUT SIGNAL vs ANODE VOLTAGE

During the c-w operation the voltage could be varied only over a quite limited range without readjustment of the cathode input power in order to maintain a clean signal. This was due to the change in the backheating which caused a corresponding change in the cathode temperature. However, when the anode voltage was varied at a 60-cycle rate, it was possible to adjust the cathode temperature so that the tube operated satisfactorily over a sweep range of 1250 volts. Thus, once the sweep range has been determined, giving an average backheating power, it is possible to adjust the cathode input power for optimum clean-signal operation of the tube.

Measurements of c-w power output and frequency were made on this tube, and the results are shown in Fig. 6.7. From these data it is seen that the power output varies between 4.5 and 16 mw over a frequency range of 1770 to 2930 mc. The discontinuities in the frequency vs. anode voltage curve are the result of readjusting the cathode input power at these points. The output signal was monitored, as shown in Fig. 6.6 to insure that power measurements of a coherent signal were being made. Since the frequency was sensitive to cathode temperature, a slight discontinuity occurred in the frequency curve each time the cathode input power was adjusted. The adjustment required was very slight. The tube tuned at the rate of approximately 0.8 mc per volt change in anode potential. The frequency-voltage relation as obtained from the Hartree relation is also plotted in Fig. 6.7 for comparison with the experimental data (the π-mode of operation is assumed).

6.2.3 Model 11B, No. 88. Although the Model 11 magnetron operates satisfactorily as a local oscillator, the electronic efficiency

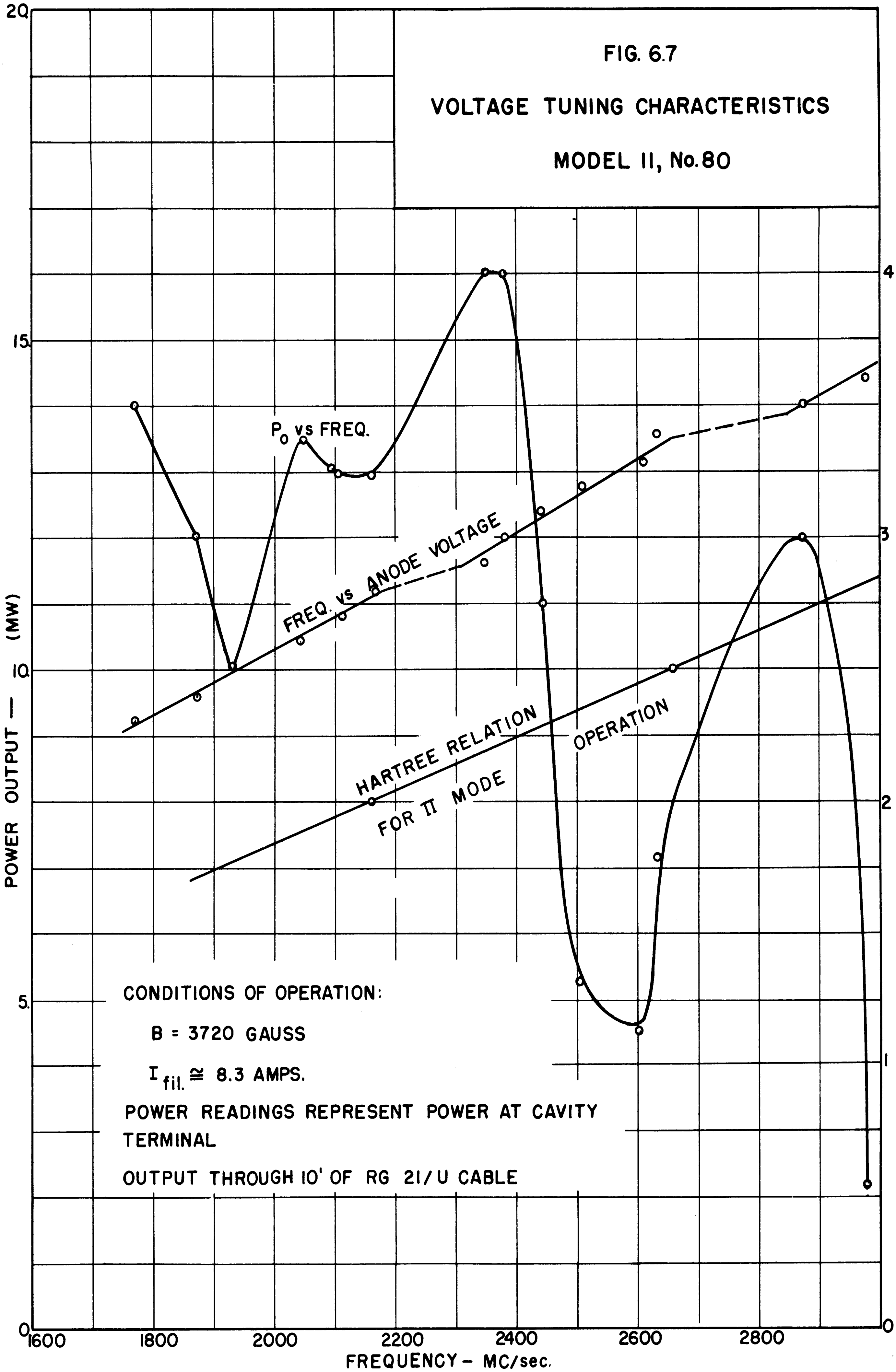
FIG. 6.7
VOLTAGE TUNING CHARACTERISTICS
MODEL II, No. 80
P_0 vs FREQ.
FREQ. vs ANODE VOLTAGE
HARTREE RELATION FOR Π MODE OPERATION
CONDITIONS OF OPERATION:
B = 3720 GAUSS
$I_{fil.} \cong$ 8.3 AMPS.
POWER READINGS REPRESENT POWER AT CAVITY TERMINAL
OUTPUT THROUGH 10' OF RG 21/U CABLE
POWER OUTPUT — (MW)
FREQUENCY – MC/sec.
0
5.
10.
15.
20
1600
1800
2000
2200
2400
2600
2800
0
1
2
3
4

is very poor. Since the impedance of the circuit is lower than for a high-Q magnetron, the r-f fields in the interaction space are very weak. To compensate for this in the Model 11B, the anode diameter was decreased (from .233 inch in the Model 11) to .205 inch. This decrease in anode diameter increased the r_c/r_a ratio to .75 (from .6 in the Model 11), allowing greater penetration of the r-f fields into the interaction space. Test results indicated a significant improvement in electronic efficiency as a consequence of these changes. The Model 11B is otherwise identical with the Model 11.

A pure tungsten cathode was used in this tube. Figure 6.8 shows the voltage tuning characteristics for this tube. These data were taken without any readjustment of the cathode input power. One terminal of the cavity was terminated in a 50-ohm load while these data were being taken. The frequency characteristic is approximately linear, having a slope of approximately 1.18 volts/mc. The sharp discontinuities which were present in the frequency characteristic curves of the other tubes are not present in this case. The frequency could be spot-tuned anywhere within the indicated frequency range without readjusting the cathode input power. When the anode voltage was modulated with a 60 cycle sine-wave voltage, the tube could be tuned from 2000 to 2730 mc with a clean signal output over the entire range. The signal was monitored, using the circuit arrangement shown in Fig. 6.5. The frequency was measured in this case by using a coaxial-type wavemeter as an absorption meter in the circuit shown in Fig. 6.5.

As indicated in Fig. 6.8, the power output varied from 100 milliwatts to 2 watts over a frequency range of approximately 500 mc. This is

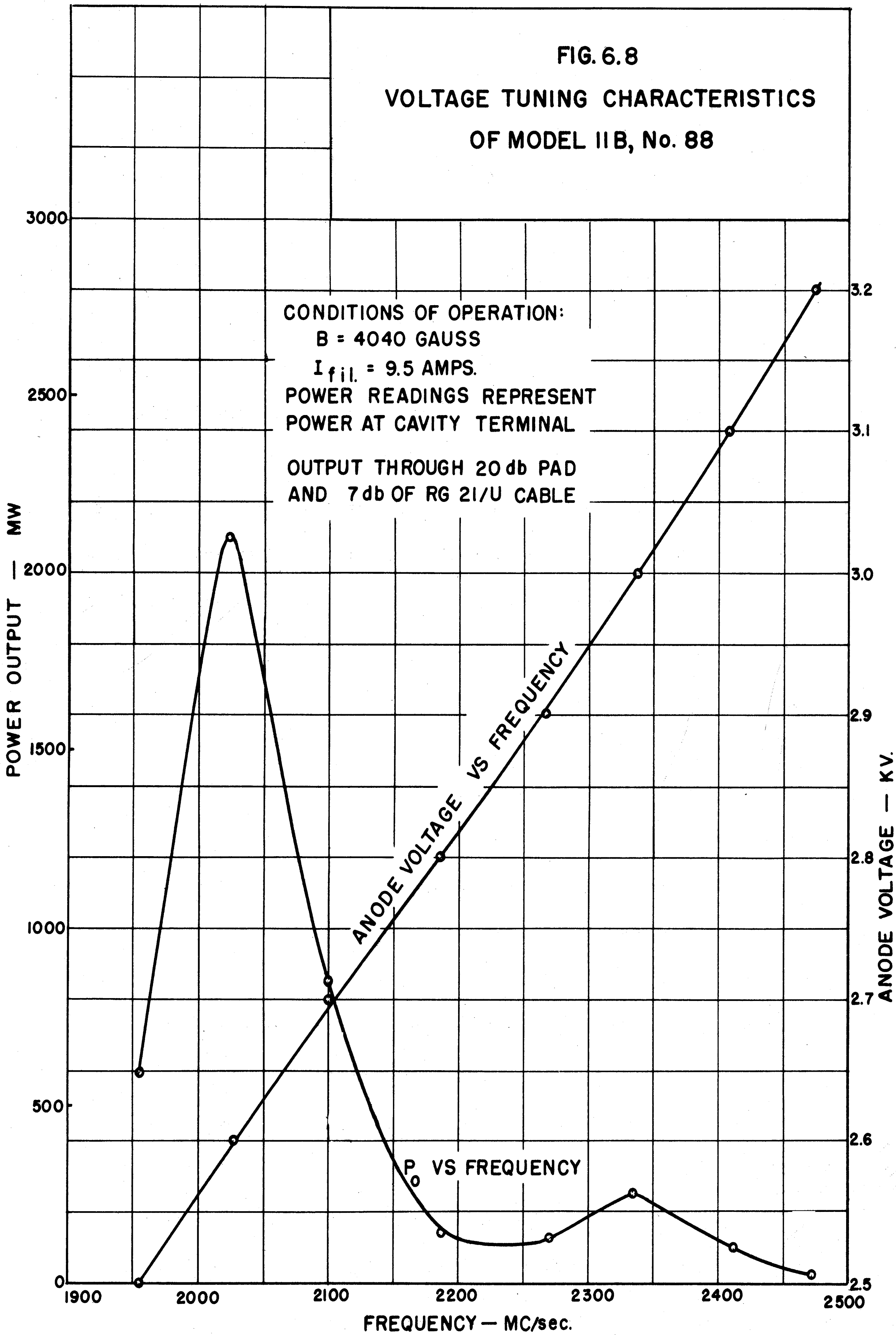

FIG. 6.8
VOLTAGE TUNING CHARACTERISTICS
OF MODEL 11B, No. 88
CONDITIONS OF OPERATION:
B = 4040 GAUSS
$I_{fil.}$ = 9.5 AMPS.
POWER READINGS REPRESENT
POWER AT CAVITY TERMINAL
OUTPUT THROUGH 20 db PAD
AND 7 db OF RG 21/U CABLE
ANODE VOLTAGE VS FREQUENCY
P_o VS FREQUENCY
POWER OUTPUT — MW
ANODE VOLTAGE — KV.
FREQUENCY — MC/sec.
0
500
1000
1500
2000
2500
3000
2.5
2.6
2.7
2.8
2.9
3.0
3.1
3.2
1900
2000
2100
2200
2300
2400
2500

considerably larger than the power output of the Model 11 tubes. Also, the operation of the tube was less senstive to small changes in the cathode input power; once the adjustment of cathode input power was made, the operation of this tube was more stable than were the Model 11 tubes.

6.2.4 Model 11B, No. 112. Tungsten rods were used as the anode bars in this tube. The heat dissipating capacity of the anode structure is increased over that of the tubes which use molybdenum anode bars. The processing technique was modified in the construction of this tube in that the cathode was vacuum-fired before mounting in the tube. This vacuum-firing of the cathode before mounting eliminated the coating of the glass envelope of the tube which had previously occurred in normal operation of the tubes. (This coating was due to molydenum evaporated from the cathode.)

This tube was tested under dynamic operating conditions, and the results are as shown in Figs. 6.9 and 6.10. The conditions of operation are indicated on the figures. A 60-cycle voltage was superimposed upon the d-c anode potential, giving an anode-voltage swing of 900 volts. Filament power was supplied from a battery to eliminate the frequency modulation caused by the variation of the magnetic field which is produced by an a-c heater current.

In addition to the voltage-tunable mode indicated in Fig. 6.9, there were two other modes which were very weak, but still detectable (by reducing the attenuation somewhat) over portions of the voltage range. One of these modes tuned from 2845 mc at 2100 volts to 3170 mc at 2300 volts; the second tuned from 4080 mc at 2050 volts to 4370 mc at 2200 volts. In the voltage range 2350 to 2850 only the main mode was present. Under

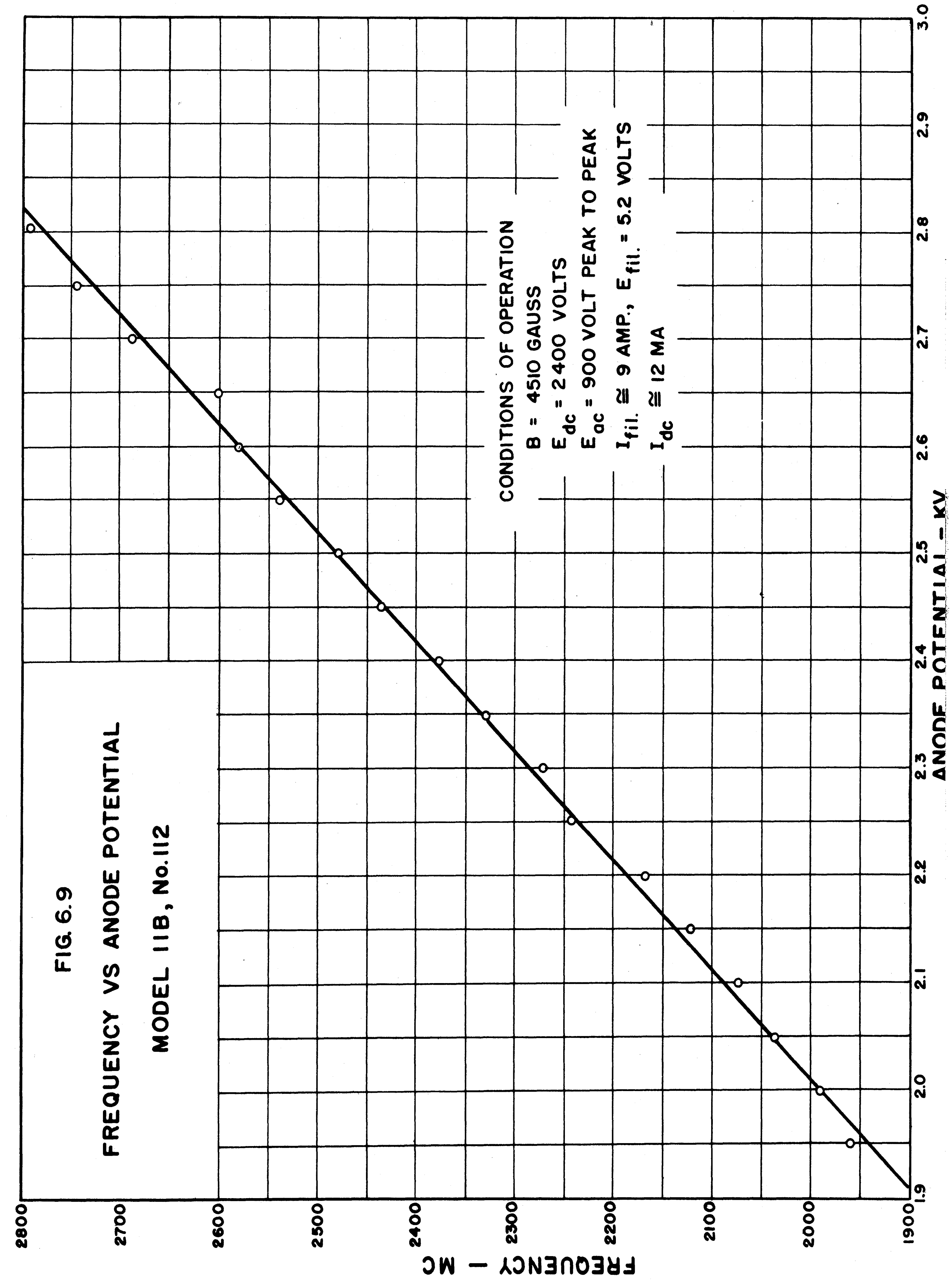

FIG. 6.9
FREQUENCY VS ANODE POTENTIAL
MODEL 11B, No.112
CONDITIONS OF OPERATION
B = 4510 GAUSS
E_{dc} = 2400 VOLTS
E_{ac} = 900 VOLT PEAK TO PEAK
$I_{fil.}$ ≅ 9 AMP., $E_{fil.}$ = 5.2 VOLTS
I_{dc} ≅ 12 MA
FREQUENCY — MC
1900
2000
2100
2200
2300
2400
2500
2600
2700
2800
ANODE POTENTIAL — KV
1.9
2.0
2.1
2.2
2.3
2.4
2.5
2.6
2.7
2.8
2.9
3.0

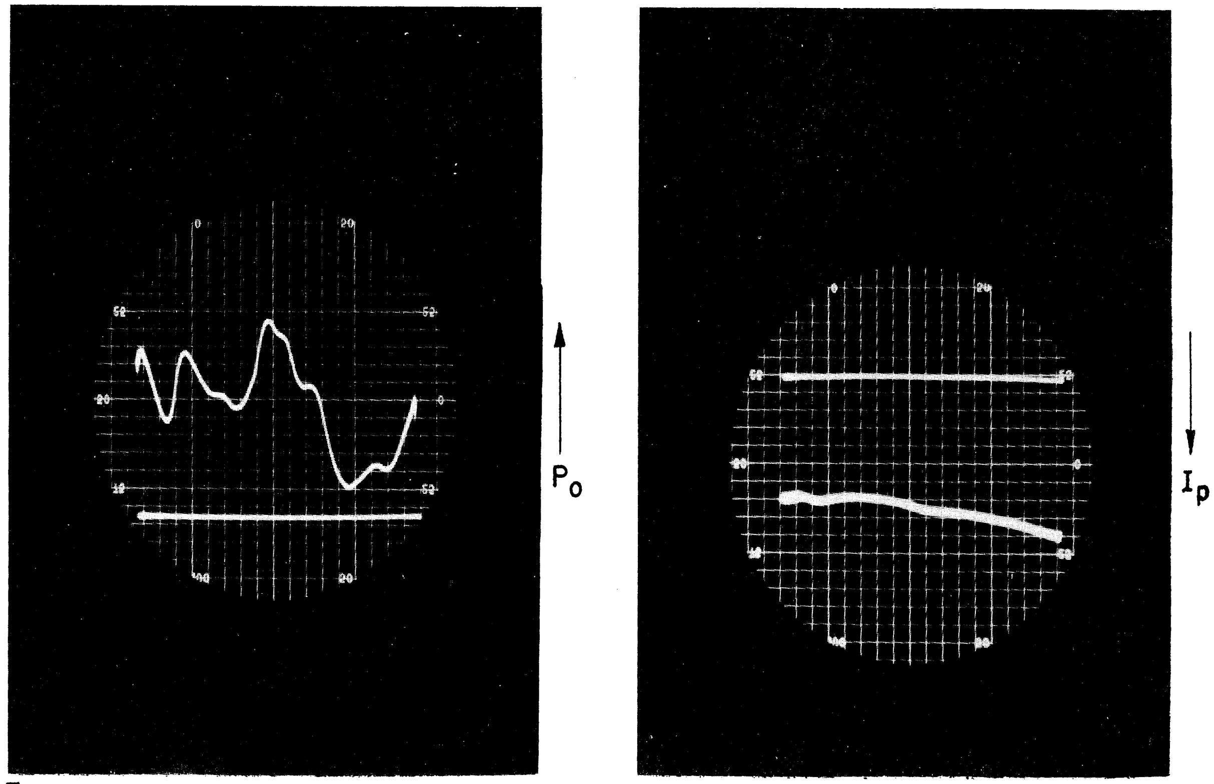

$E_a \longrightarrow$ P_o VS E_a

(a)

$E_a \longrightarrow$ I_p VS E_a

(b)

FIG. 6.10

POWER AND CURRENT CHARACTERISTICS
OF MODEL 11B, No. 112

B = 4510 GAUSS

E_{dc} = 2400 VOLTS

E_{ac} = 900 VOLTS PEAK TO PEAK

$I_{fil.} \cong$ 9 AMP

$I_{dc} \cong$ 15 AMP

$E_{fil.}$ = 5.2 VOLTS

certain conditions of operation, there are discontinuities in the operation of the main mode. These discontinuities in the operation are detectable in either the power output or anode current curves (shown in Fig. 6.10). Continuous operation can be obtained by proper adjustment of the various parameters. Frequency deviations of 400 to 600 mc can be obtained with no difficulty in maintaining continuous operation; for frequency deviations of the order of 800 to 1000 mc, the adjustment of the cathode temperature becomes more critical.

With the modulation voltage reduced to 450 volts peak-to-peak, the frequency of operation could be shifted as much as 50 mc by varying the filament heater current and still maintain coherent operation over the voltage range. An increase in cathode temperature decreases the frequency of oscillation. The tube seemed to operate best at, or near, the lower cathode temperature.

For c-w operating conditions it was possible to vary the filament current from 8.9 amps to 9.3 amps, and still maintain a coherent signal output. The power output varied from 52 mw at an anode current of 5 ma to 350 mw at an anode current of 18.75 ma. The corresponding frequency variation was from 2450 mc to 2320 mc.

Figure 6.10 shows the variation in power output and anode current with the anode voltage. The frequency range in Fig. 6.10 is approximately 900 mc (as shown in Fig. 6.9) and the peak power is of the order of 550 milliwatts. Figure 6.10(b) shows the variation of anode current with anode voltage, the average current being approximately 15 ma. It should be noted that there are no discontinuities in the operation and it was determined that the tube was oscillating coherently throughout the range. The decrease in the power output in the right (high frequency) side of Fig. 6.10(a) is due to the loading of the cathode circuit at that frequency.

This tube was operated with battery supplies for the filament and anode, and an electrically regulated power supply for the electromagnet. Under these conditions, the output signal (as observed on a spectrum analyser) was stable; no jitter was present in c-w operation. The output could be tuned over several hundred mcs without readjusting the cathode temperature. Qualitative measurements using the spectrum analyser indicated that the coherent output signal was at least 65 db above the noise present in the output signal.

Satisfactory operation was obtained with anode voltages as low as 800 volts and frequencies in the order of 2000 mc.

Under these conditions the output power was reduced but the signal was stable and free of noise.

6.2.5 Model 11A. The Model 11A is similar to the Model 11 except that square anode bars are used. The anode bars are .030 inch square and are arranged such that the spacing between bars is approximately .030 inch. The inside anode diameter is .235 inch; this is approximately equal to the inside anode diameter in the Model 11. The original design of the Model 11 was based on the assumption that round anode bars would reduce the higher space harmonics in the interaction space and thus improve the operation of a low-Q voltage-tunable magnetron. The Model 11A was constructed for the purpose of comparing the operation of similar tubes with round and with square anode bars. The Model 11 and Model 11A are identical except for the shape, size, and spacing of anode bars.

Since the Model 11 has more desirable characteristics as a voltage-tunable magnetron, it is concluded that a large portion of this improvement may be attributed to the use of round anode bars. This improvement could be due to the phase shift of the third harmonic or to the reduction in anode-to-anode capacitance.

6.3 Summary of Conclusions. A voltage-tunable magnetron has been developed with operating characteristics that make the tube useful as a source of microwave power. It has been shown that the tube is satisfactory as the local oscillator of a spectrum analyser and as an r-f power source for most r-f measurement applications.

A pure tungsten cathode was found to give better voltage-tunable operation than either an oxide-coated or a thoriated-tungsten cathode. The cathode support and the filament leads were found to cause variations in the power output of the tube. Further work is required to eliminate these effects (See Section 9 of this report).

It was shown that round anode bars improve the operation of the Model 11 magnetrons over that obtained with square anode bars. It was also shown that an increase in the r_c/r_a ratio over the value used in conventional magnetrons improves voltage-tunable operation. Further research is necessary to determine the optimum value for this ratio. With the present circuit arrangement, the anode-to-anode capacitance appears to be the limiting factor in obtaining higher power from the tubes. A reduction in the value of this capacitance is necessary if significantly higher powers are to be obtained. Some improvement in efficiency and power output may be obtained by increasing the external circuit impedance; however, the improvement to be obtained in this way is limited.

A theoretical voltage-tuning curve for a magnetron is derived and experimental data are compared to the theoretical results. The operating anode voltage was found to be higher than predicted by the Hartree equation, assuming π-mode of operation. This increase in operating voltage is attributed primarily to the electrons reaching the anode with considerable radially directed velocity. It is proposed that the sensitivity of voltage-tunable operation to cathode temperature is due primarily to the low impedance which is presented to the electrons by the anode and cavity structure.

7. A Ten-Watt Interdigital Voltage-Tunable Magnetron (Model 12) (P. E. Dicker)

In his study of the Model 11 magnetron, Mr. J. A. Boyd showed experimentally that the tube and its associated circuit behave very well in voltage-tuned operation.

The circuit, which Dr. H. W. Welch, Jr., showed theoretically (Technical Report No. 12) to be one of the limiting parameters of the power in voltage-tunable operation, was designed to give a low conductance and an inductive susceptance which varied slowly with frequency, i.e., low Q circuit. For voltage-tunable operation the impedance of this low Q circuit should be as high as possible. The structure used consisted of a tapered, ridged guide having a characteristic impedance of approximately 165 ohms at 10 cm. This structure is shown in Fig. 6.1. The VSWR varied between 1.25 and 4.5 from 2160 to 3400 mc. Using this structure Model 11 tubes were operated with a power output between 100 and 650 mw in the frequency range of 1300 to 4000 mc. Under certain conditions of operation up to 1.5 watts of power have been observed.

The Model 12 magnetron was designed to have a useful power output of 10 watts and a center frequency of 9 cm. A picture of the tube is shown in Fig. 7.1. It has an interdigital anode structure and associated cathode within a vacuum envelope. The structure differs little from that of the Model 11 tube in order that comparison of performance could be made using the same external circuit. One of the serious limitations of the Model 11 tube was its inability to dissipate large amounts of power in the glass seal. A number of tubes failed because the glass envelope melted in operation, despite their being subjected to an air jet. An analysis of the heat problem in the Model 11 was made and these findings were incorporated into the design of the Model 12 tube.

The essential design data for the tube was as follows:

$$N = 16$$

$$\lambda = 9 \text{ cm}$$

$$\frac{r_c}{r_a} = .7$$

$$r_a = .17 \text{ inch}$$

$$E_o = 380 \text{ volts}$$

$$B_o = 580 \text{ gauss}$$

The anode bars were .035 inch diameter molybdenum rods. No attempt was made to plug the holes in the power output vs. frequency characteristic by building an internal by-pass into the cathode line. It was felt that if the tube performed well this could easily be done at a later date.

With these design considerations two tubes were built and tested.

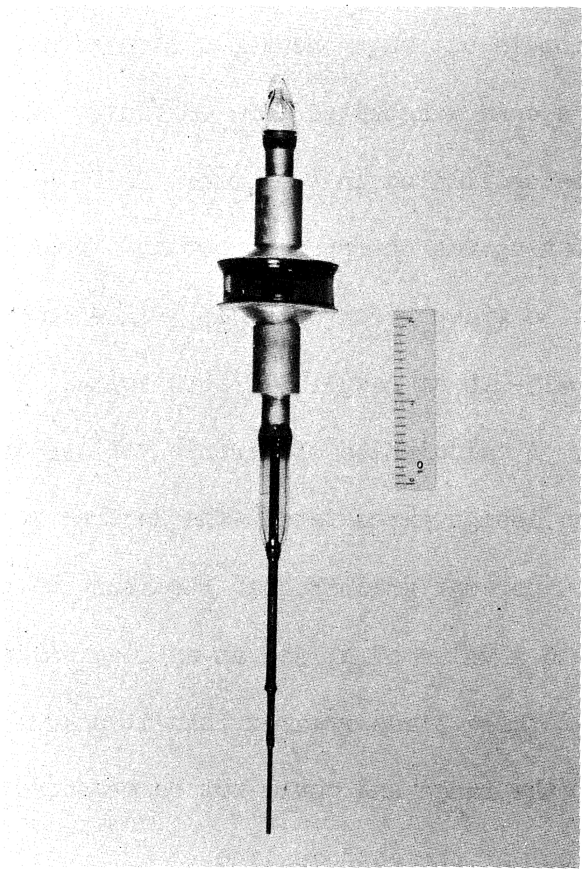

FIG. 7,1

HIGH POWER S-BAND
INTERDIGITAL MAGNETRON

It was discovered that they had a serious flaw. The design of the end hats did not sufficiently confine the electrons to the interaction space to keep the leakage current at a minimum. The tubes appeared to be able to withstand high power inputs although one was destroyed during test by excessive power input. The second was tested more carefully and the following results obtained. The tube oscillated in two modes, 2230-2410 mc/sec and 3150-3485 mc/sec. Voltage tuning was observed in both of these regions. The voltage variation required to sweep through the 13.4-12.4 cm range was 900-1200 volts and for the 9.5-8.6 cm range 1300-1600 volts. The field was approximately 3800 gauss. A calculation of Hartree voltage was made using the experimental data and design parameters. The Hartree potential thus determined was about 300 percent greater than the measured operating voltage. This corresponded to a value of N, for an applied voltage equal to the Hartree voltage, about three times greater than it actually was. The power output varied over the range and could not be measured. A large amount of power was coupled out of the cathode line.

This tube was redesigned to allow for larger end hats. In this Model 12A, tungsten bars replaced the molybdenum anodes. This was done because experience with the molydenum indicated that under high temperatures it had a tendency to release gas bursts which caused arcing with subsequent destruction of the anode bars. Preliminary tests indicated a power output of 2 to 3 watts in the range 2000-3000 mc/sec. The problem of leakage current which caused the failure of the first tube was materially reduced but there still appeared to be a large number of electrons escaping past the end hat shields and striking the iron pole pieces. This was evidenced by the fact that the pole pieces continued to break down.

A third modification of the body resulted in the Model 12B. It was believed that the end-hat construction of the cathode was one of the factors limiting the output power. Both the upper and lower end hats were tightly capacitively coupled to the pole pieces with the result that a short of the r-f field could exist. A decrease in the size of the upper end hat was effected and the results described below followed.

Magnetic field = 5800 gauss

I_{fil} = 9.2 d-c amperes

V_{d-c} = 4700 volts

I_{d-c} = 12 ma

V_{a-c} (sweep) = 900 volts peak-to-peak

The frequency range over which voltage tuning existed was approximately 1665 mc to 2730 mc. The average power, with the sweep in operation, measured out of one end of the cavity was 2 watts. The tube operation was sensitive to cathode temperature as evidenced by change in frequency, power level and cleanliness of signal. The frequency shift with temperature was approximately one percent. Power varied over a 3 to 1 range. An optimum clean signal could be obtained once the sweep range had been determined.

The pole pieces which have been melting under the heat of operation are being redesigned. The current belief is that these pole pieces become hot enough to reach the Curie point. With the loss of the magnetic field, higher currents are drawn and an arc from the cathode to the pole piece forms causing the pole piece to melt. A new cavity similar in construction to the old, but presenting a higher impedance to the tube, has been designed. Plans are also under way to operate the tube with indirectly heated cathodes.

8. A Study of the Effect of the Cathode-Filament System on the Operation of Magnetrons (G. E. Dombrowski)

The anode structure of the insertion magnetron (Model 9) and interdigital magnetron (Model 11) are electrically coupled to the cathode-heater system. This may result in undesirable leakage of r-f power through the heater leads and conversely, the cathode-heater structure may produce undesirable effects on the magnetron interaction itself. One of these effects, conceivably, is that the cathode potential may become unbalanced with respect to the potentials of alternate anode surfaces. Another is the effect of the impedance coupled into the anode circuit. This study was to determine the extent of these effects and to obtain a suitable cathode structure from these considerations. A separate report will be published on this subject as Technical Report No. 18.

It is convenient to consider separately the two expected effects of the cathode system:

(a) the "circuit effect", in which the cathode system couples impedance into the anode cavity, thereby altering its characteristics, such as resonant frequency and circuit efficiency; and

(b) the "electronic effect", in which the cathode system causes an alternation of the interaction forces, resulting in modified electronic efficiency, mode spectrum, and so forth.

The circuit effect is readily discussed with reference to the simplified equivalent circuit of Fig. 8.1. If the cathode line is a simple lossless structure which does not radiate, then the impedance it couples into the anode circuit will be essentially as shown in Fig. 8.2. It is seen that the most appreciable loading caused by the cathode structure occurs when the line is inductive and in series resonance with the vane-to-cathode capacitance. Also shown is the expected variation of the resonant frequency of the magnetron, under the assumption of constant electron-stream susceptance, i.e., with

$$B_{cavity} + B_{anode} + B_{cathode} = \text{constant.}$$

The cathode system thus "pulls" the frequency, much the same as does the r-f load (indeed, a "pulling figure" could be suitably defined).

Referring again to Fig. 8.1, it will be seen that depending on the impedance of the cathode structure, the cathode may assume various potentials relative to the anode sets. Since only reactive elements comprise the circuit, the fields are all in the same phase, and the potential can be plotted as in Fig. 8.3. Assuming, for the sake of argument, that the power output varies with unbalance as shown in the center curve, then the resultant variation of power output will be expected as shown in the lower part of Fig. 8.3. The condition for "power drop-out" in Fig. 8.3 is the series resonant cathode structure identified by the severe frequency pulling of Fig. 8.2.

The curves of Figs. 8.5 and 8.6 show what actually occurred at the mode boundary of a Model 9B insertion magnetron operating into the high Q cavity of Fig. 8.4. Here the role of the cathode line is clearly seen.

Figs. 8.5 and 8.6 serve to confirm the expectations regarding

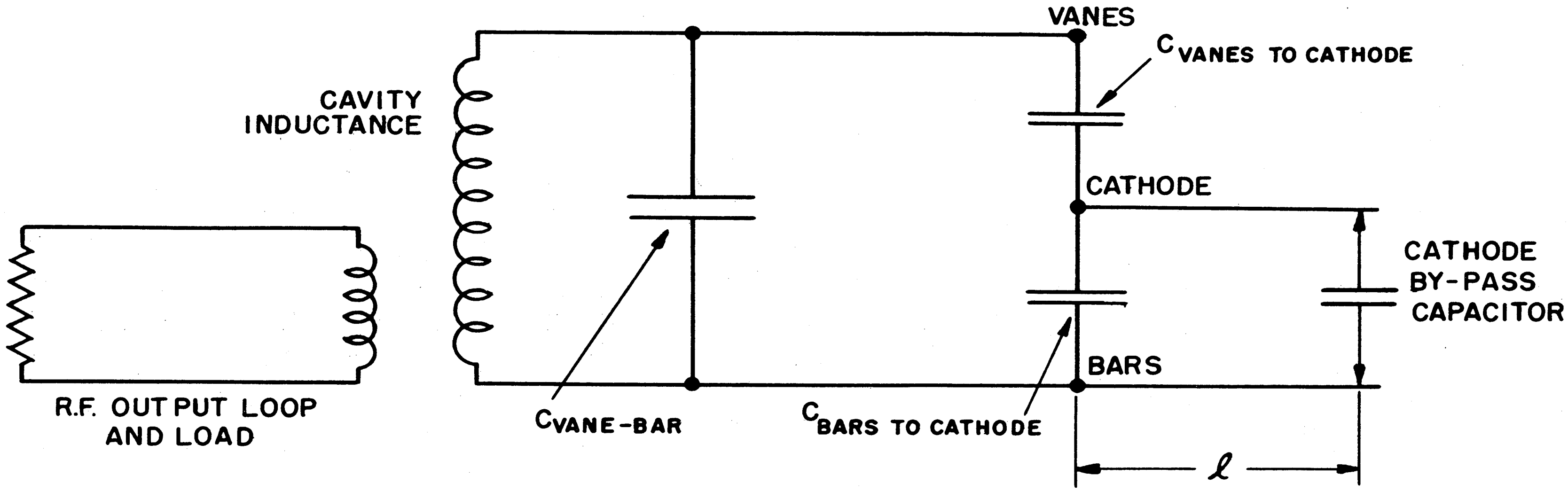

FIG.8.1

EQUIVALENT CIRCUIT OF MAGNETRON AND CAVITY

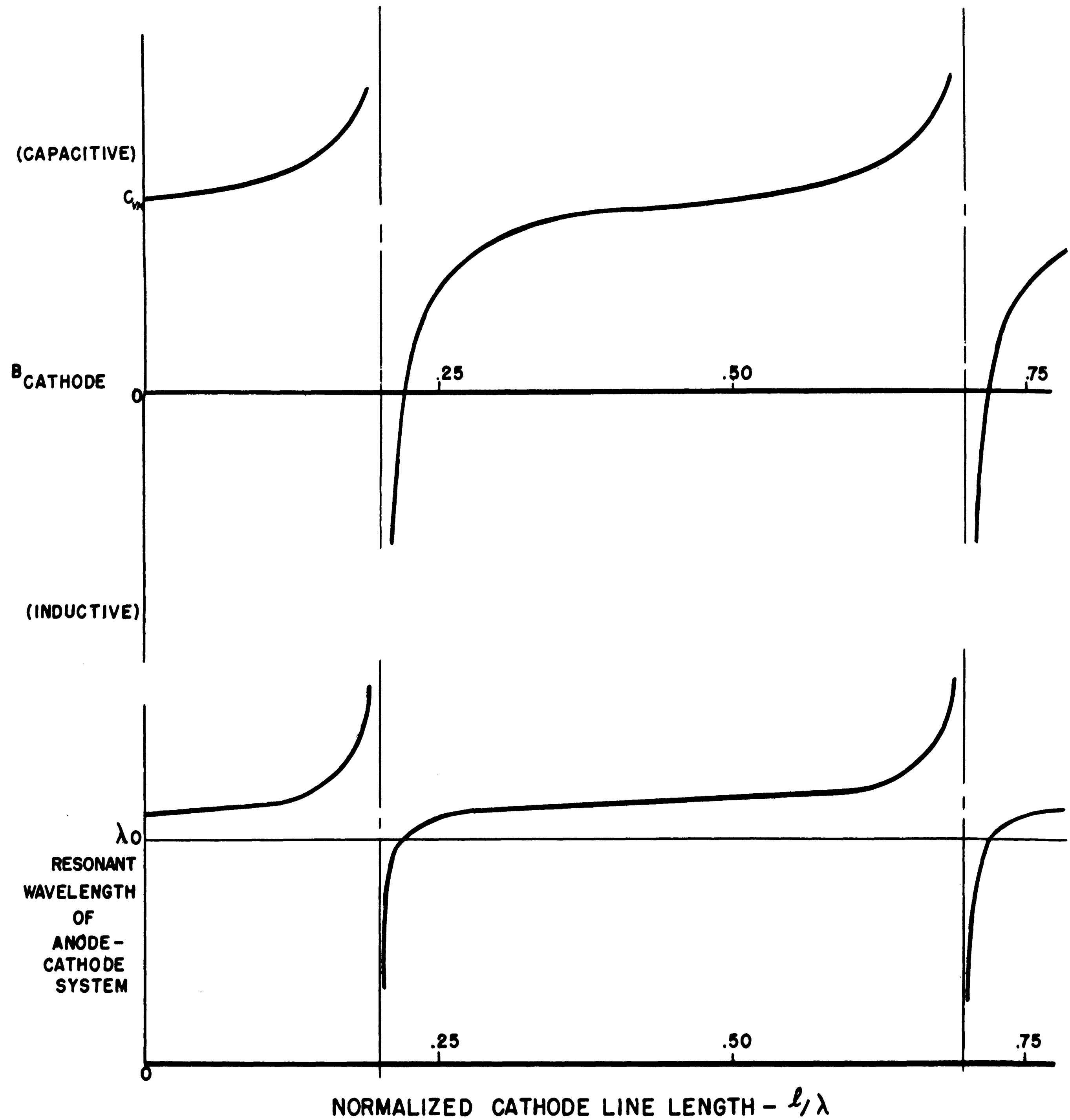

FIG.8.2 EXPECTED CIRCUIT EFFECT FOR SIMPLE CATHODE LEAD STRUCTURE

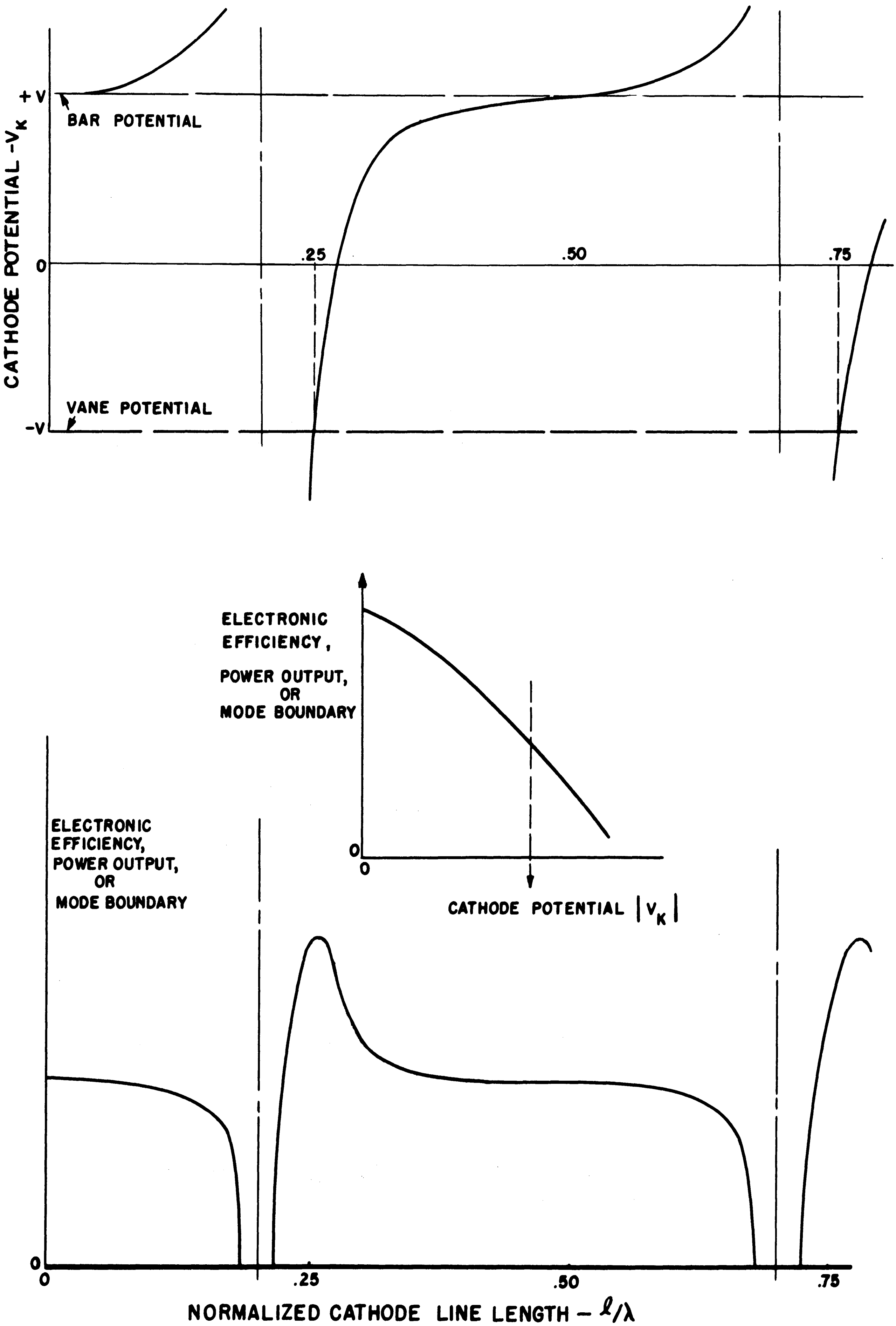

FIG. 8.3 EXPECTED CATHODE UNBALANCE EFFECT FOR SIMPLE CATHODE BY-PASS STRUCTURE

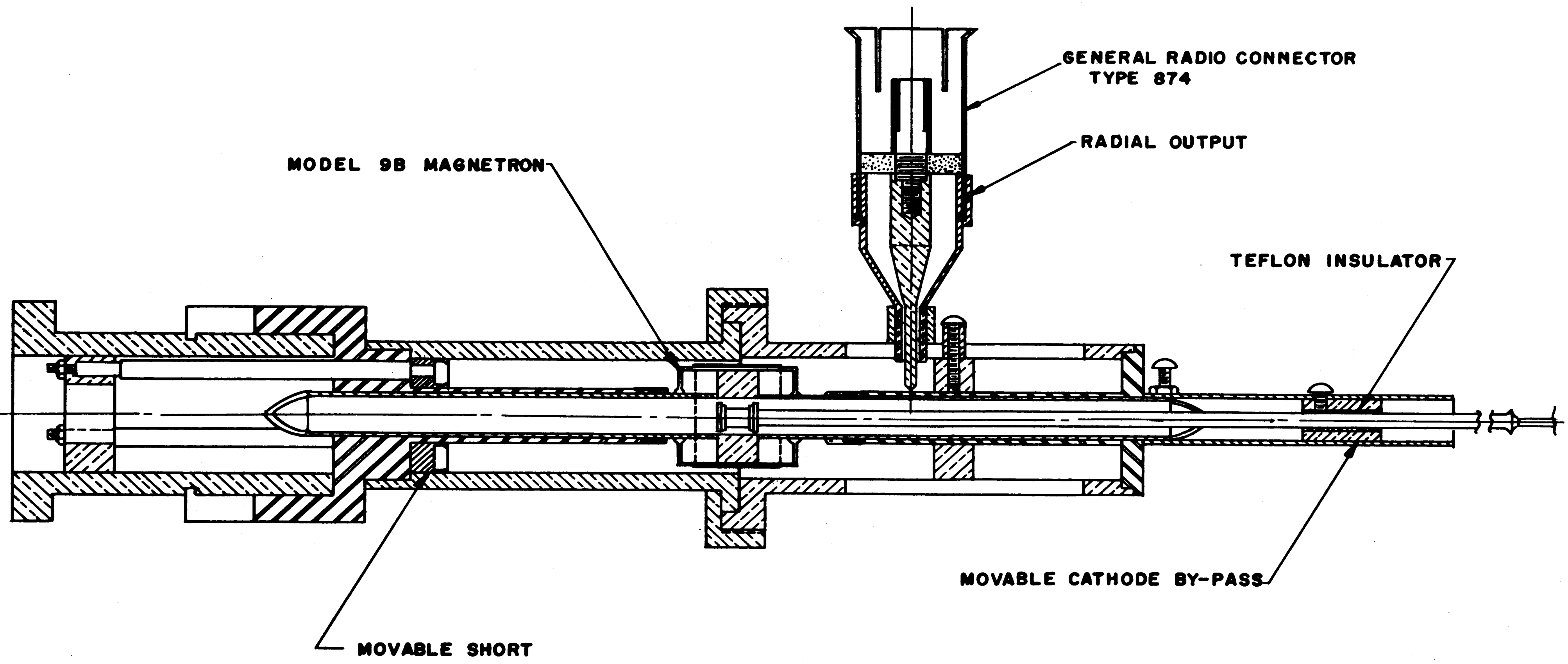

FIG.8.4

ASSEMBLY OF MAGNETRON CAVITY
AND EXPERIMENTAL BY-PASS STRUCTURE

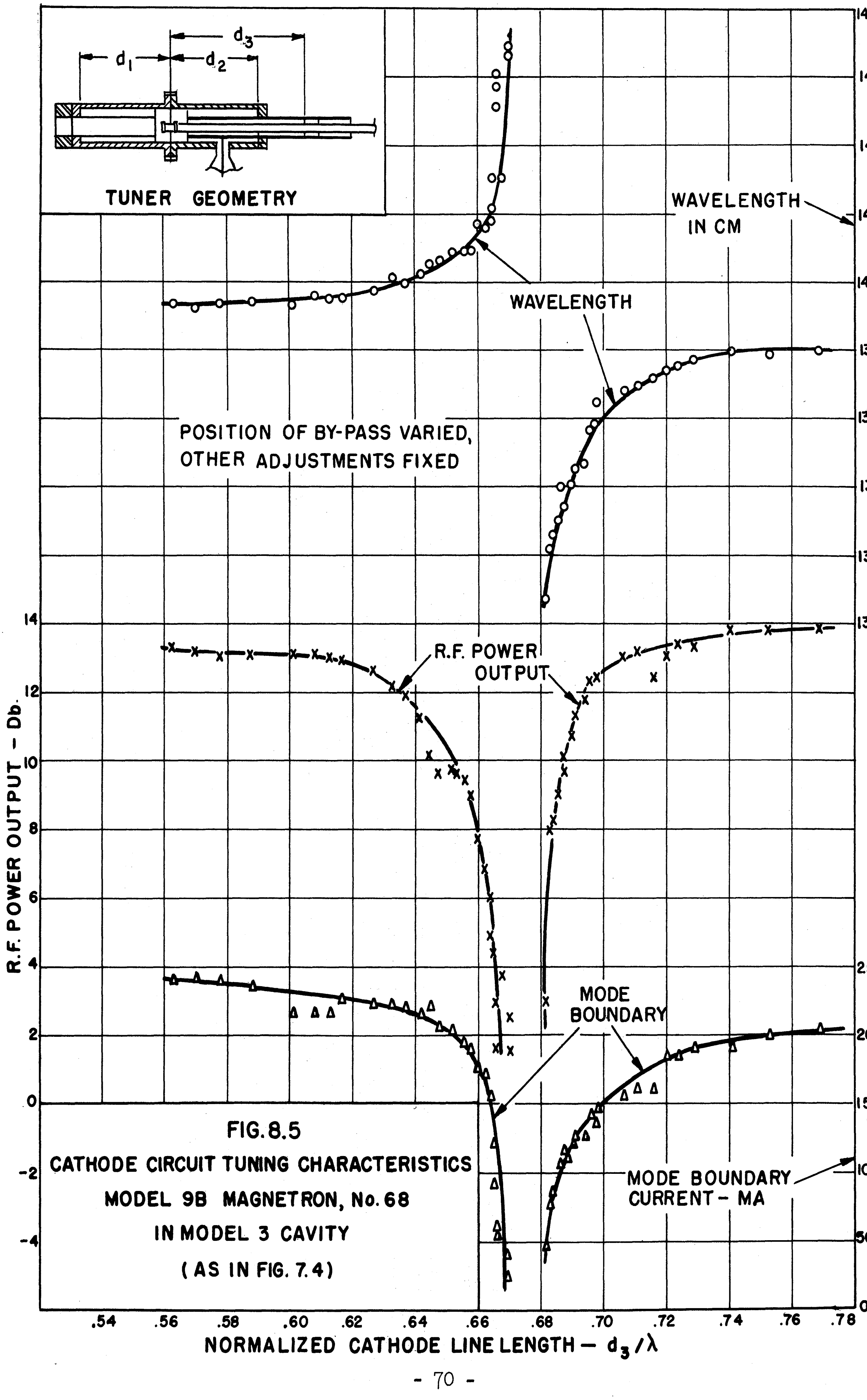

FIG. 8.5
CATHODE CIRCUIT TUNING CHARACTERISTICS
MODEL 9B MAGNETRON, No. 68
IN MODEL 3 CAVITY
(AS IN FIG. 7.4)

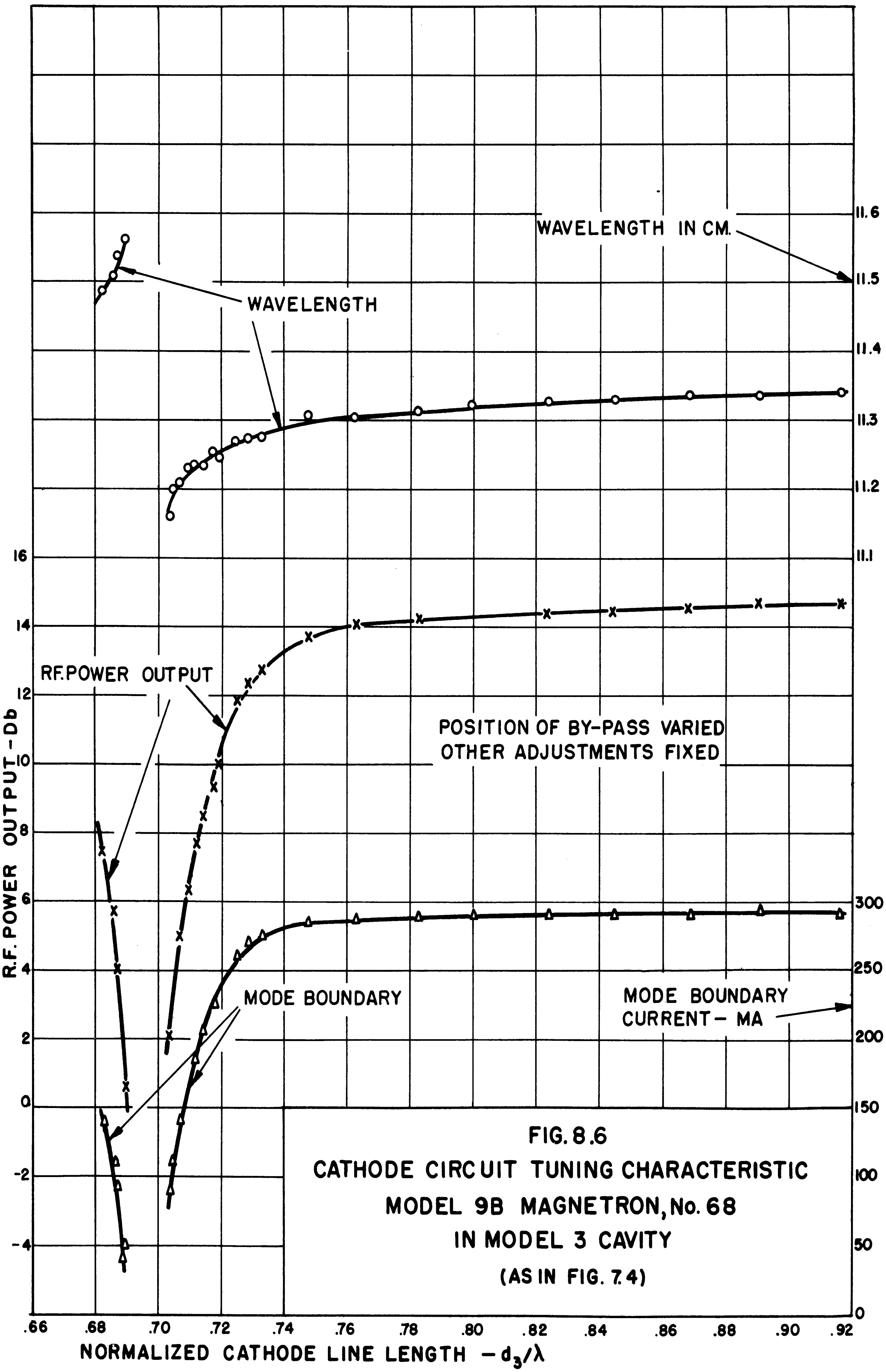

FIG. 8.6
CATHODE CIRCUIT TUNING CHARACTERISTIC
MODEL 9B MAGNETRON, No. 68
IN MODEL 3 CAVITY
(AS IN FIG. 7.4)

the "circuit" effect. It will be noted, however, that the peaks predicted in power output and mode boundary from unbalance considerations, (Fig. 8.3, did not occur. Furthermore, the mode boundary current and the power output varied similarly. Thus, the efficiency also tended to remain constant, even near the power drop-out. It is therefore concluded that cathode potential unbalance is not serious in the "normal range", viz., close to, or somewhere between, the anode potentials.

The effect of the series resonance on the magnetron performance is pronounced. Since the circuit impedance and the cathode potential unbalance are intimately related, and the mode boundary and electronic efficiency are dependent on the circuit in a complicated way; little can be said as to the exact nature of the power drop-out. For practical purposes, nevertheless, the indication is clear: that the cathode line must not present an inductive impedance which can resonate with the interelectrode capacitance between the cathode and the "free" anode segments. It is evidently permissible to by-pass the cathode to the anode set, as the potential unbalance is not important.

This result relating to cathode unbalance may be applied to the heavily loaded voltage-tunable Model 11B magnetron, in which the r-f potentials are quite small in comparison with the d-c anode-cathode potential. An experimental Model 11C magnetron was constructed incorporating a cathode line designed to present an impedance which avoids the series resonance over a wavelength range from 4 to 14 cm. The design is shown in Fig. 8.7, which also shows a modified "free" end hat to avoid a capacitive loading of the cavity.

Elimination of cathode-line resonsnces served to make the effect

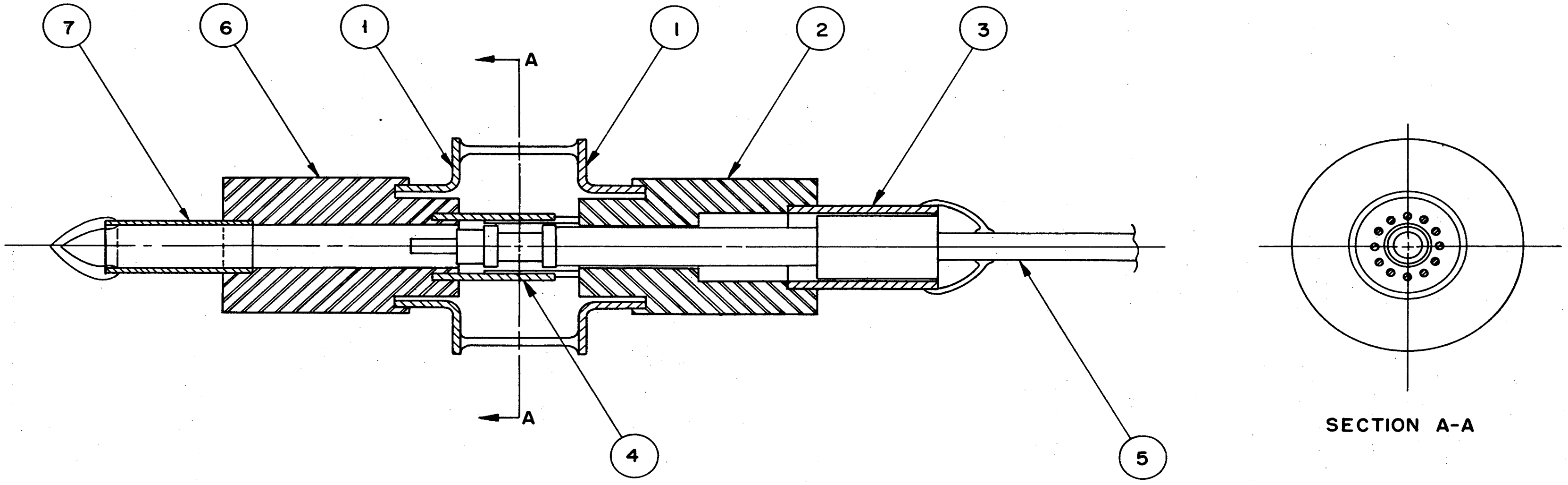

FIG. 8.7

ALL DIMENSIONS UNLESS OTHERWISE SPECIFIED MUST BE HELD TO A TOLERANCE - FRACTIONAL ± 1/64," DECIMAL ± .005," ANGULAR ± 1/2°

		ENGINEERING RESEARCH INSTITUTE UNIVERSITY OF MICHIGAN ANN ARBOR MICHIGAN	DESIGNED BY G.E.D.	APPROVED BY
			DRAWN BY P.L.W.	SCALE 2X
			CHECKED BY	DATE 12-18-52
		PROJECT 2009	TITLE INTERDIGITAL EXTERNAL CAVITY MAGNETRON MODEL 11C	
1	12-18-52	CLASSIFICATION	DWG. NO. B- 10,011C	
ISSUE	DATE			

DWG. NO. B

DWG. NO. B

of the filament-line structure of the Model 11 series more prominent. Since the emitting cathode is a helical wire, it is possible to excite its interior supporting filament lead. A complete equivalent circuit showing this aspect is shown in Fig. 8.8.

Actually, the impedance of the helical filament is not a simple inductance, but is that of a helical transmission line modified by the presence of the center support rod and by the anodes as a shield. Such a transmission line is similar to those used in traveling-wave tubes and can be analysed accordingly. Measurement on a models shows that this helical transmission line is highly dispersive in the operating frequency range, Fig. 8.9.

Also shown is the estimated characteristic impedance, based on the very-low frequency approximation to a coaxial line, and on the very-high frequency (non-dispersive) character of helices[1]. Thus,

$$Z_o \approx 60 \left(\ln \frac{a}{b}\right) \frac{c}{v} \; e^{\frac{-2\pi a}{\lambda g}} \text{ ohms,}$$

where a = mean helix radius, cm.

b = radius of center rod, cm.

c = free-space propagation velocity

v = phase velocity on transmission line

λ_g = "guide" wavelength, cm.

The impedance of the helix which appears between the end hats is therefore

$$Z_{helix} \approx Z_o \tan \frac{2\pi \ell_{helix}}{\lambda_g} ,$$

1 Pierce, J. R., "Traveling-Wave Tubes," Bell System Technical Journal, Vol. 29, p. 27 ff, January 1950.

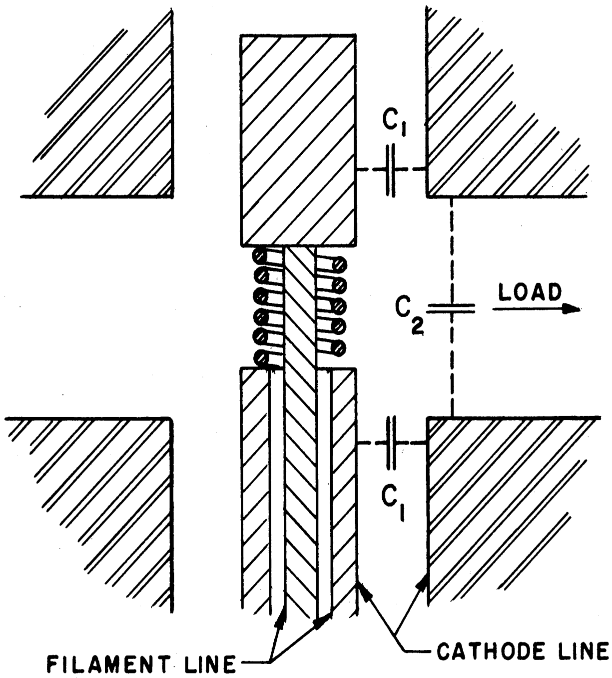

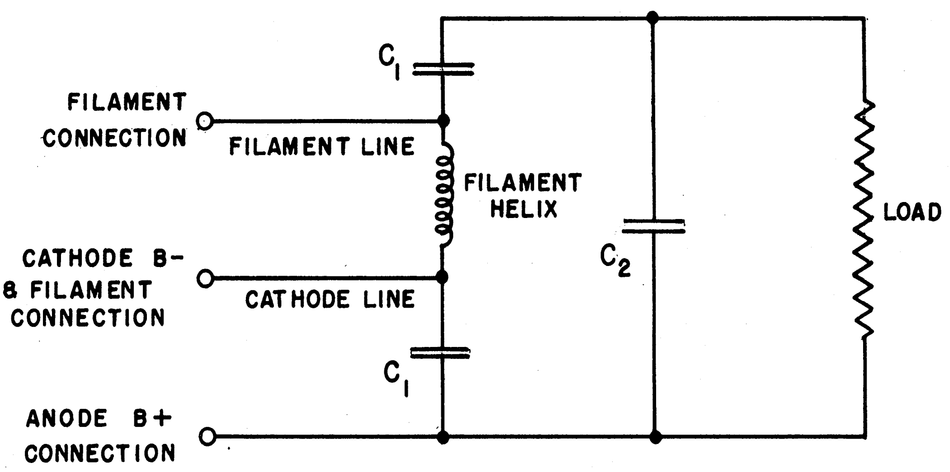

C_1 –CAPACITANCE BETWEEN CATHODE END HAT AND ADJACENT ANODE

C_2– CAPACITANCE BETWEEN ANODES

FIG. 8.8

EQUIVALENT CIRCUIT OF MAGNETRON AND CAVITY

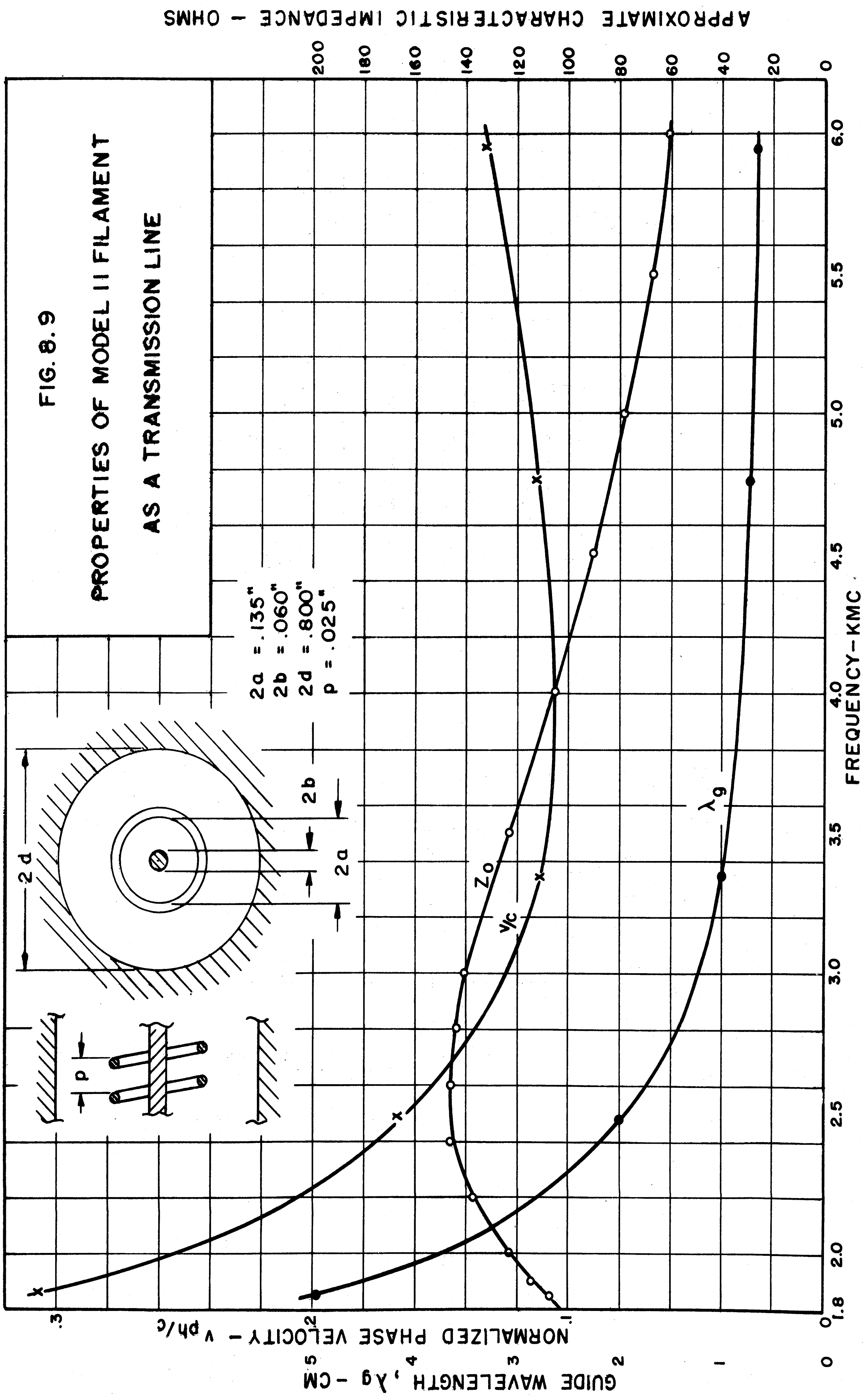

FIG. 8.9
PROPERTIES OF MODEL II FILAMENT
AS A TRANSMISSION LINE

where it is assumed that the voltage drop along the center rod is negligible.

From the above filament impedance and the other tube parameters the magnetron circuit impedance can be calculated. This was done for variations of the Model 11B structures. The results are compared with the operating characteristics in Fig. 8.10.

The peak occurs when the filament-cathode system introduces sufficient inductive impedance into the anode to resonate with the anode capacitance. At slightly lower frequencies this inductive impedance series resonates with end-hat capacitance, C_3, thus heavily loading the anode. The sharpness of the impedance peak for Model 11CA is owing to its smaller end-hat-to-anode capacitance. The broad peak for Modified Model 11B is the result of cathode-line resonance, rather than the filament-line resonances of the other magnetrons.

Because the temperature-limited voltage-tuned magnetron acts as a constant-current generator, and because the load conductance is nearly constant, the power output is proportional to the impedance magnitude plotted. The experimental oscillograms bear this out, but indicate a lower frequency for the peak output, possibly because of under-estimated anode capacitance. The relative natures of the peaks are correctly predicted however. Of further interest is the fact that the magnetron appears to perform equally well with inductive and capacitive loading. This analysis ignores the effect of the r-f helix fields on the electron interaction; the adequacy of the analysis indicates that these fields are not important in the present case. The r-f electric field of the helix is mainly axial, and would cause slight axial motion of the electron and may lower the elec-

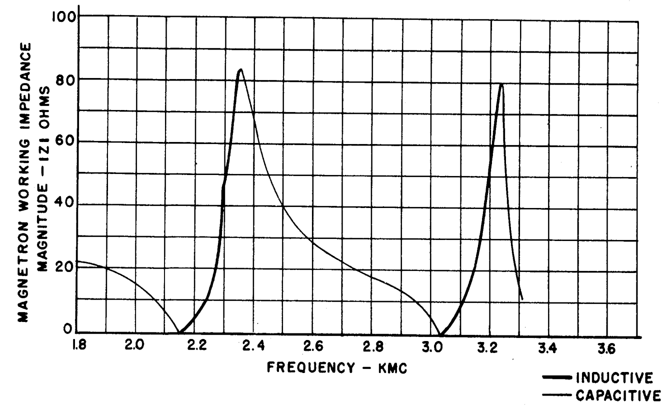

CALCULATED IMPEDANCE

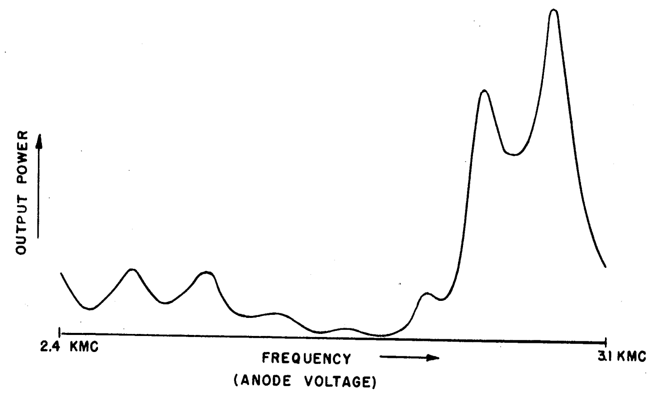

EXPERIMENTAL OSCILLOGRAM

a. MODEL 11B

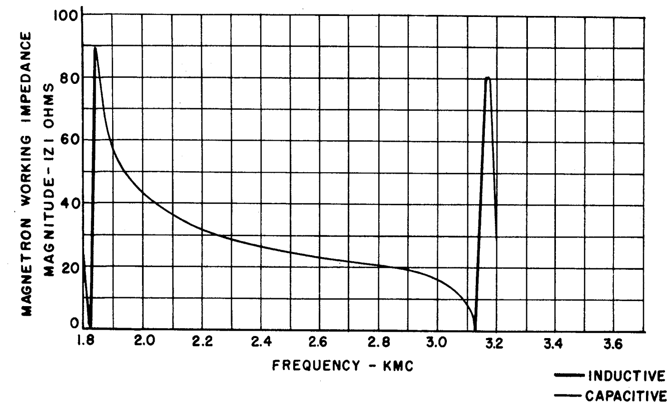

CALCULATED IMPEDANCE

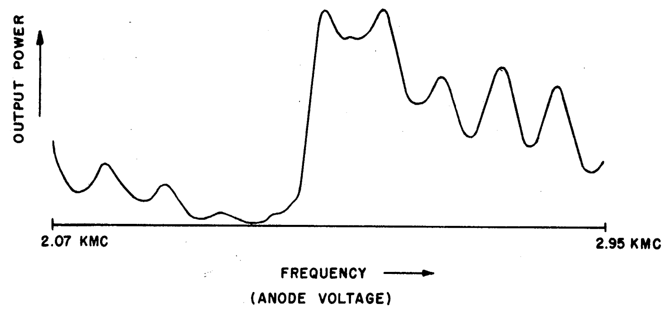

EXPERIMENTAL OSCILLOGRAM

b. MODEL 11CA

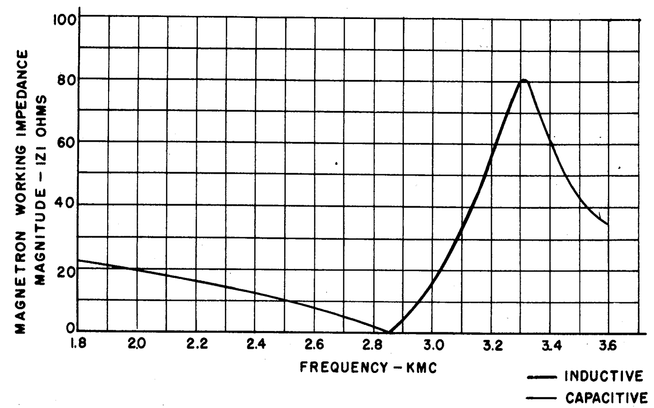

CALCULATED IMPEDANCE

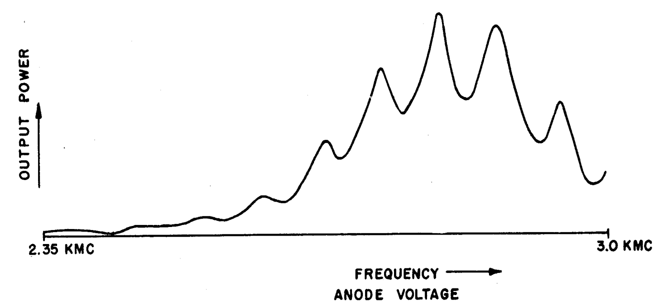

EXPERIMENTAL OSCILLOGRAM

c. MODEL 11B WITH MODIFIED FILAMENT LEADS

FIG. 8.10 COMPARISON OF CALCULATED IMPEDANCE AND EXPERIMENTAL CHARACTERISTICS.

tronic efficiency somewhat. There is no synchronism with the traveling-waves on the helix, hence no traveling-wave helix interaction.

These results indicate that by suitable redesign of the cathode line, the filament line and the filament helix itself, the variations of impedance (power output) can be eliminated in the operating range of the magnetron.

9. An Experimental Investigation of the Effects of the Interaction Space Geometry on the Operation of Voltage-Tunable Magnetrons (P. E. Dicker)

The superior operation of the interdigital voltage-tunable magnetron over the coaxial insertion tube is attributed to the increased magnetic field, its uniformity, the low anode capacity and the relatively high impedance presented to the tube by the waveguide structure.

The heat dissipating ability of the anode bars in the interdigital tube is inferior to the anode sectors of the hole-and-slot or vane-type tube. Although this may not be serious in high Q structures at S-band, this becomes serious at higher frequencies and at lower Q's. In an effort to maintain a high impedance across the anode sections small anode wires have been used to keep C_A low and as a result the power handling capacity of the anode was reduced.

The first step in the study was to investigate the effect of increase of C_A on the operation of the Model 11 tubes. If an increase in C_A did not greatly affect the behavior of the tube, larger anodes could be incorporated in the structure. Tests performed indicated that any change which increased the total capacitance across the anodes such as increasing the anode wire size, increasing the length of the interaction space, or increasing the top end hat-to-pole piece capacitance lowers the power output.

Experiments with Model 11 and 11B tubes indicated that an r_c/r_a ratio higher than that predictable from experience with high Q magnetrons was desirable. The laboratory constructed a number of tubes having different anode to cathode ratios with the following results:

1. The first tube changed was a Model 11. It originally had an r_c/r_a = .643 and gave a peak power output of 16 mw. Upon modification the anode bar diameter was made 0.235 inch and the cathode diameter was kept at 0.150 inch. This gave an r_c/r_a = 0.73. The power output jumped to a value of .5-1 watt.

2. The second modification was one in which the Model 11 tube kept its original pole piece structure and anode bar radius of 0.268 inch. The cathode diameter was increased from 0.150 to 0.170 again giving an r_c/r_a ratio of .73. This tube was operated under two different sets of conditions. One point of operation gave a maximum power output of approximately 2 watts with an average power of 630 mw. Power varied approximately 4-1 over a frequency range of 1945 to 3120 mc/sec. The second point of operation yielded a peak power of 3 watts with only slight increase in minimum power levels. The frequency range was 1765 mc/sec to 3000 mc/sec. Indications were that an increase in cathode to anode radius ratio from 0.6 to 0.75 gave increase in power by a factor of ten.

3. A Model 11F tube was built which was identical with the Model 11 except that the interaction space was increased. The anode wires and the cathode were lengthened .372 inches to .872 inches allowing the tube to operate directly across a 1 x 2 inch guide having no ridge. The tube be-

haved very poorly, voltage tuning at very low levels only below 1500 mc. Several high Q modes appeared which were non-voltage-tunable. In general, the behavior of the tube bears out our prediction that it would be poor mainly due to the low impedance presented by the high capacitance of the anode structure.

One relatively major change in the cathode of the Model 11 series was made. Mr. C. Litton of Litton Industries indicated that backheating of the cathode structure could be greatly reduced by causing the cathode to present as nearly a cylindrical surface as possible to the interaction space. This was accomplished by grinding the outside surface of the tungsten helix to as near a cylindrical surface as possible. Helices of this type have been employed in several of the Model 11 series magnetrons. The noise figure appears to be greatly improved over the round helix cathode and in some instances power increase has been improved by a factor of ten. No reduction in backheating power was noted.

10. The Trajectron -- An Experimental D-C Magnetron (W. W. Peterson)

The purpose of the research reported in this section was to learn as much as possible about the potential distribution, space charge distribution, and electron orbits in a d-c magnetron through an experimental technique which we have named the "trajectron" method.

The trajectron, the d-c magnetron used in the experiments, consists of a magnetron diode with concentric cylindrical anode and cathode. An electron gun is placed in the same envelope at one end of the diode, and a fluorescent screen is placed at the other end. The electron beam is placed so that the beam electrons enter the diode as closely as possible to the cathode surface and with their velocity as nearly parallel with the axis of the cathode as possible. Then the forces on the beam electrons are the same as the forces on electrons emitted by the magnetron cathode, and the deflection of the beam in its passage through the diode is the same as the displacement of an emitted electron after the same transit time[1]. The transit time of beam electrons can be varied by varying beam potential, and thus the orbit of an emitted electron can be traced out on the fluorescent screen, and electron displacement as a function of transit time can be found[2]. If the electron displacement as a function of time could be found sufficiently accurately, it would be possible to calculate potential distribution and space charge distribution. Thus the trajectron method might be expected to answer all the pertinent questions about space charge in a d-c magnetron.

10.2 Status of the Work. The experimental work on this problem is considered complete. A report is being prepared on this work. It will discuss the experiment and the results in detail. A tentative Table of Contents, several figures, and a brief statement of the conclusions is included for reference.

The Trajectron -- An Experimental D-C Magnetron

TABLE OF CONTENTS

List of Illustrations

Abstract

Acknowledgements

---

1 This assumes that end effects of the fields are negligible and that the initial radial and angular velocities of the beam electrons match those of emitted electrons.

2 This method was first used by R. Svensson, but his experiments were of very limited scope.

1. Introduction
    1.1. Statement of the Problem
    1.2. Outline of Previous Work on the D-C Magnetron
        1.2.1. Introduction
        1.2.2. Theoretical Studies
        1.2.3. Experimental Studies
2. Theory of the D-C Magnetron
    2.1. Introduction
    2.2. The Motion of Electrons in the Fields of a Planar Magnetron
    2.3. The Self-Consistent Field Solution for the Planar Magnetron
    2.4. The Motion of Electrons in the Fields of a Cylindrical Magnetron
    2.5. The Self-Consistent Field Solution for a Cylindrical Magnetron
    2.6. Secular Space Charge and Its Influence on the Self-Consistent Field Solutions
        2.6.1. Secular Space Charge
        2.6.2. Self-Consistent Field Solution with Secular Space Charge
        2.6.3. Conclusions
3. The Design of the Trajectron
    3.1. Basic Design Parameters
    3.2. Details of Tube Construction
    3.3. The Magnetic Field
    3.4. Instruments and Recording of Data
    3.5. Auxiliary Equipment
    3.6. Processing of Cathodes
4. Control Experiments
    4.1. Introduction
    4.2. The Electron Beam
    4.3. The Case of Non-Emitting Cathode with No Magnetic Field
    4.4. The Case of Non-Emitting Cathode with Magnetic Field
    4.5. The Case of Emitting Cathode with No Magnetic Field
    4.6. Discussion of the Trajectron Method
5. The D-C Magnetron Case
    5.1. Introduction
    5.2. End Effects
    5.3. Initial Velocities
    5.4. The Cutoff D-C Magnetron
    5.5. The Conducting D-C Magnetron
    5.6. Irregularities in the Volt-Ampere Characteristics of the D-C Magnetron
6. Conclusions
    6.1. The Trajectron Method
    6.2. The D-C Magnetron

<u>10.3 Typical Trajectron Data.</u> An assembly drawing of the trajectron is shown in Fig. 10.1. The trajectron is shown with the solenoid and camera in place in Fig. 10.2, and the tube, vacuum station, and power

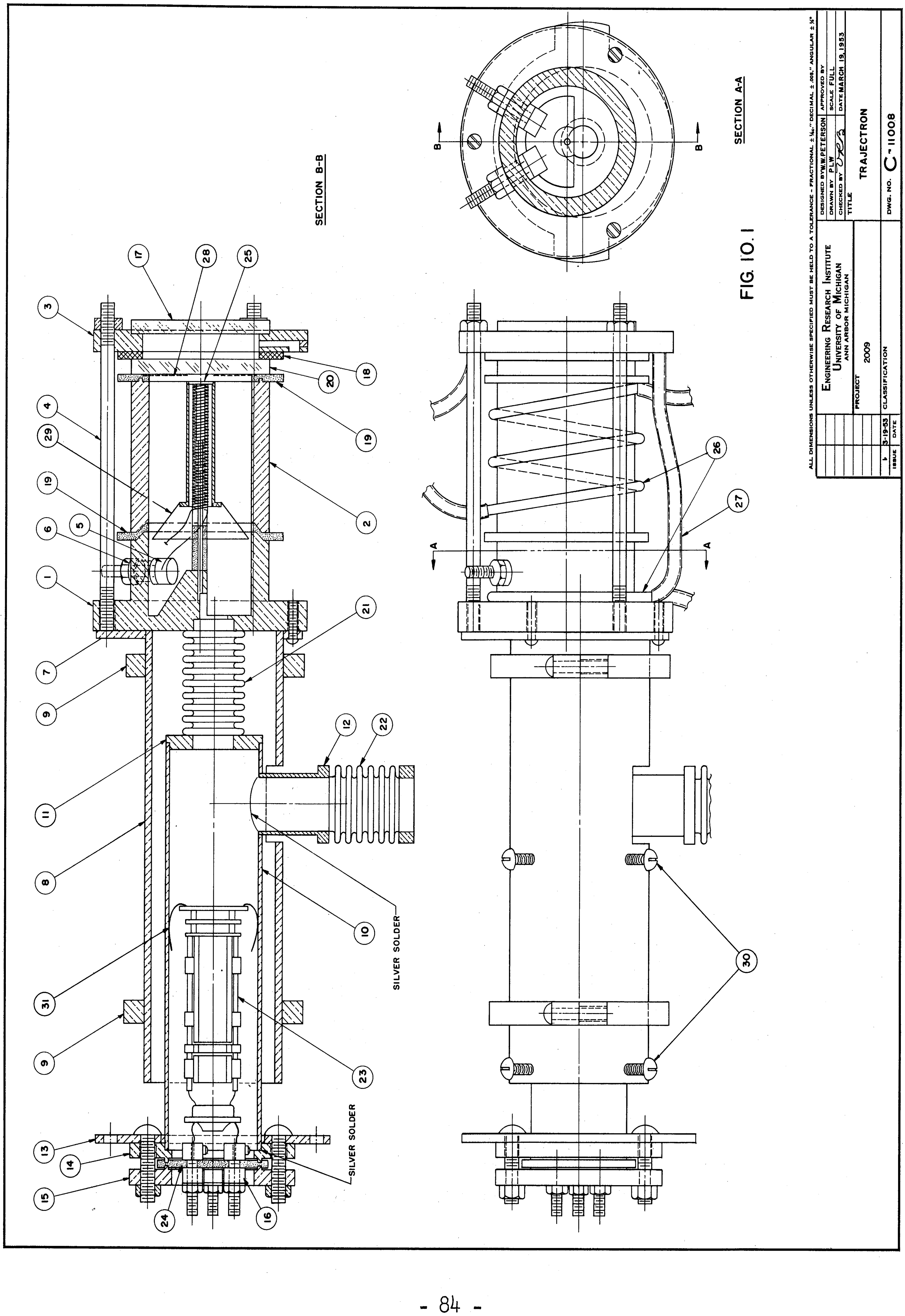
SECTION B-B
SECTION A-A
FIG. 10.1
SILVER SOLDER
SILVER SOLDER
ALL DIMENSIONS UNLESS OTHERWISE SPECIFIED MUST BE HELD TO A TOLERANCE - FRACTIONAL ± 1/64" DECIMAL ± .005" ANGULAR ± 1/2°
ENGINEERING RESEARCH INSTITUTE
UNIVERSITY OF MICHIGAN
ANN ARBOR MICHIGAN
DESIGNED BY W.W. PETERSON
DRAWN BY PLW
CHECKED BY
APPROVED BY
SCALE FULL
DATE MARCH 19, 1953
PROJECT
2009
TITLE
TRAJECTRON
CLASSIFICATION
DWG. NO. C-11008
ISSUE
DATE
3-19-53
DWG. NO. C

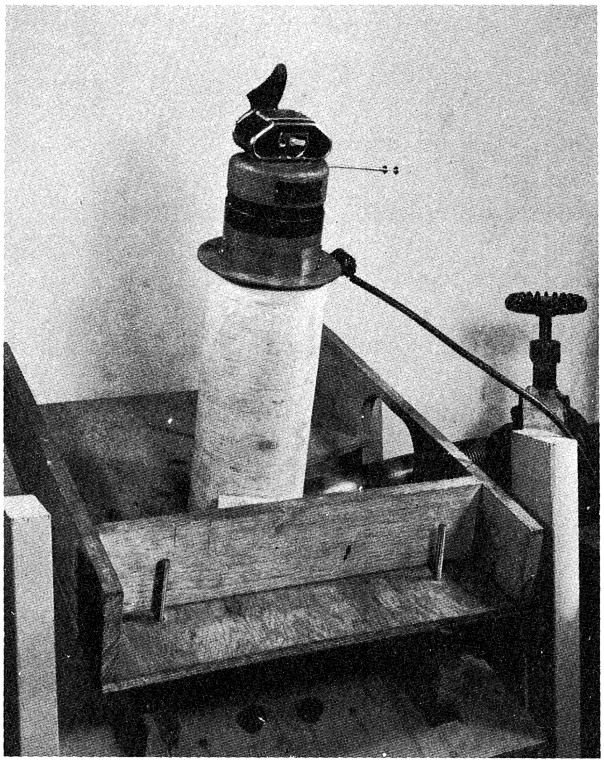

FIG. 10.2 THE TRAJECTRON READY FOR RECORDING OF DATA

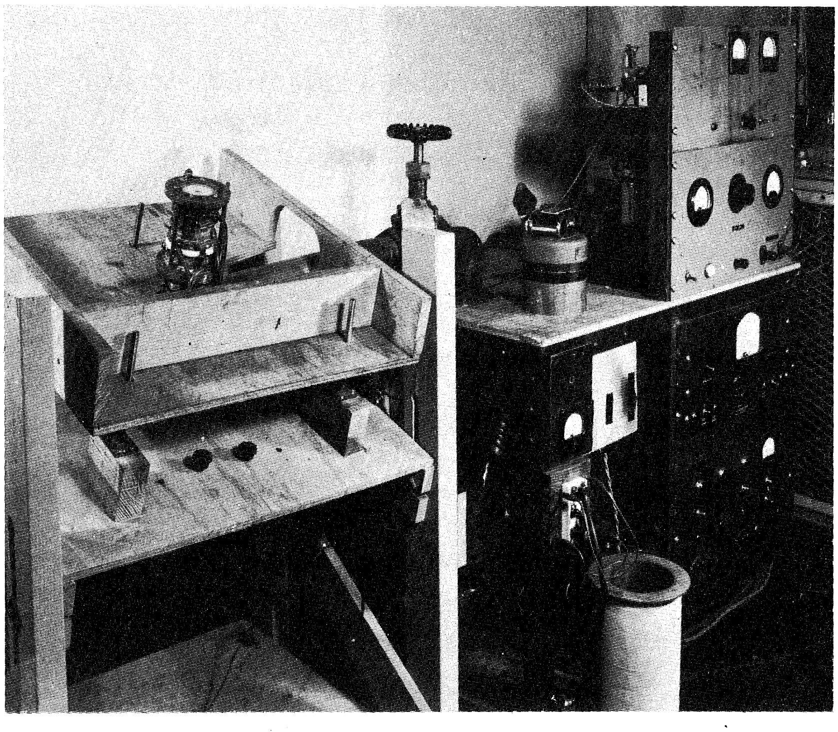

FIG. 10.3 THE TRAJECTRON, VACUUM STATION AND POWER SUPPLIES

supplies can be seen in Fig. 10.3.

This tube could be operated in any one of four conditions:

(1) Non-emitting cathode with no magnetic field,

(2) Non-emitting cathode with magnetic field,

(3) Emitting cathode with no magnetic field,

(4) Emitting cathode with magnetic field.

The trajectron experiment was undertaken as a study of the fourth case, the magnetron case. The other three were studied as control experiments.

In Fig. 10.4 data are shown for the trajectron operating with a magnetic field and a non-emitting cathode. In the photograph there are many exposures of the spot. In each case there is an exposure with no anode voltage applied. Then with the anode voltage applied and held constant exposures were made at several beam voltages. At each beam voltage an exposure was made, the magnetic field was reversed, and another exposure was made. A circle showing the projection of the cathode surface is drawn on the photograph. The other curve drawn on each photograph is the theoretical electron orbit neglecting end effects and initial velocities. The theoretical curves and the data from the photographs are replotted in Fig. 10.5 to show R and θ as functions of transit time. The time was calculated by dividing the length of the diode by the velocity of the beam calculated from the potential of the cathode of the electron gun.

In Fig. 10.6 data are presented for the case of no magnetic field and cathode with space-charge limited emission. The arrows mark theoretical deflection based on the theory in which initial velocities of emitted electrons are neglected.

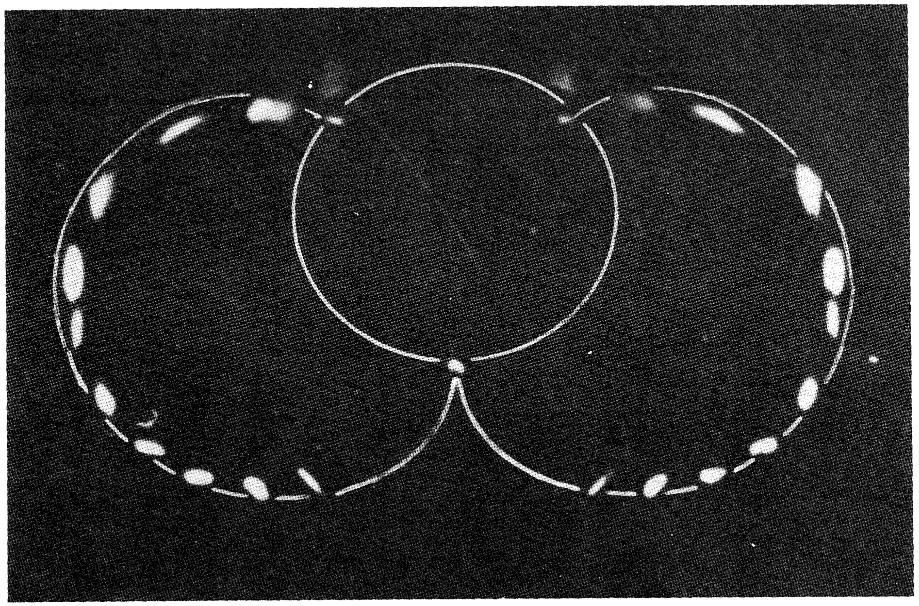

WITHOUT MESH SHIELD

ϕ_a = 700 V.

I_m = 3.0 AMPS

ϕ_{BEAM} = 4390, 3220, 2500, 1980, 1580, 1220, 1000, 810, 605, 450, 280, 195 VOLTS.

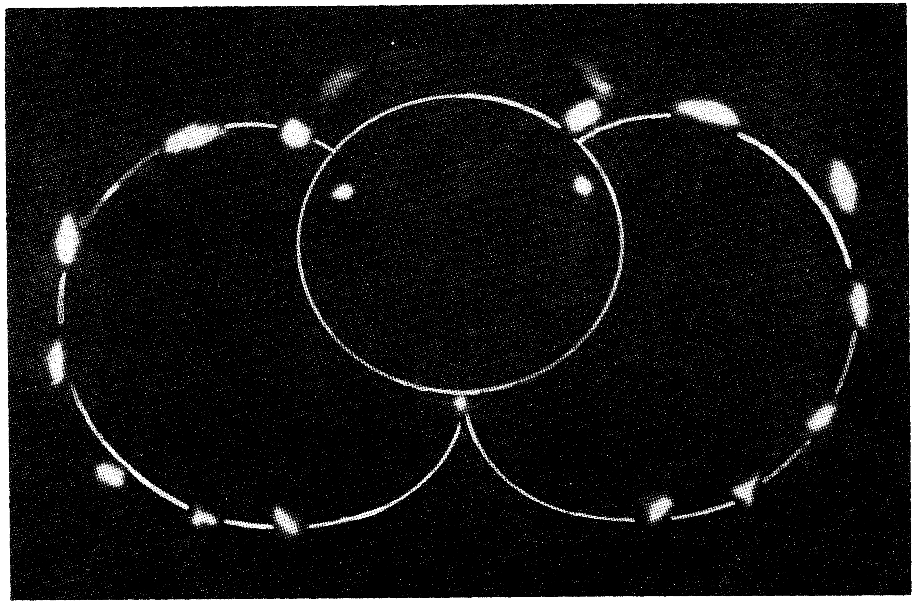

WITH MESH SHIELD

ϕ_a = 798 VOLTS

I_m = 3.2 AMPS

ϕ_{BEAM} = 4000, 2800, 2020, 1420, 1010, 760, 510, 330, 185 VOLTS

FIG. 10.4

TRAJECTRON DATA FOR THE CASE OF NON-EMITTING CATHODE WITH MAGNETIC FIELD (a = 2.48)

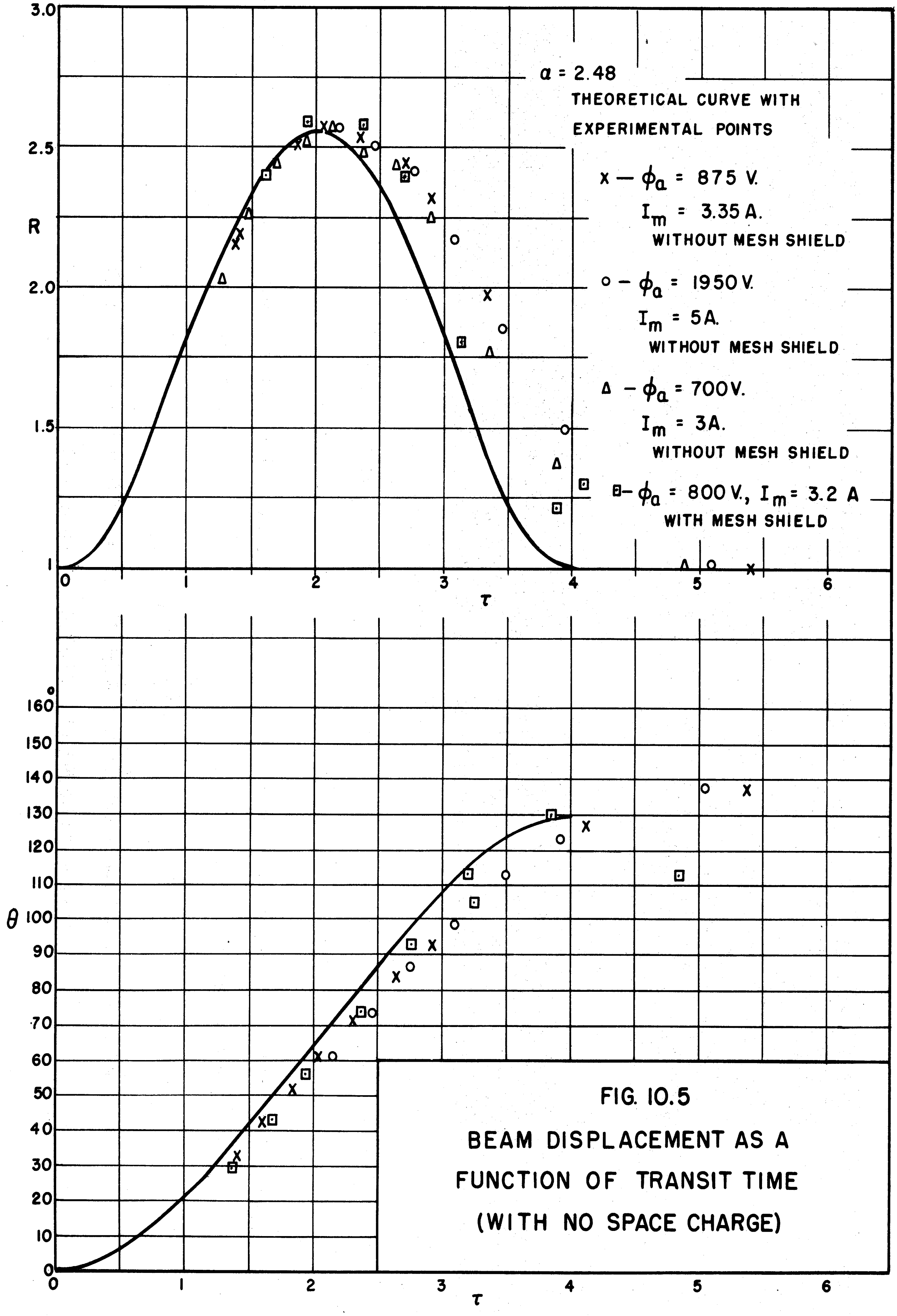

FIG. 10.5

BEAM DISPLACEMENT AS A FUNCTION OF TRANSIT TIME (WITH NO SPACE CHARGE)

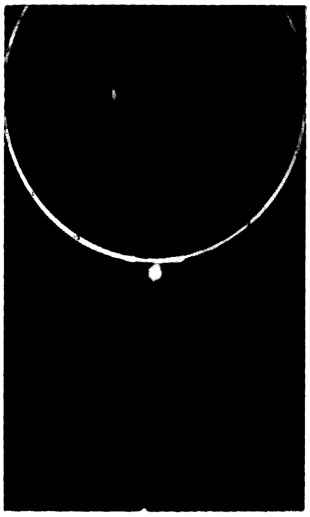

$\phi_a = 0$

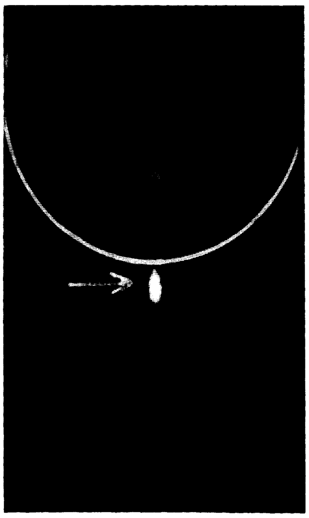

$\phi_{BEAM} = 4220$ V.

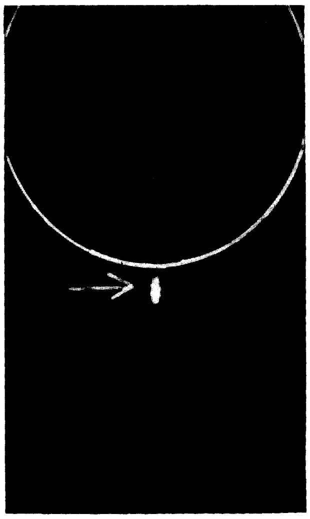

$\phi_{BEAM} = 3820$ V.

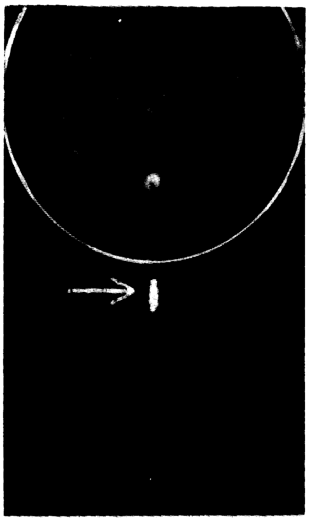

$\phi_{BEAM} = 3220$ V.

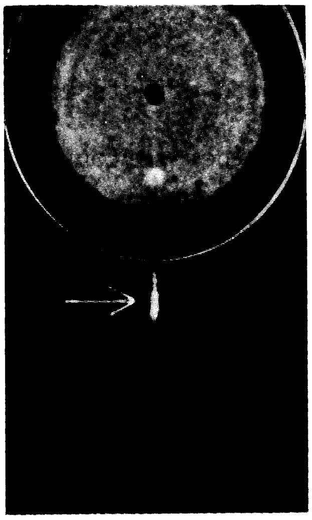

$\phi_{BEAM} = 2400$ V.

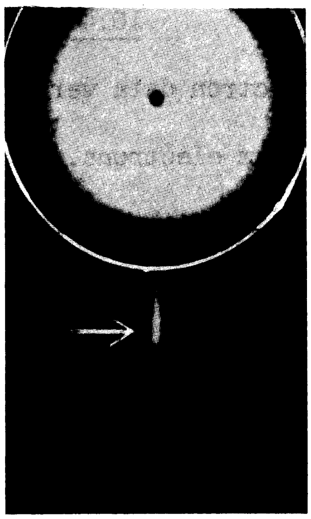

$\phi_{BEAM} = 1780$ V.

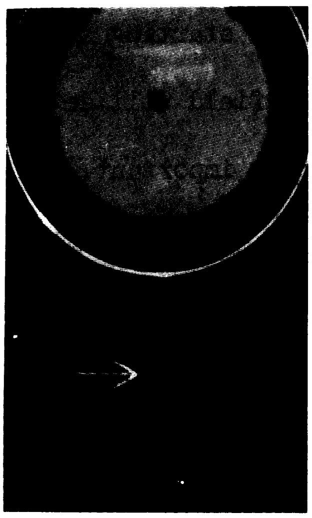

$\phi_{BEAM} = 1280$ V.

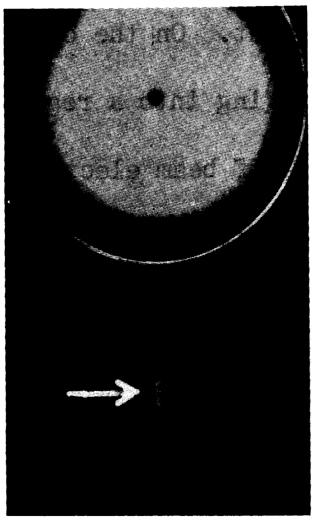

$\phi_{BEAM} = 1000$ V.

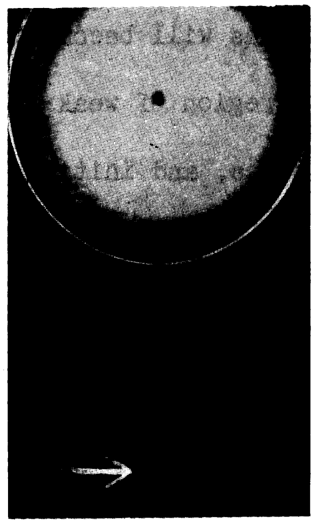

$\phi_{BEAM} = 710$ V.

FIG. 10.6

TRAJECTRON DATA FOR THE CYLINDRICAL DIODE

($\phi_a = 217$ V., $I_a = 120$ ma., $I_m = 0$)

Typical data photographs for the cutoff magnetron case are shown in Fig. 10.7. Each photograph includes several exposures of the spot. There is an exposure with the anode voltage removed showing the undeflected position of the spot. The other exposures are taken with fixed anode voltage and with several different beam voltages. The only difference in conditions between the two figures is in the orientation of the magnetic field.

10.4 Conclusions. The important sources of error in the trajectron data were found to be end effects and the initial conditions of beam electrons. In spite of rather serious end effects the data for the cases with non-emitting cathode agreed reasonably well with theoretical trajectories. It appears that end effects could be reduced in many problems to the point where fairly accurate trajectories could be traced out by the trajectron method.

A beam starting in a region of strong field and moving into a region of weak field will tend to focus, and differences in initial conditions will become less important. On the other hand a beam starting in a region of weak field and moving into a region of strong field will defocus, and initial conditions of beam electrons become more important. The extreme case occurs when part of the beam enters where the field is zero. In this case the deflected beam spreads out so much that it always extends back to the cathode. (See Fig. 10.6.) The trajectron cannot be used to obtain displacement as a function of time for this case. The shape of the orbit may or may not be given by the spot. There is an area of zero field near the cathode of any space-charge-limited vacuum tube, so that this extreme case is an important one.

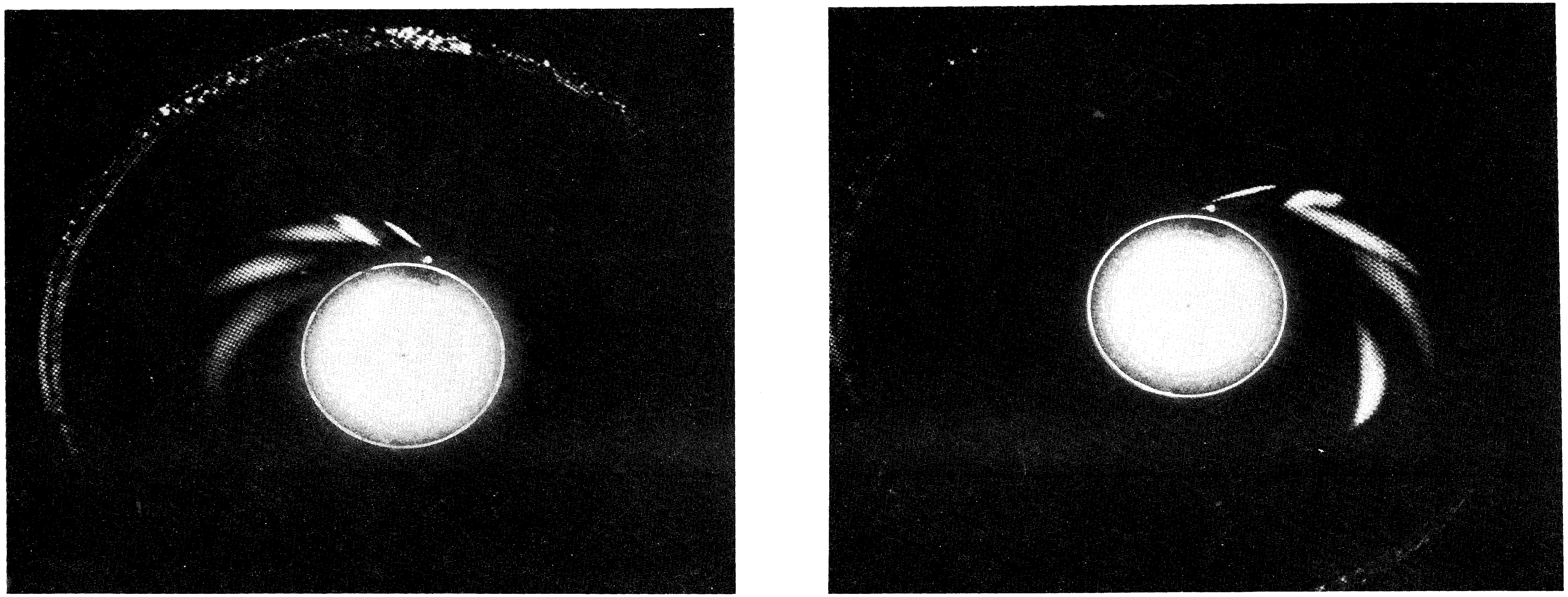

ϕ_a = 1550 VOLTS ; I_a = 10 MA ; I_m = 4 AMPS

ϕ_{BEAM} = 710, 1000, 1480, 2500, 4020 VOLTS

FIG. 10.7 TYPICAL DATA PHOTOGRAPHS FOR CUTOFF MAGNETRON CASE

For the magnetron the trajectron data could not be considered as representing the displacement of emitted electrons as a function of time, as is apparent from the size of the spots in Fig. 10.7. The reason is that the initial velocities and displacements of beam electrons differed too much from the initial conditions of emitted electrons. Although the data would be improved and more useful if the beam were made smaller and were more accurately aligned, the trajectron cannot be made to work as it was intended to, i.e., to have the spot position closely approximate displacement as a function of transit time for emitted electrons. It is pointed out in the preceding paragraph that the trajectron will never be successful when the beam must enter in a region where the field is zero, as it is near the cathode of any space-charge-limited vacuum tube.

In spite of this it is possible to obtain some information from the trajectron data because the character of the field is reflected in the shape and position of the deflected spots. The first observation that was made is that the beam electrons did not move as far from the cathode as would be expected if there were no secular space charge[1]. The conclusion is that the secular space charge is far from negligible, contrary to the usual assumption. A very rough estimate for typical conditions indicated that if the secular space charge distribution is that of the B_o solution (single-stream, or Brillouin solution), its density was approximately 58 percent of that of the B_o solution.

The second observed fact is that the spots in the trajectron data at the maximum radius part of their loop have a much greater radial width than predicted by calculations in which secular space charge was

---

1 Hok, G., "Space-Charge Equilibrium in a Magnetron -- A Statistical Approach," Technical Report No. 10, July 1951.

neglected. Two factors probably contribute to this. The first modification of the potential distribution due to the presence of secular space charge. The second is fluctuations of the electric field, which are known to occur in the d-c magnetron. Calculations indicate that both of these should have the same effect on the beam spot, to make it take on the shape and size which it is observed to have. It does not appear possible to tell the relative importance of these two phenomena.

The third observation on the cutoff magnetron concerns regions of negative resistance and inflections observed in the anode current-anode voltage curves in the cutoff region. These inflections in anode current were associated by Delcroix[1] with changes in the character of the space charge from one type of electron orbits to another. Some calculations neglecting secular space charge were made showing roughly the expected spot configuration for a beam entering space charge of the B_0, B_1, and B_2 types. The calculated beam spots indicated that changes from one type space charge to another should have resulted in a conspicuous change in the spot configuration. No such changes were observed in the spot configuration. There appear to be two possible explanations. The inflections may not be associated with changes in space charge type, but rather with some other phenomenon. The second possible explanation is that the inflections are associated with changes in the type of orbits of the electrons as they leave the cathode (i.e., the cathode accessible electrons), but these electrons contribute so little and the secular space charge contributes so much to the total space charge that changes in the orbits of

---

1 Delcroix, J. L., "Le Magnetron en Regime Statique de Coupure: Etude Expermentale," Comptes Rendus de l'Academie des Sciences, Vol. 234, June 9, 1952, pp. 2347-2349.

the cathode accessible space charge have a negligible effect on the beam spots.

11. Conclusions. (J. R. Black)

The Model 8 rectangular type cavity employing interdigital type anodes appears to be a promising structure for a wide variety of magnetron types.

A circuit has been developed for use with the Model 9 coaxial vane-bar anode magnetron to produce a mechanically tunable signal from 375 to 3750 mc. Also voltage tuning over a frequency range of 3000-4800 mc has been obtained using this tube in a waveguide circuit.

High power voltage-tunable operation employing a coaxial vane-bar anode circuit does not look promising mainly due to the low shunt impedance appearing across the anode sets.

Voltage-tunable magnetrons employing interdigital anodes and operating in a ridge waveguide circuit have been developed for operation in the S-band region. Frequency deviations of 1000 mc can be obtained which are a linear function of the anode voltage. The power output may vary from 200 mw to 2 watts over this frequency range. Although the cathode temperature is quite critical for good operation this temperature can be readily adjusted for a stabel signal. A total of four such tubes with one ridge-waveguide circuit were shipped to the Signal Corps for evaluation.

The possibility of obtaining ten watts of wide band voltage-tunable power from an interdigital anode magnetron appears quite encouraging at this stage although this hasn't been accomplished.

An analysis has been made of the role the cathode circuit plays in the behavior of magnetrons. This analysis has led to the design of cathode structures having little effect on magnetron operation over a frequency range greater than three to one.

The experimental investigation of the space-charge distribution within a d-c smooth bore magnetron has been completed. An analysis of the results is being made and will be published in the near future. Although the experiment was discouraging in that the exploring electron beam displacement could not be measured with sufficient accuracy to calculate the potential distribution and therefore the space-charge distribution, the character of the electric field could be determined.

A theoretical study of the initiation of oscillations in electron streams through crossed fields has been made and published as a Technical Report.

12.

APPENDIX

12A. Tubes Constructed Within the Period Covered by This Report

(J. W. Van Natter)

A history of tubes constructed during this period is presented in Table 12A.1. Construction was started on a total of sixty-eight tubes, five of which were not completed. Most tubes were rebuilt several times mainly for repair or for changing the type cathode employed.

Considerable difficulty was encountered initially when molybdenum wires were used as anodes in the Model 11 series of magnetron. Complete outgassing of the molybdenum was difficult resulting in an arc occurring between the cathode and one anode wire which melted the molybdenum anode. The use of tungsten for the anodes eliminated this trouble.

Out of the total of sixty-three tubes completed two were never operated due to breakage and a leak.

Of the sixty-one tube bodies operated thirty-two are still in operating order.

Actually more than sixty-one tubes were tested due to the fact that some tube bodies were operated with a variety of changes.

TABLE 12A.1

Tube No.	Model No.	Date Assembled	History	Operated	Present Condition
64	9B	12-51	1. Oxide cathode. 2. Cracked glass - repaired.	Yes	Operable
65	9B	11-51	1. Oxide cathode. 2. Gassy.	Yes	Inoperable
66	9B	11-51	1. Tungsten cathode.	Yes	Operable
	9B	11-51	1. Oxide cathode.	Yes	Operable
68	9B	11-51	1. Oxide cathode No. 8022. 2. Broken - repaired. 3. Cracked seal - repaired, inserted oxide cathode No. 8026. 4. Cracked seal - repaired.	Yes	Operable
69	9B	11-51	1. Modified QK-59 cathode emission area 2/3 of original.	Yes	Operable
70	9C	12-51	1. Cathode No. 8022.	Yes	Inoperable
71	9C	11-51	1. Not completed.	No	Inoperable
72	9C	11-51	1. Not completed.	No	Inoperable
73	10	2-52	1. Litton cathode No. 1-10-A. 2. Cracked seal - repaired - gassy.	Yes	Inoperable

Tube No.	Model No.	Date Assembled	History	Operated	Present Condition
74	11	2-52	1. Oxide cathode No. 8027. 2. Backheating melted cathode. 3. Repaired cathode No. 8027 4. Broken glass seal - repaired. 5. Backheating melted cathode.	Yes	Inoperable
75	9E	3-52	1. Oxide cathode No. 8022.	Yes	Operable
76	9E	5-52	1. Oxide cathode No. 8022.	Yes	Inoperable
77	11	2-52	1. Thoriated tungsten cathode No. 8030. 2. Anode melted.	Yes	Inoperable
78	9B	5-52	1. Cathode No. 8026. 2. Cracked seal - repaired. 3. Tube broken - repaired. 4. Gassy.	Yes	Inoperable
79	8D	5-52	1. Continuously pumped - porous cavity.	Yes	Inoperable
80	11	5-52	1. Oxide cathode No. 8027. 2. Cracked seal - repaired. 3. Thoriated tungsten cathode No. 8030. 4. Glass surrounding anode structure melted - repaired. 5. AuCu joint leaked - repaired. 6. Anode melted.	Yes	Inoperable
81	11	6-51	1. Oxide button cathode No. 8032. 2. Coated with nickel - repaired. 3. Tungsten cathode No. 8030. 4. Anode melted - repaired. 5. Tungsten cathode No. 8030 6. Anode melted.	Yes	Inoperable

TABLE 12A.1 (Contd.)

Tube No.	Model No.	Date Assembled	History	Operated	Present Condition
82	11	6-51	1. Oxide button cathode No. 8032. 2. Melted cathode.	Yes	Inoperable
83	11	7-51	1. Oxide button cathode No. 8032. 2. Tungsten cathode No. 8030. 3. Anode melted - repaired. 4. Tungsten cathode No. 8030. 5. Glass surrounding anode structure melted - repaired. 6. AuCu joint leaked - repaired. 7. Broken.	Yes	Inoperable
84	11	8-51	1. Oxide button cathode No. 8032. 2. Cathode melted - repaired. 3. Tungsten cathode No. 8030. 4. Glass surrounding anode structure melted - repaired. 5. Anode melted.	Yes	Inoperable
85	11	8-51	1. Tungsten cathode No. 8039. 2. Glass surrounding anode structure melted - repaired. 3. Anode melted - repaired. 4. Glass surrounding anode structure melted - repaired. 5. AuCu joint leaked - repaired. 6. Pole piece converted to make Model 11B	Yes	Operable
86	9B	8-51	1. Oxide button cathode No. 8032	Yes	Inoperable

Tube No.	Model No.	Date Assembled	History	Operated	Present Condition
87	11B	11-51	1. Oxide button cathode No. 8034. 2. Anode shorted to cathode. 3. Tungsten cathode No. 8030. 4. Anode melted - repaired. 5. Glass surrounding anode structure melted - repaired. 6. Anode melted.	Yes	Inoperable
88	11B	11-51	1. Tungsten cathode No. 8034. 2. Anode melted - repaired. 3. Anode melted - repaired. 4. Anode melted - repaired.	Yes	Operable
89	11A	9-51	1. Tungsten cathode No. 8030. 2. Anode melted - repaired. 3. Glass surrounding anode structure melted - repaired. 4. Glass surrounding anode structure melted - repaired. 5. Anode melted.	Yes	Inoperable
90	11A	9-51	1. Thoriated tungsten cathode No. 8039. 2. Glass surrounding anode structure melted - repaired. 3. Cracked glass seal - repaired.	Yes	Operable
91	9B	8-51	1. Tungsten cathode No. 8031.	Yes	Inoperable
92	11B	10-51	1. Tungsten cathode No. 8039. 2. Anode melted - repaired.	Yes	Inoperable
93	11	2-53	1. Tungsten cathode No. 8040.	Yes	Operable

TABLE 12A.1 (Contd.)

Tube No.	Model No.	Date Assembled	History	Operated	Present Condition
94	11	2-53	1. Tungsten cathode No. 8041. 2. Cathode shorted - repaired. 3. Tube flashed with copper - repaired.	Yes	Operable
95	11E	5-53	1. Tungsten cathode No. 8044. 2. Broken.	No	Inoperable
96	11E	5-53	1. Tungsten cathode No. 8044. 2. Broken - repaired. 3. Broken.	Yes	Inoperable
97	11D	6-53	1. Tungsten cathode No. 8049.	Yes	Operable
98	11D	7-53	1. Oxide cathode No. 8027.	Yes	Operable
99	11B	4-53	1. Tungsten cathode No. 8044. 2. Cathode vaporized - repaired. 3. Shipped to Electronic Defense Group, University of Michigan	Yes	Operable
100	11B	3-53	1. Tungsten cathode No. 8044. 2. Shipped to Signal Corps.	Yes	Operable
101	11C	12-52	1. Tungsten cathode No. 8043. 2. Leaked - repaired. 3. Misaligned cathode - repaired. 4. Anode melted.	Yes	Inoperable
102	12	1-53	1. Tungsten cathode No. 8042.	Yes	Operable

Tube No.	Model No.	Date Assembled	History	Operated	Present Condition
103	12	1-53	1. Tungsten cathode No. 8042. 2. Pole piece melted.	Yes	Inoperable
104	11CA	2-53	1. Tungsten cathode No. 8043. 2. Anode melted - repaired. 3. Anode melted - repaired.	Yes	Operable
105	12A	5-53	1. Tungsten cathode No. 8053. 2. Modified cathode. 3. Anode melted.	Yes	Inoperable
106	12A	4-53	1. Tungsten cathode No. 8050. 2. Anode melted.	Yes	Inoperable
107	11B	3-53	1. Tungsten cathode No. 8044. 2. Shipped to Signal Corps.	Yes	Operable
108	11B	4-53	1. Tungsten cathode No. 8044. 2. Shipped to Signal Corps.	Yes	Operable
109	11B	5-53	1. Tungsten cathode No. 8044. 2. Tungsten cathode No. 8051.	Yes	Operable
110	11B	4-53	1. Tungsten cathode No. 8044. 2. Pole piece overheated melting copper - repaired. 3. Overheated cathode - repaired.	Yes	Inoperable
111	11B	4-53	1. Tungsten cathode No. 8044. 2. Glass surrounding anode structure melted - repaired.	Yes	Operable
112	11B	4-53	1. Tungsten cathode No. 8044. 2. Shipped to Signal Corps.	Yes	Operable

TABLE 12A.1 (Contd.)

Tube No.	Model No.	Date Assembled	History	Operated	Present Condition
113	11B	4-53	1. Tungsten cathode No. 8048.	Yes	Inoperable
114	13	5-53	1. Tungsten cathode No. 8044. 2. Cathode removed - used for cold test.	Yes	Inoperable
115	13	5-53	1. Tungsten cathode No. 8044.	Yes	Operable
116	11B	4-53	1. Tungsten cathode No. 8051. 2. Glass cracked - repaired. 3. Shipped to Electronic Defense Group, University of Michigan	Yes	Operable
117	11GA	12-53	Not completed	No	Inoperable
118	11F	8-53	1. Tungsten cathode No. 8045. 2. Tungsten cathode No. 8054.	Yes	Operable
119	11FA	10-53	1. Tungsten cathode No. 8055. 2. Tungsten cathode No. 8061.	Yes	Operable
120	14	10-53	1. Tungsten cathode No. 8044. 2. Melted copper on pole piece.	Yes	Inoperable
121	11B		1. Not completed.	No	Inoperable
122	11CA		1. Not completed.	No	Inoperable
123	12A	10-53	1. Tungsten cathode No. 8057 2. Melted pole piece.	Yes	Inoperable

Tube No.	Model No.	Date Assembled	History	Operated	Present Condition
124	12B	10-53	1. Tungsten cathode No. 8060. 2. Pole piece melted.	Yes	Inoperable
125	11G	11-53	1. Tungsten cathode No. 8062. 2. Pole piece overheated, melting copper - repaired.	Yes	Operable
126	11G	11-53	1. Tungsten cathode No. 8062. 2. Shipped to Electronic Defense Group, University of Michigan.	Yes	Operable
127	11G	11-53	1. Tungsten cathode No. 8062.	Yes	Operable
128	11B	11-53	1. Tungsten cathode No. 8055.	Yes	Operable
129	11B	11-53	1. Tungsten cathode No. 8044. 2. Leaky seal.	No	Inoperable
130	12B	11-53	1. Tungsten cathode No. 8059. 2. Tungsten cathode No. 8059 modified. 3. Melted pole piece.	Yes	Inoperable
131	15	11-53	1. Tungsten cathode No. 8062 2. Melted pole piece.	No	Inoperable

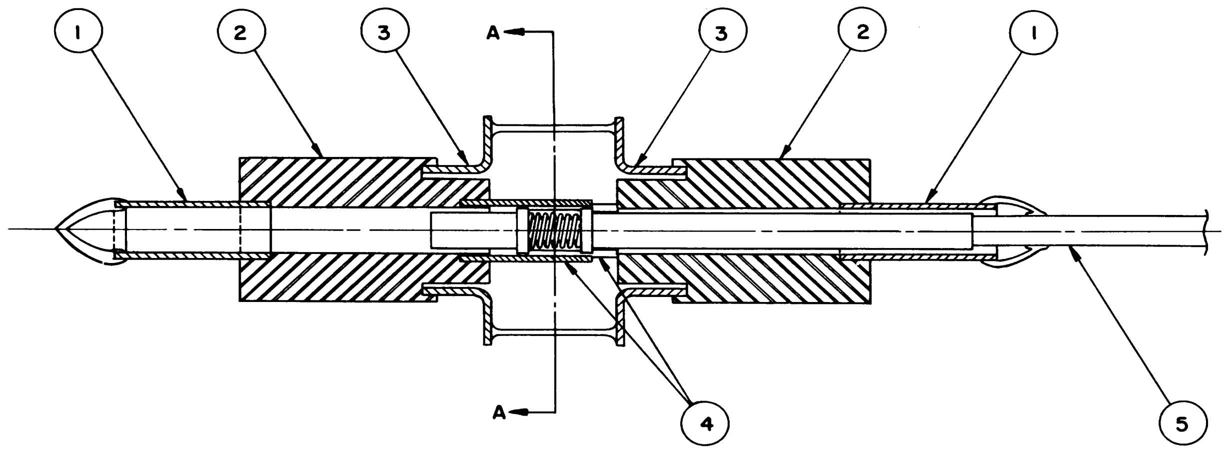

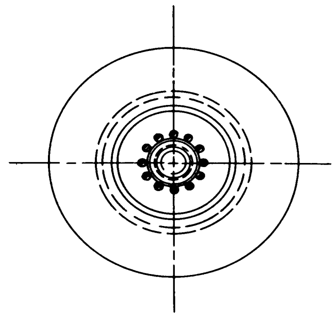

SECTION A-A

FIG. 12B.1

ALL DIMENSIONS UNLESS OTHERWISE SPECIFIED MUST BE HELD TO A TOLERANCE - FRACTIONAL ± 1/64," DECIMAL ± .005," ANGULAR ± 1/2°

ENGINEERING RESEARCH INSTITUTE UNIVERSITY OF MICHIGAN ANN ARBOR MICHIGAN	DESIGNED BY J.A. BOYD DRAWN BY PKW CHECKED BY	APPROVED BY SCALE 2X DATE 9-12-52
PROJECT 2009	TITLE INTERDIGITAL EXTERNAL CAVITY MAGNETRON MODEL 11B	
CLASSIFICATION	DWG. NO. B-10,011 B	
ISSUE / DATE		

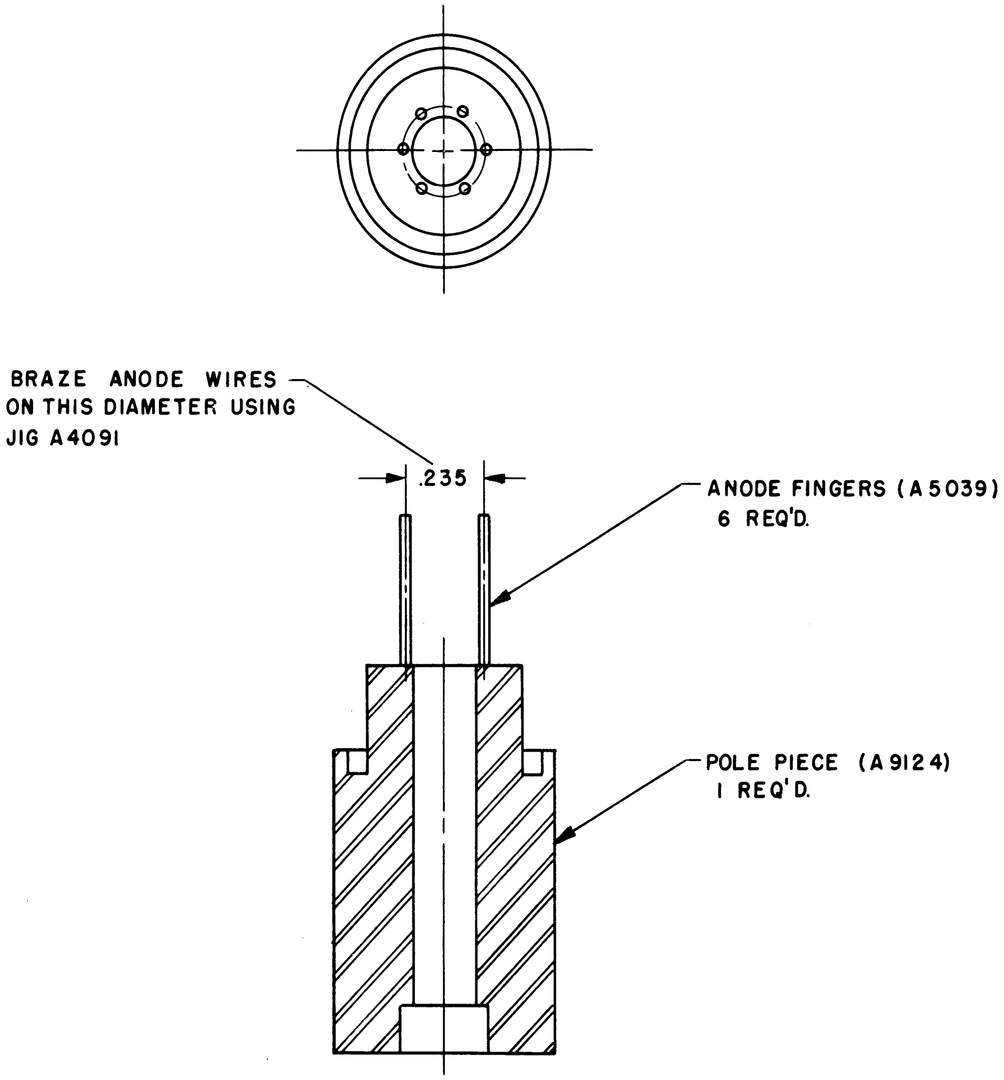

FIG. 12B.2

SUB—ASSEMBLY — 2 REQ'D.

ALL DIMENSIONS UNLESS OTHERWISE SPECIFIED MUST BE HELD TO A TOLERANCE - FRACTIONAL ± 1/64," DECIMAL ± .005," ANGULAR ± 1/2°

ENGINEERING RESEARCH INSTITUTE
UNIVERSITY OF MICHIGAN
ANN ARBOR MICHIGAN

DESIGNED BY JAB	APPROVED BY
DRAWN BY PLW	SCALE 2 X
CHECKED BY V.R.B.	DATE 12-17-53

PROJECT
2009

TITLE
ANODE AND POLE PIECE
SUB-ASSEMBLY

ISSUE	DATE
2	12-17-53

CLASSIFICATION

DWG. NO. A-10,011B-1

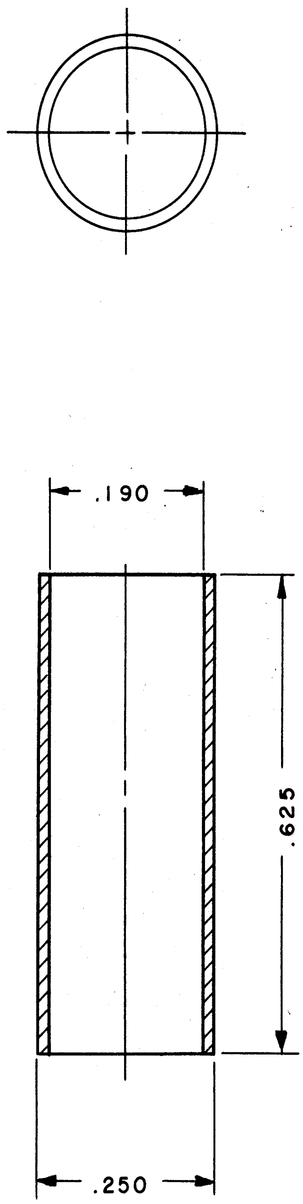

FIG.12B.3

KOVAR TUBING (STUPAKOFF #90250018) – 2 REQ'D.

ALL DIMENSIONS UNLESS OTHERWISE SPECIFIED MUST BE HELD TO A TOLERANCE - FRACTIONAL ± 1/64," DECIMAL ± .005," ANGULAR ± 1/2°

ENGINEERING RESEARCH INSTITUTE UNIVERSITY OF MICHIGAN ANN ARBOR MICHIGAN	DESIGNED BY J.A.B. / APPROVED BY DRAWN BY N.N. / SCALE 4X CHECKED BY V.R.B. / DATE 4-10-52
PROJECT 2009	TITLE KOVAR SLEEVE
ISSUE 2 / DATE 4-10-53 / CLASSIFICATION	DWG. NO. A- 9097

DWG. NO. A

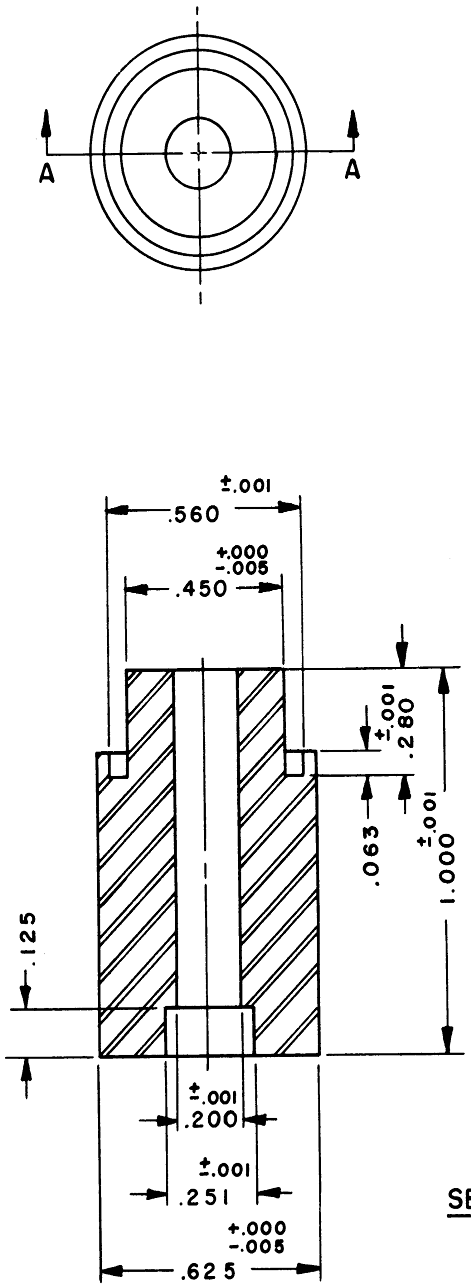

SECTION A-A

FIG. 12B.4

HRS — 2 REQ'D.

ALL DIMENSIONS UNLESS OTHERWISE SPECIFIED MUST BE HELD TO A TOLERANCE - FRACTIONAL ± 1/64," DECIMAL ± .005," ANGULAR ± 1/2°

		ENGINEERING RESEARCH INSTITUTE UNIVERSITY OF MICHIGAN ANN ARBOR MICHIGAN	DESIGNED BY JRB	APPROVED BY
			DRAWN BY PLW	SCALE 2X
			CHECKED BY	DATE 10-19-53
		PROJECT 2009	TITLE POLE PIECE	
1	10·19·53	CLASSIFICATION	DWG. NO. A- 9124	
ISSUE	DATE			

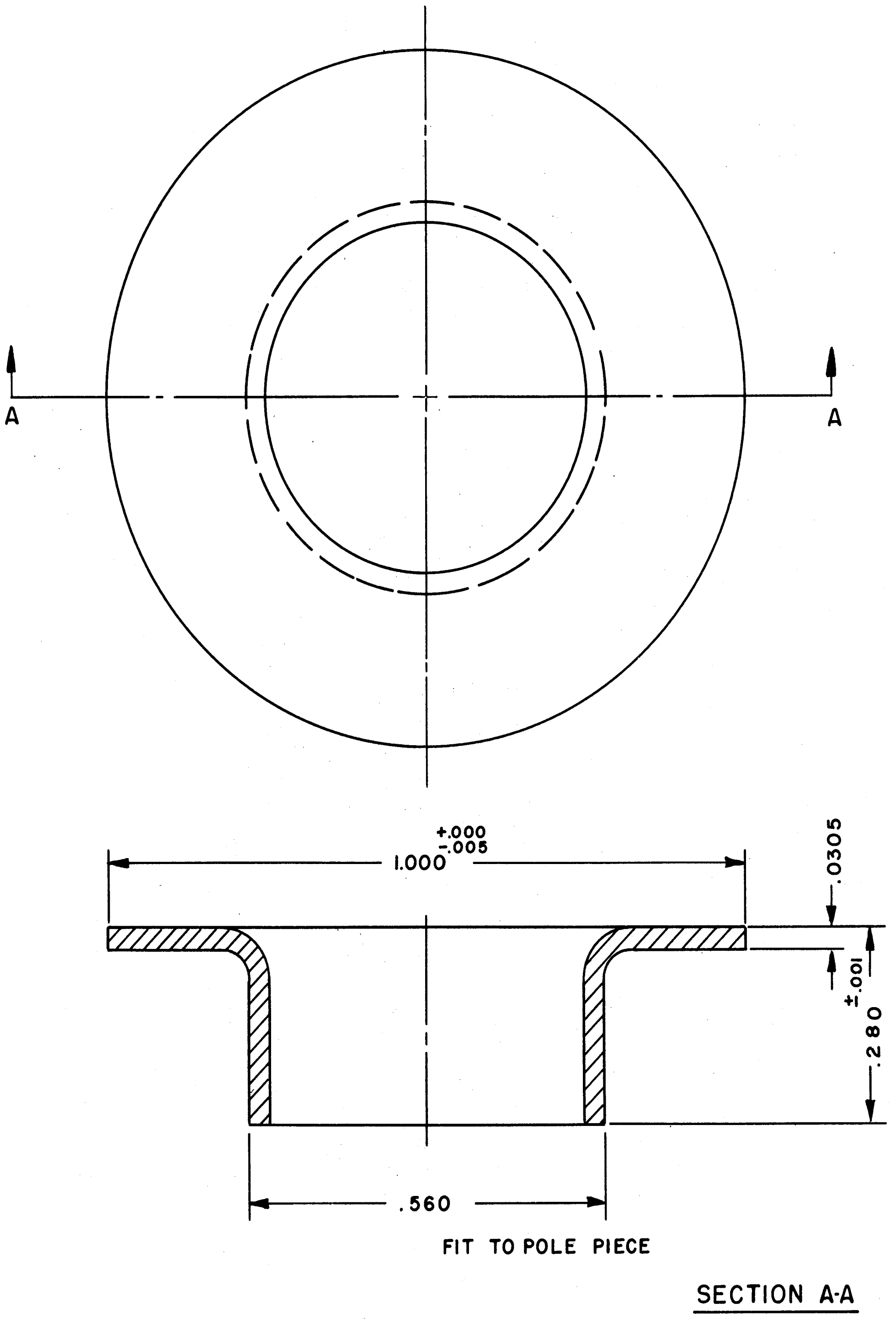

FIG. 12B.5

KOVAR (STUPAKOFF #941002) — 2 REQ'D.

ALL DIMENSIONS UNLESS OTHERWISE SPECIFIED MUST BE HELD TO A TOLERANCE - FRACTIONAL ± 1/64," DECIMAL ± .005," ANGULAR ± 1/2°

		ENGINEERING RESEARCH INSTITUTE UNIVERSITY OF MICHIGAN ANN ARBOR MICHIGAN	DESIGNED BY J.A.B.	APPROVED BY
			DRAWN BY N.N.	SCALE 4X
			CHECKED BY V.R.B.	DATE 4-9-52
		PROJECT 2009	TITLE KOVAR FLANGED FLAT-BOTTOM CUP	
2	4-9-53	CLASSIFICATION	DWG. NO. A-9098	
ISSUE	DATE			

LET.	DATE	APPR.	CHANGE
A	5-19-53	V.R.B.	.445 WAS .520
B	"	"	TUNGSTEN WAS MOLY.
C	12-17-53		.395 WAS .445

DWG. NO. A

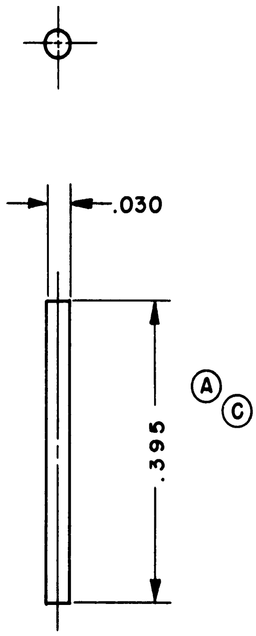

FIG. 12B.6

(B)

TUNGSTEN WIRE – 12 REQ'D.

ALL DIMENSIONS UNLESS OTHERWISE SPECIFIED MUST BE HELD TO A TOLERANCE - FRACTIONAL ± 1/64" DECIMAL ± .005" ANGULAR ± 1/2°

ENGINEERING RESEARCH INSTITUTE
UNIVERSITY OF MICHIGAN
ANN ARBOR MICHIGAN

DESIGNED BY J.A.B.	APPROVED BY
DRAWN BY P.L.W.	SCALE 4 X
CHECKED BY V.R.B.	DATE 9-11-52

PROJECT 2009

TITLE
ANODE FINGERS –
MODEL 11B MAGNETRON

ISSUE	DATE
12	9-11-52

CLASSIFICATION

DWG. NO. A-5039

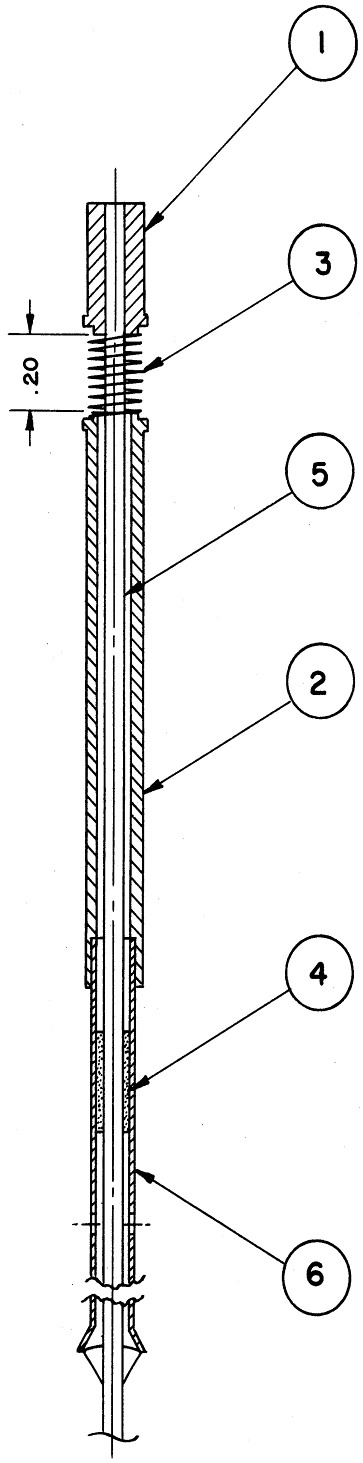

FIG. 12B.7

ALL DIMENSIONS UNLESS OTHERWISE SPECIFIED MUST BE HELD TO A TOLERANCE - FRACTIONAL ± 1/64," DECIMAL ± .005," ANGULAR ± 1/2°

		ENGINEERING RESEARCH INSTITUTE UNIVERSITY OF MICHIGAN ANN ARBOR MICHIGAN	DESIGNED BY VAN NATTER	APPROVED BY
			DRAWN BY PLW	SCALE 2X
			CHECKED BY [signature]	DATE 1-23-53
		PROJECT 2009	TITLE TUNGSTEN CATHODE FOR MODELS 11B & 11E MAGNETRONS	
1	1-23-53	CLASSIFICATION	DWG. NO. A-8044	
ISSUE	DATE			

DWG. NO. A

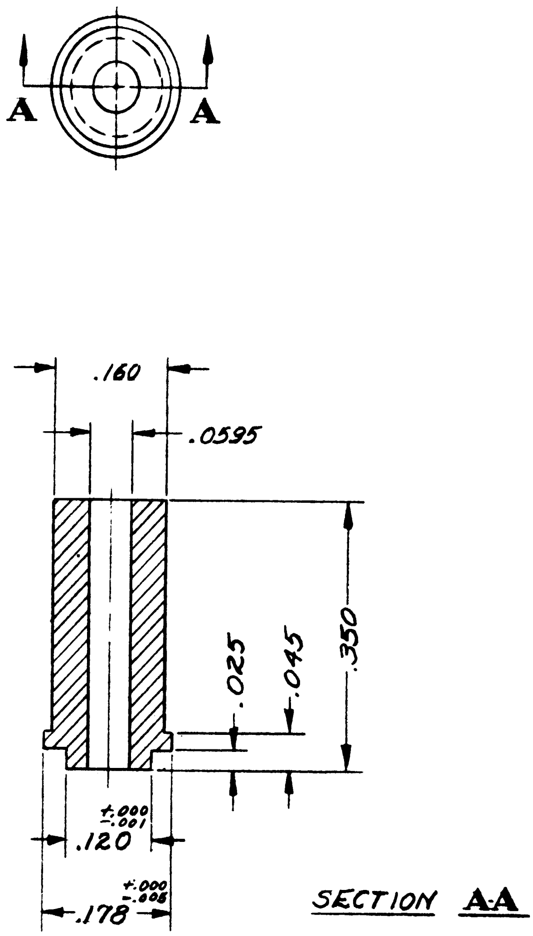

FIG. 12B.8

MOLYBDENUM - 1 REQ'D.

ALL DIMENSIONS UNLESS OTHERWISE SPECIFIED MUST BE HELD TO A TOLERANCE - FRACTIONAL ± 1/64," DECIMAL ± .005," ANGULAR ± 1/2°

ENGINEERING RESEARCH INSTITUTE UNIVERSITY OF MICHIGAN ANN ARBOR MICHIGAN	DESIGNED BY VAN NATTER	APPROVED BY
	DRAWN BY PLW	SCALE 4X
	CHECKED BY VRB	DATE 1-23-53
PROJECT 2009	TITLE UPPER END HAT	
CLASSIFICATION	DWG. NO. A- 8044-1	

ISSUE	DATE

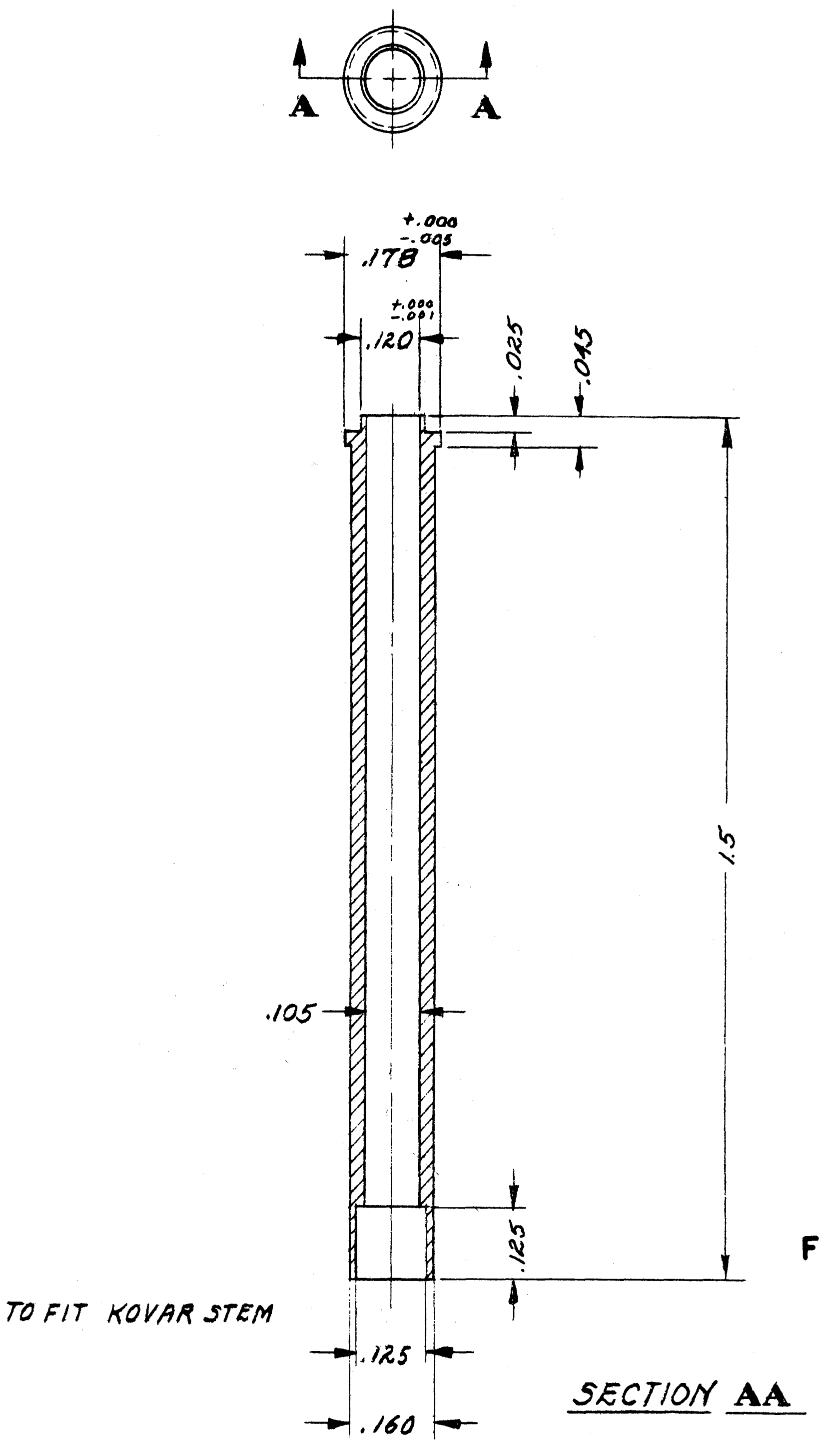

FIG. 12B.9

MOLYBDENUM - 1 REQ'D

ALL DIMENSIONS UNLESS OTHERWISE SPECIFIED MUST BE HELD TO A TOLERANCE - FRACTIONAL ± 1/64," DECIMAL ± .005," ANGULAR ± 1/2°

		ENGINEERING RESEARCH INSTITUTE UNIVERSITY OF MICHIGAN ANN ARBOR MICHIGAN	DESIGNED BY VAN NATTER	APPROVED BY
			DRAWN BY PLW	SCALE 3X
			CHECKED BY VRB	DATE 1-22-53
		PROJECT 2009	TITLE LOWER END HAT	
1	1-22-53	CLASSIFICATION	DWG. NO. A-8044-2	
ISSUE	DATE			

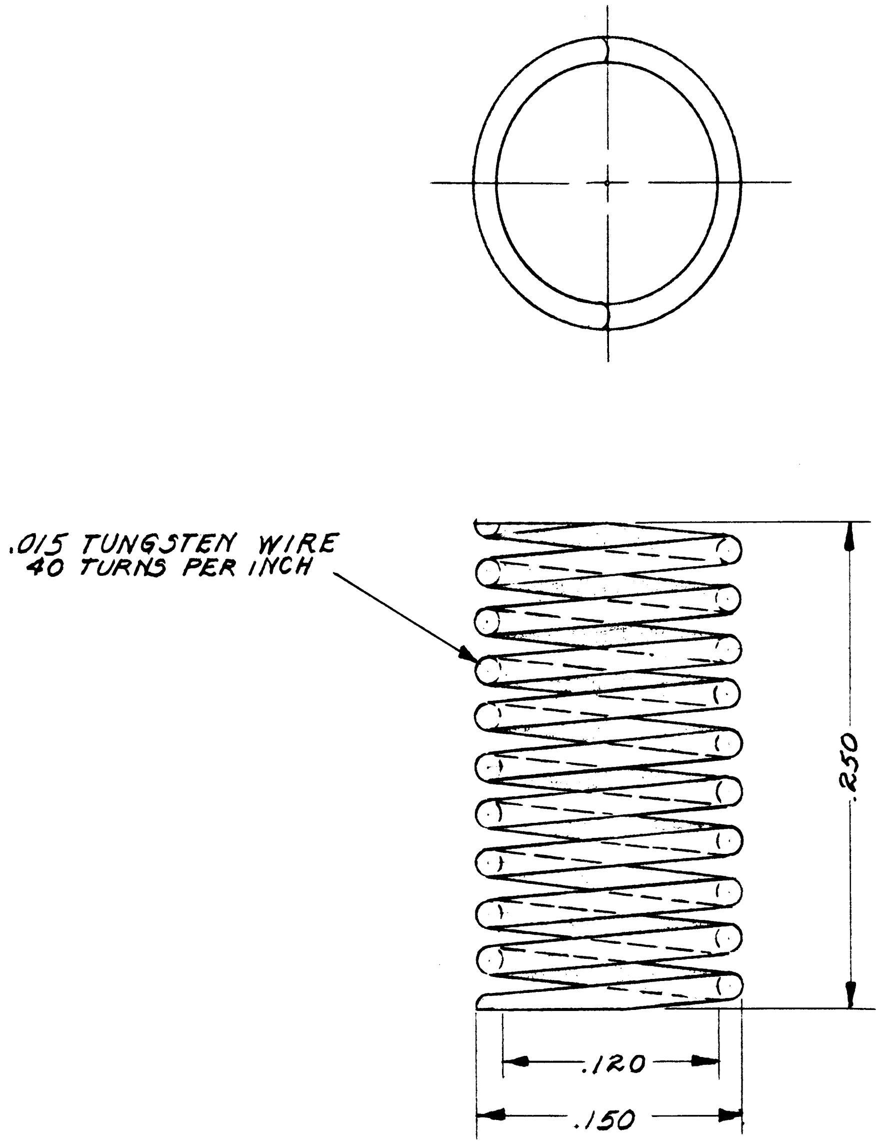

FIG. 12 B.10

.015 TUNGSTEN WIRE - 1 REQ'D.

ALL DIMENSIONS UNLESS OTHERWISE SPECIFIED MUST BE HELD TO A TOLERANCE - FRACTIONAL ± 1/64," DECIMAL ± .005," ANGULAR ± 1/2°

ENGINEERING RESEARCH INSTITUTE
UNIVERSITY OF MICHIGAN
ANN ARBOR MICHIGAN

DESIGNED BY VAN NATTER	APPROVED BY
DRAWN BY PLW	SCALE 10X
CHECKED BY [illegible]	DATE 1-23-53

PROJECT 2009

TITLE TUNGSTEN FILAMENT

CLASSIFICATION

ISSUE | DATE

DWG. NO. A-8044-3

DWG. NO. A

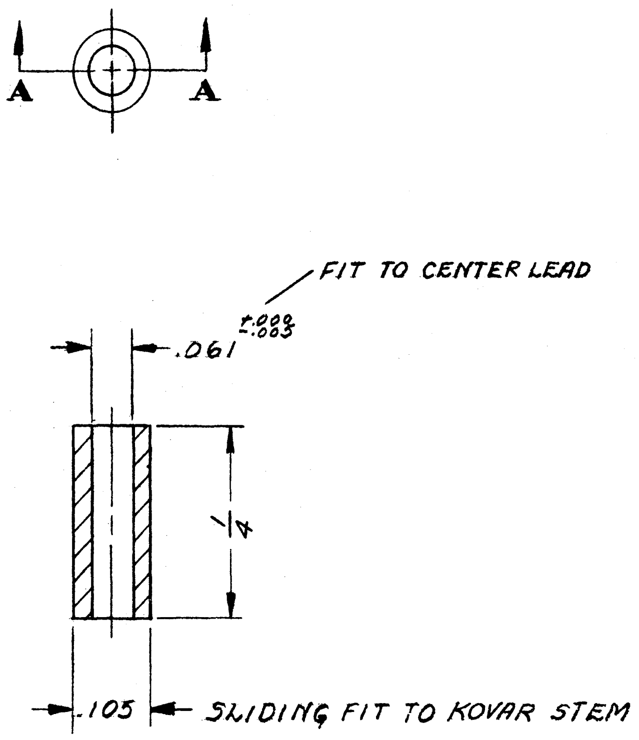

SECTION A-A

FIG. 12B. 11

ALSIMAG 222 - 1 REQ'D.

ALL DIMENSIONS UNLESS OTHERWISE SPECIFIED MUST BE HELD TO A TOLERANCE - FRACTIONAL ± 1/64," DECIMAL ± .005," ANGULAR ± 1/2°

ENGINEERING RESEARCH INSTITUTE UNIVERSITY OF MICHIGAN ANN ARBOR MICHIGAN	DESIGNED BY VAN HATTER — APPROVED BY DRAWN BY PLW — SCALE 4X CHECKED BY VRB — DATE 1-26-53
PROJECT 2009	TITLE INSULATOR
CLASSIFICATION	DWG. NO. A-8044-4
ISSUE 1 — DATE	

DWG. NO. A

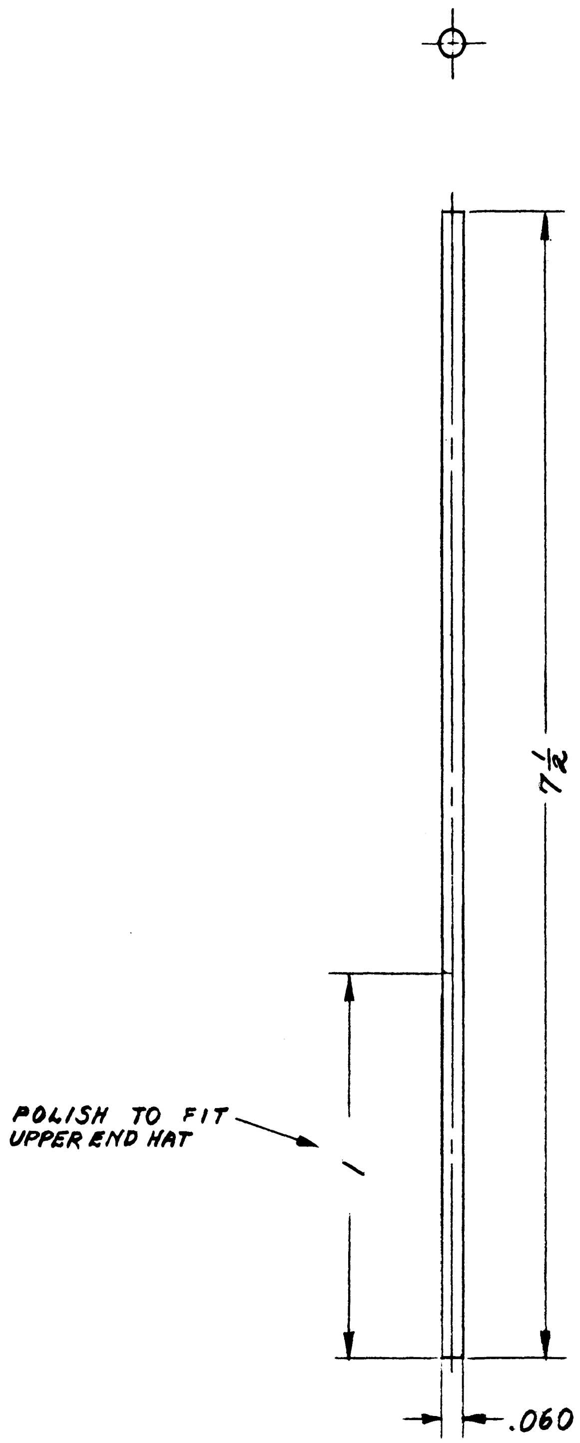

FIG. 12B. 12

MOLYBDENUM - 1 REQ'D.

ALL DIMENSIONS UNLESS OTHERWISE SPECIFIED MUST BE HELD TO A TOLERANCE - FRACTIONAL ± 1/64." DECIMAL ± .005." ANGULAR ± 1/2°

ENGINEERING RESEARCH INSTITUTE UNIVERSITY OF MICHIGAN ANN ARBOR MICHIGAN	DESIGNED BY DICKER	APPROVED BY JRB
	DRAWN BY PLW	SCALE 2X
	CHECKED BY VKR	DATE 11-17-52
PROJECT 2009	TITLE CENTER CONDUCTOR	
CLASSIFICATION	DWG. NO. A-8040-3	

ISSUE	DATE

	CHANGES	DATE	APPR.
A	ADDED NOTE "#55 DRILL THRU" & DIM 3/4.	11-25-52	

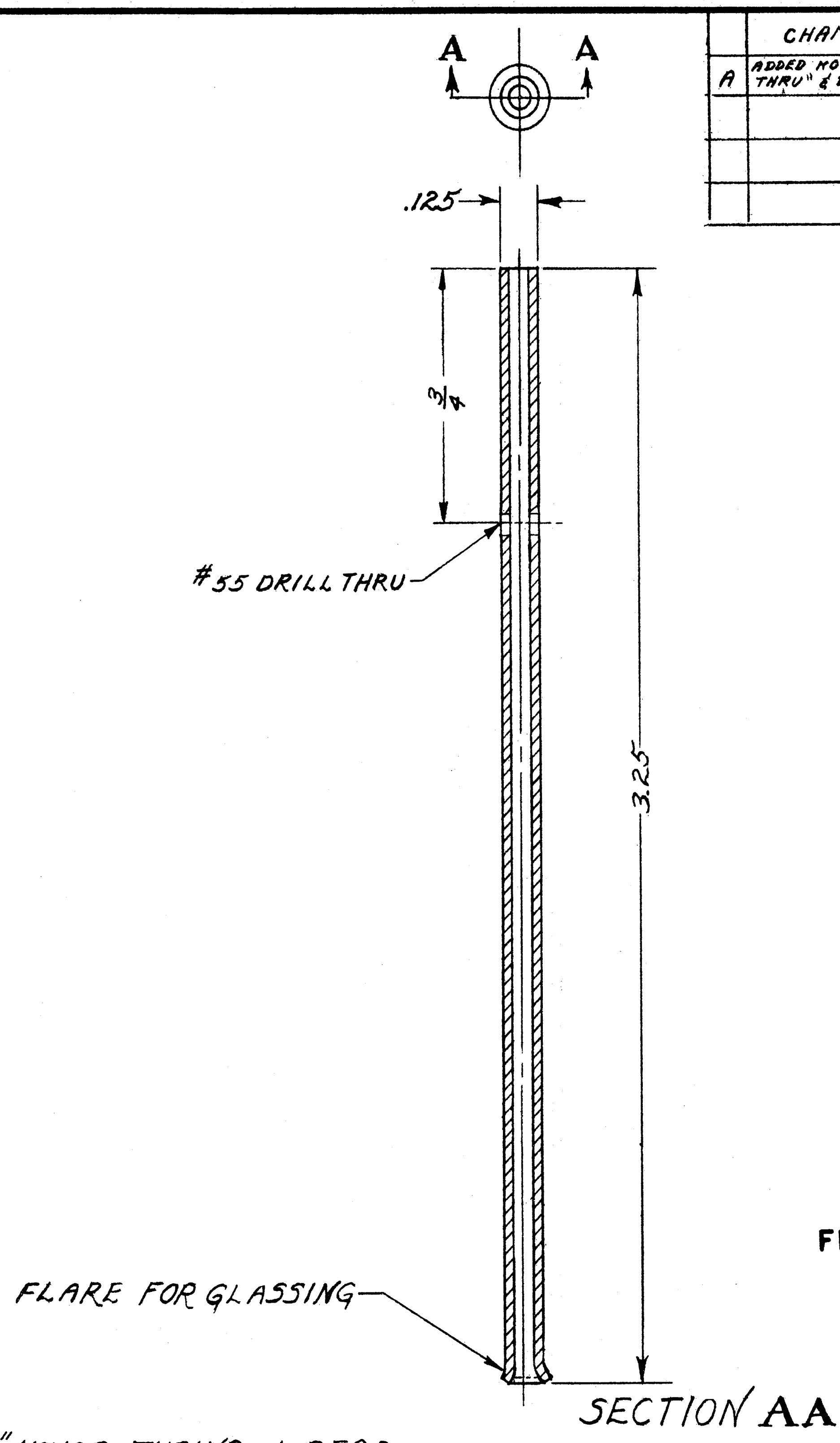

FIG. 12B. 13

1/8" KOVAR TUBING 1 REQD.

ALL DIMENSIONS UNLESS OTHERWISE SPECIFIED MUST BE HELD TO A TOLERANCE - FRACTIONAL ± 1/64," DECIMAL ± .005," ANGULAR ± 1/2°

ENGINEERING RESEARCH INSTITUTE
UNIVERSITY OF MICHIGAN
ANN ARBOR MICHIGAN

DESIGNED BY JAB | APPROVED BY JRB
DRAWN BY PLW | SCALE 2X
CHECKED BY [illegible] | DATE 7-1-52

PROJECT 2009

TITLE LOWER STEM

ISSUE 1 | DATE 7-1-52

CLASSIFICATION

DWG. NO. A- 8030-6

12C. Construction Techniques Employed in the Assembly of the Voltage-Tunable Magnetrons (J. W. Van Natter)

The following is a brief discussion of the techniques employed in the assembly of voltage-tunable magnetrons constructed at this laboratory. In general, standard construction techniques are used. A Model 11B assembly drawing is referred to in this description for clarity, however, the techniques described apply to all voltage-tunable magnetrons.

Brazing Operations

Three gold-copper (63% copper) brazes per pole piece made in a hydrogen atmosphere are required for the assembly of all tubes of the Model 11, 12, and 15 series. One ring of solder wire, .025 inch in diameter, is used for each braze. The iron pole pieces are copper plated before the brazes are made.

Braze No. 1, Kovar Tube to Pole Piece. The kovar tube (Part 1 of Fig. 12.B.1) is held in position by a counterbore provided in the pole piece.

Braze No. 2, Anode Bars to Pole Piece. In the second braze the anode bars (Part 4 of Fig. 12.B.1) are positioned by an oxidized stainless steel jig, properly machined for the geometry desired. A brazing jig for the Model 11B is shown in Fig. 12.C.2 and 12.C.3). Flash copper plating the ends of the anode bars will assure proper wetting of the solder.

Earlier models used molybdenum anodes which were relatively short lived. It is believed that the evolution of absorbed gas from the anodes caused an arc discharge between the cathode and anode resulting in the melting of one of the anode wires. The following treatment of tungsten anode wire appears to have completely eliminated this source of difficulty.

a. Brief immersion in mixture of 1 part H_2NO_3 and 1 part HFl,

b. Fire at temperature of 1700° C in H_2 atmosphere,

c. Fire at temperature of 1400° C in vacuum at pressure of 2 to 6 x 10^{-7} mm of Hg.

Any bars not immediately used may be stored without further contamination by wrapping in clean, dry tissue and storing in hot box with dehydrating agent. Any adsorbed gas will be readily removed by bombarding during evacuation.

Braze No. 3, Kovar Flange to Pole Piece. A kovar flange is finally brazed to the pole piece. The position of this flange is determined by a counterbore in the pole piece.

Glassing

The two pole piece assemblies are glassed together in one operation by means of r-f induction heating in a stainless steel jig which provides for adjustable spacing between pole pieces. (See Figs. 12C.4, 12C.5, 12C.6 and 12C.7.) A pole piece assembly is placed in each retainer of the glassing jig and the jig is then assembled. Spacing between anode bars is determined by loosening the lock screws in one of the retainers and rotating the pole piece to a position determined by inserting feeler gauges between the anode bars. With the pole piece properly oriented and locked the upper retainer may be removed from the centering rod and a piece of glass tubing .015 to .020 inch longer than the required spacing between flanges is then put in place and the jig reassembled. The ends of the glass cylinder should be clean and parallel. After glassing in the induction heater the lock screws in both retainers are immediately loosened.

The extremities of the tube are glassed with a hand torch.

Cleaning Tube Body

1. Clean tungsten anode structure after glassing by passing an alternating current between anodes while tube is filled with solution of 20 percent KOH. Rinse with water.

2. Partially fill tube with warm Oakite 32 and shake until all interior kovar and copper plate is free from oxides. Rinse thorougly in warm running water, then distilled water followed by an acetone rinse. Dry with nitrogen stream passed through tube.

Cathode

Certain cathode assembly techniques not immediately evident from the drawings (Figs. 12B.7 through 12B.13) will be described.

1. The ceramic insulator is secured to the center conductor by painting it with heater coating solution and firing in hydrogen at 1600° C for 5 minutes.

2. The upper end hat is secured to the center conductor by arc welding in a hydrogen atmosphere.

3. The helix is attached to the end hats by sintering with tungsten powder. A mixture of tungsten powder in a vehicle consisting of 15 percent nitrocellulose and 85 percent ethyl acetate is painted on each joint. After thoroughly drying, the assembly is fired at a temperature of 1700° C in a hydrogen atmosphere for 15 minutes. The cathode should be thoroughly vacuum fired before sealing in to the tube to remove oxides formed during sintering in hydrogen which is not moisture free.

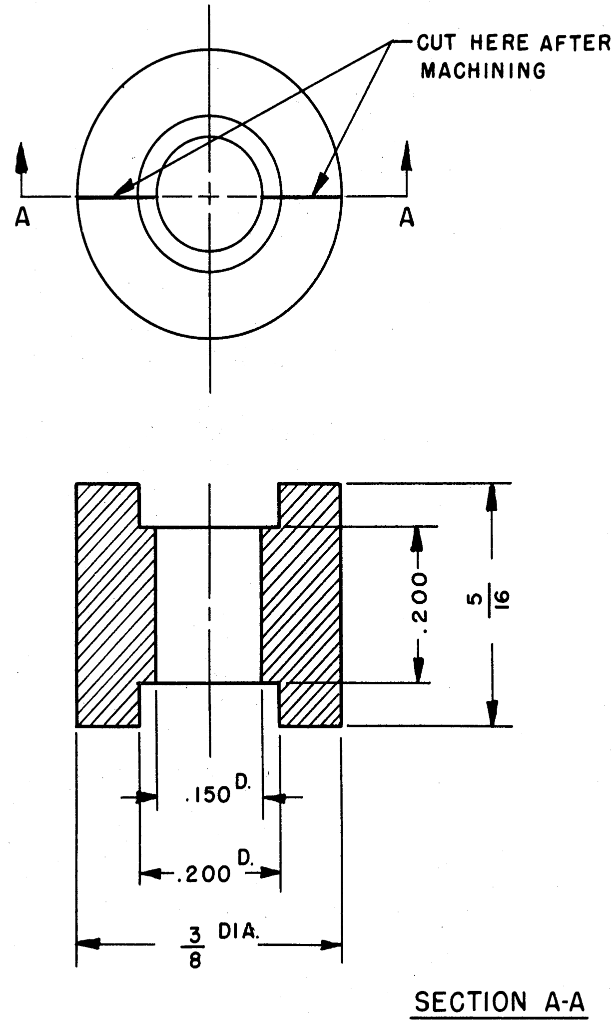

FIG. 12C.1

MOLYBDENUM — 1 REQ'D.

ALL DIMENSIONS UNLESS OTHERWISE SPECIFIED MUST BE HELD TO A TOLERANCE - FRACTIONAL ± 1/64," DECIMAL ± .005," ANGULAR ± 1/2°

ENGINEERING RESEARCH INSTITUTE
UNIVERSITY OF MICHIGAN
ANN ARBOR MICHIGAN

DESIGNED BY VAN NATTER	APPROVED BY
DRAWN BY PLW	SCALE 4 X
CHECKED BY VRB	DATE 9-5-52

PROJECT 2009

TITLE FILAMENT FIRING JIG— MODEL II MAGNETRON

ISSUE	DATE
1	9-5-52

CLASSIFICATION

DWG. NO. A- 4076

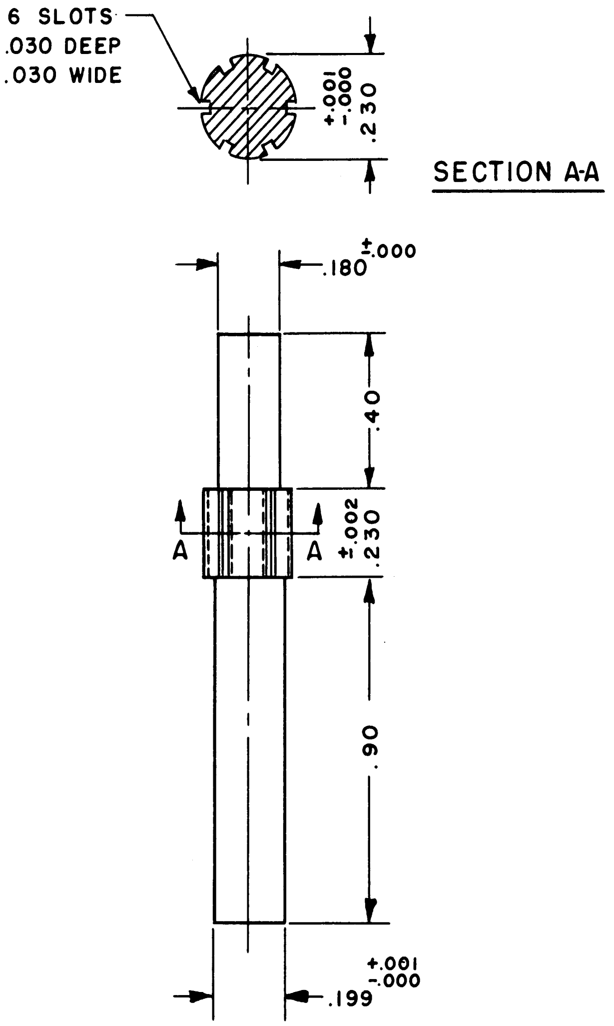

FIG. 12C.2

ALL DIMENSIONS UNLESS OTHERWISE SPECIFIED MUST BE HELD TO A TOLERANCE - FRACTIONAL ± 1/64," DECIMAL ± .005," ANGULAR ± 1/2°

ENGINEERING RESEARCH INSTITUTE
UNIVERSITY OF MICHIGAN
ANN ARBOR MICHIGAN

DESIGNED BY J V'N	APPROVED BY
DRAWN BY PLW	SCALE 2X
CHECKED BY	DATE 12-2-53

PROJECT 2009

TITLE BRAZING JIG FOR MODELS 11B, 11G, 11GA, 13, & 14 MAGNETRONS

ISSUE	DATE
1	12-2-53

CLASSIFICATION

DWG. NO. A- 4091-1

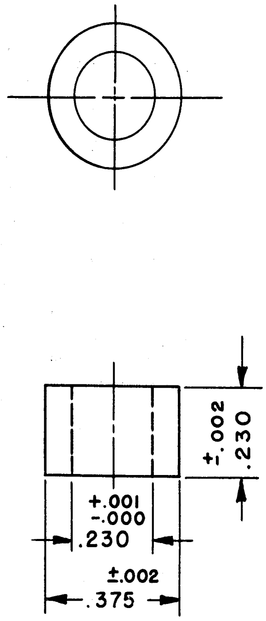

THIS DETAIL TO SLIP OVER
SLOTTED CYLINDER TO RETAIN
WIRES IN SLOTS

FIG. 12 C.3

STAINLESS STEEL — 1 REQ'D.

ALL DIMENSIONS UNLESS OTHERWISE SPECIFIED MUST BE HELD TO A TOLERANCE - FRACTIONAL ± 1/64," DECIMAL ± .005," ANGULAR ± 1/2°

		ENGINEERING RESEARCH INSTITUTE UNIVERSITY OF MICHIGAN ANN ARBOR MICHIGAN	DESIGNED BY J V'N DRAWN BY P L W CHECKED BY	APPROVED BY SCALE 2 X DATE 12-2-53
		PROJECT 2009	TITLE ANODE WIRE BRAZING JIG	
1	12-1-53	CLASSIFICATION	DWG. NO. A- 4091-2	
ISSUE	DATE			

DWG. NO. A

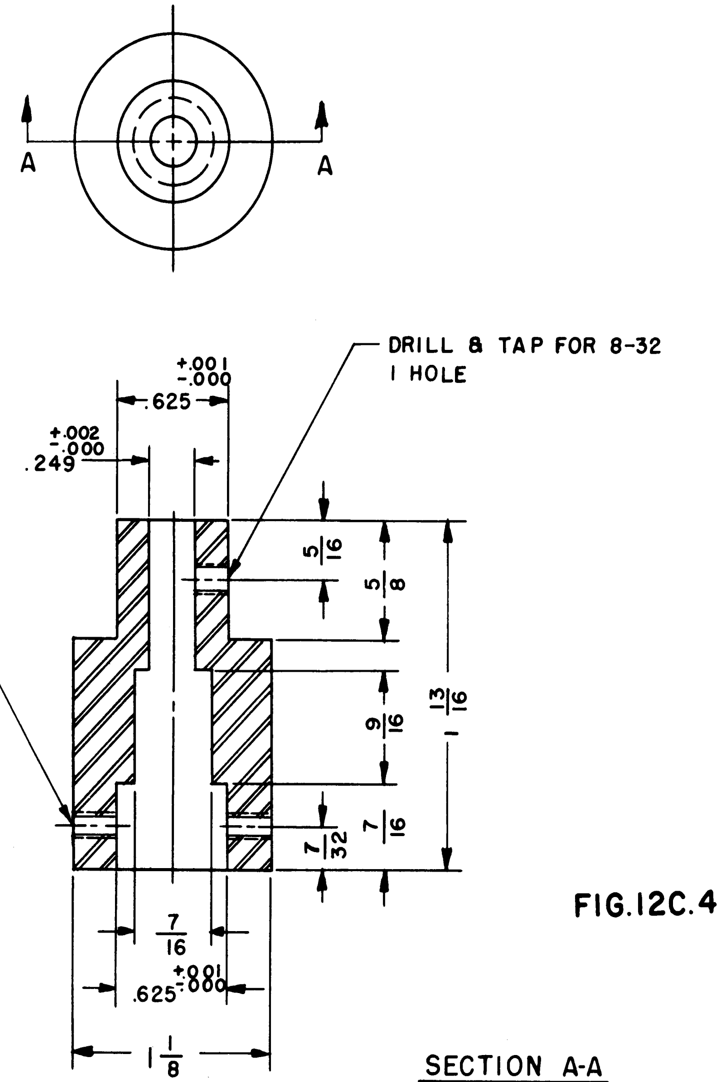

FIG.12C.4

SECTION A-A

NOTE-
USED IN MAGNETRON MODELS 11, 11A, 11B, 11C, 11 CA, 11 D, 11 F, 11G, 11GA, 12, 12A, 12B, 13, 14, AND 15

STAINLESS STEEL — 1 REQ'D.

ALL DIMENSIONS UNLESS OTHERWISE SPECIFIED MUST BE HELD TO A TOLERANCE - FRACTIONAL ± 1/64," DECIMAL ± .005," ANGULAR ± 1/2°

		ENGINEERING RESEARCH INSTITUTE UNIVERSITY OF MICHIGAN ANN ARBOR MICHIGAN	DESIGNED BY J. V'N.	APPROVED BY
			DRAWN BY PLW	SCALE FULL
			CHECKED BY VRB	DATE 12-28-53
		PROJECT 2009	TITLE GLASSING JIG	
1	12-28-53	CLASSIFICATION	DWG. NO. A- 4092-1	
ISSUE	DATE			

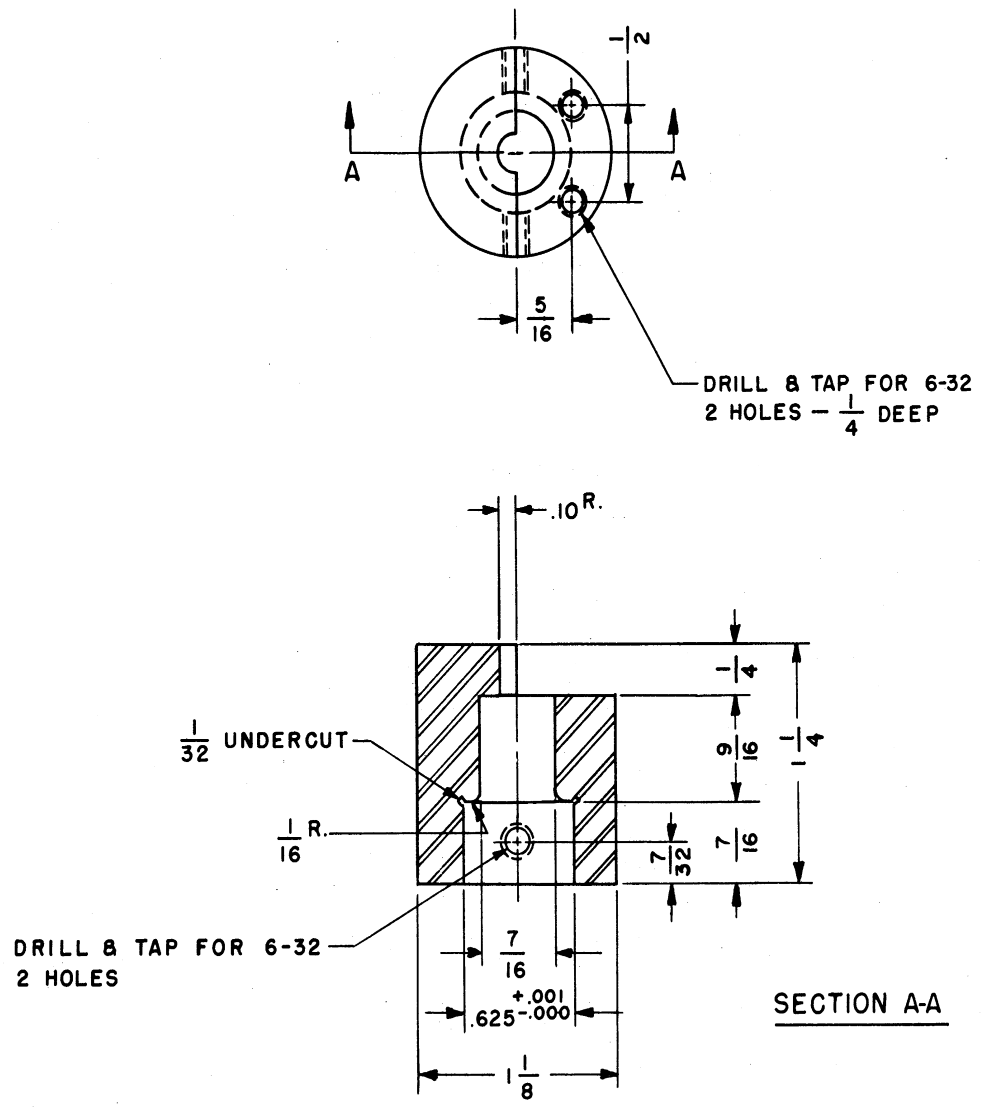

FIG. 12C. 5

NOTE -
USED ON MAGNETRONS 11, 11A, 11B, 11C, 11CA, 11 D, 11E, 11F, 11G, 11GA; 12, 12A, 12 B, 13, 14, AND 15

STAINLESS STEEL — 1 REQ'D.

ALL DIMENSIONS UNLESS OTHERWISE SPECIFIED MUST BE HELD TO A TOLERANCE - FRACTIONAL ± 1/64," DECIMAL ± .005," ANGULAR ± 1/2°

		ENGINEERING RESEARCH INSTITUTE UNIVERSITY OF MICHIGAN ANN ARBOR MICHIGAN	DESIGNED BY J. V'N.	APPROVED BY
			DRAWN BY PLW	SCALE FULL
			CHECKED BY [signature]	DATE 12-28-53
		PROJECT 2009	TITLE GLASSING JIG	
1	12-28-53	CLASSIFICATION	DWG. NO. A- 4092-2	
ISSUE	DATE			

DWG. NO. A

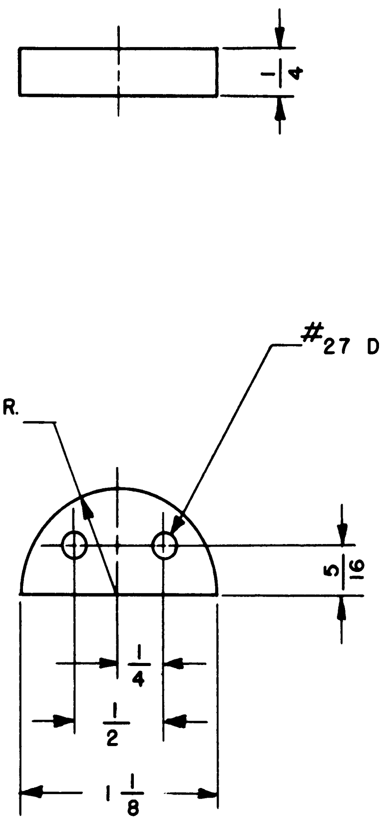

FIG. 12C.6

NOTE —
USED IN MAGNETRON MODELS 11, 11A, 11B, 11C, 11CA, 11D, 11E, 11F 11G, 11GA, 12, 12A, 12B, 13, 14, AND 15.

STAINLESS STEEL — 1 REQ'D.

ALL DIMENSIONS UNLESS OTHERWISE SPECIFIED MUST BE HELD TO A TOLERANCE - FRACTIONAL ± 1/64," DECIMAL ± .005," ANGULAR ± 1/2°

ENGINEERING RESEARCH INSTITUTE UNIVERSITY OF MICHIGAN ANN ARBOR MICHIGAN	DESIGNED BY J V'N.	APPROVED BY
	DRAWN BY PLW	SCALE FULL
	CHECKED BY VRB	DATE 12-28-53
PROJECT 2009	TITLE GLASSING JIG	
ISSUE 1 · DATE 12-28-53	CLASSIFICATION	DWG. NO. A- 4092-3

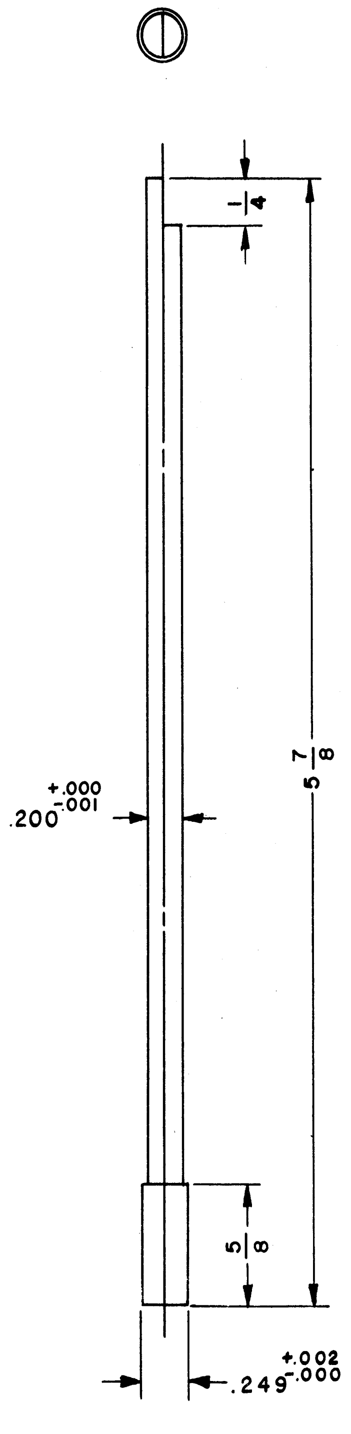

FIG. 12C.7

NOTE –
USED ON MAGNETRON MODELS 11, 11A, 11B, 11C, 11CA, 11D, 11E, 11F, 11G, 11GA, 12, 12A, 12B, 13, 14, AND 15

STAINLESS STEEL – 1 REQ'D.

ALL DIMENSIONS UNLESS OTHERWISE SPECIFIED MUST BE HELD TO A TOLERANCE - FRACTIONAL ± 1/64." DECIMAL ± .005." ANGULAR ± 1/2°

ENGINEERING RESEARCH INSTITUTE UNIVERSITY OF MICHIGAN ANN ARBOR MICHIGAN	DESIGNED BY J. V'N. / APPROVED BY DRAWN BY PLW / SCALE FULL CHECKED BY [illegible] / DATE 12-28-53
PROJECT 2009	TITLE GLASSING JIG
ISSUE 1 / DATE 12-28-53 / CLASSIFICATION	DWG. NO. A- 4092-4

DISTRIBUTION LIST

20 copies - Director, Evans Signal Laboratory
Belmar, New Jersey
FOR: Chief, Thermionics Branch

10 copies - Chief, Bureau of Ships
Navy Department
Washington 25, D.C.
ATTENTION: Code 930A

10 copies Chief, Engineering and Technical Service
Office of the Chief Signal Officer
Washington 25, D.C.

10 copies Director, Air Materiel Command
Wright Field
Dayton, Ohio
ATTENTION: Electron Tube Section

2 copies - Mr. John Keto
Director, Aircraft Radiation Laboratory
Air Materiel Command
Wright Field
Dayton, Ohio

2 copies - Document File
Electronic Defense Group
Engineering Research Institute
University of Michigan
Ann Arbor, Michigan

1 copy - H. W. Welch, Jr., Project Supervisor
Electronic Defense Group
Engineering Research Institute
University of Michigan
Ann Arbor, Michigan

Engineering Research Institute File
University of Michigan
Ann Arbor, Michigan

W. E. Quinsey, Assistant to the Director
Engineering Research Institute
University of Michigan
Ann Arbor, Michigan

W. G. Dow, Professor
Department of Electrical Engineering
University of Michigan
Ann Arbor, Michigan

Gunnar Hok, Professor
Department of Electrical Engineering
University of Michigan
Ann Arbor, Michigan

J. R. Black, Research Engineer
Engineering Research Institute
University of Michigan
Ann Arbor, Michigan

J. S. Needle, Assistant Professor
Department of Electrical Engineering
University of Michigan
Ann Arbor, Michigan

Bell Telephone Laboratories
Murray Hill, New Jersey
ATTENTION: S. Millman

Microwave Research Laboratory
University of California
Berkeley, California
ATTENTION: Professor D. Sloan

Air Force Cambridge Research Laboratories
Library of Geophysics Directorate
230 Albany Street
Cambridge, Massachusetts
ATTENTION: Dr. E. W. Beth

Air Force Cambridge Research Laboratories
Library of Radiophysics Directorate
230 Albany Street
Cambridge, Massachusetts

Collins Radio Company
Cedar Rapids, Iowa
ATTENTION: Robert M. Mitchell

Columbia Radiation Laboratory
Columbia University
Department of Physics
New York 27, New York

Department of Physics
Cornell University
Ithaca, New York
ATTENTION: Dr. L. P. Smith

Industry and Science Department
Enoch Pratt Free Library
Baltimore 1, Maryland

Vacuum Tube Department
Federal Telecommunication Laboratories, Inc.
500 Washington Avenue
Nutley 10, New Jersey
ATTENTION: A. K. Wing, Jr.

General Electric Co.
General Engineering Laboratory Library
Building 5, Room 130
1 River Road
Schenectady 5, N. Y.

General Electric Research Laboratory
Schenectady, New York
ATTENTION: Dr. A. W. Hull

General Electric Research Laboratory
Schenectady, New York
ATTENTION: P. H. Peters

Mr. A. C. Gable
Ind. and Trans. Tube Dept.
General Electric Co. (Bldg. 269)
Schenectady, New York

Mrs. Marjorie L. Cox, Librarian
G-16, Littauer Center
Harvard University
Cambridge 38, Massachusetts

Cruft Laboratory
Harvard University
Cambridge, Massachusetts
ATTENTION: Professor E. L. Chaffee

Electron Tube Laboratory
Research and Development Laboratory
Hughes Aircraft Company
Culver City, California
ATTENTION: G. R. Brewer

Electron Tube Laboratory
Department of Electrical Engineering
University of Illinois
Urbana, Illinois

Mr. R. Konigsberg
Radiation Laboratory
Johns Hopkins University
1315 St. Paul's Street
Baltimore, Maryland

Department of Electrical Engineering
University of Kentucky
Lexington, Kentucky
ATTENTION: Professor H. Alexander Romanowit

Gift and Exchange Division
University of Kentucky Libraries
University of Kentucky
Lexington, Kentucky

Mr. R. E. Harrell, Librarian
West Engineering Library
University of Michigan
Ann Arbor, Michigan

Department of Electrical Engineering
University of Minnesota
Minneapolis, Minnesota
ATTENTION: Professor W. G. Shepherd

Document Office - Room 20B-221
Research Laboratory of Electronics
Massachusetts Institute of Technology
Cambridge 39, Massachusetts
ATTENTION: John H. Hewitt

National Bureau of Standards Library
Room 203, Northwest Building
Washington 25, D. C.

Dr. D. L. Marton
Chief, Electron Physics Section
National Bureau of Standards
Washington 25, D. C.

Mr. Stanley Ruthberg
Electron Tube Laboratory
Bldg. 83
National Bureau of Standards
Washington 25, D. C.

National Research Council of Canada
Radio and Electrical Engineering Division
Ottawa, Ontario
Canada

Dr. O. S. Duffendack, Director
Phillips Laboratories, Inc.
Irvington-on-Hudson, New York

Polytechnic Institute of Brooklyn
55 Johnson Street
Brooklyn 1, New York
Attention: Dr. E. Webber

Department of Electrical Engineering
Pennsylvania State College
State College, Pennsylvania
ATTENTION: Professor A. H. Waynick

Radio Corporation of America
RCA Laboratories Division
Princeton, New Jersey
ATTENTION: Fern Cloak, Librarian

Mr. C. L. Cuccia
RCA Laboratories Division
Radio Corporation of America
Princeton, New Jersey

Radio Corporation of America
RCA Laboratories Division
Princeton, New Jersey
ATTENTION: Mr. J. S. Donal, Jr.

Radio Corporation of America
RCA Victor Division
415 South 5th Street
Harrison, New Jersey
ATTENTION: Hans K. Jenny

Raytheon Manufacturing Company
Research Division
Waltham 54, Massachusetts
ATTENTION: W. M. Gottschalk

Magnetron Developement Laboratory
Power Tube Division
Raytheon Manufacturing Company
Waltham 54, Massachusetts
ATTENTION: Edward C. Dench

Magnetron Development Laboratory
Power Tube Division
Raytheon Manufacturing Company
Waltham 54, Massachusetts
ATTENTION: W. C. Brown

Sanders Associates, Inc.
135 Bacon Street
Waltham 54, Massachusetts
ATTENTION: Mr. James D. LeVan

Sperry Gyroscope Company
Library Division
Great Neck, Long Island, New York

Department of Electrical Engineering
Stanford University
Stanford, California
ATTENTION: Dr. S. Kaisel

Sylvania Electric Products, Inc.
70 Forsyth Street
Boston 15, Massachusetts
ATTENTION: Mrs. Mary Timmins, Librarian

Sylvania Electric Products, Inc.
Woburn, Massachusetts
ATTENTION: Mr. Marshall C. Pease

Department of Electrical Engineering
Yale University
New Haven, Connecticut
ATTENTION: Dr. L. P. Smith

J. A. Boyd, Assistant Supervisor
Electronic Defense Group
Engineering Research Institute
University of Michigan
Ann Arbor, Michigan

Dr. J. H. Findlay
Director of Research
Electronic Products Company
111 E. 3 Street
Mount Vernon, New York